LAURA CRISTINA LIMA DINIZ

Avaliação biológica de peptídeos antimicrobianos isolados da hemolinfa do *Triatoma infestans* (Hemiptera:Reduviidae).

São Paulo
2020

LAURA CRISTINA LIMA DINIZ

Avaliação biológica de peptídeos antimicrobianos isolados da hemolinfa do *Triatoma infestans* (Hemiptera:Reduviidae).

Tese apresentada ao Programa de Pós-Graduação Interunidades em Biotecnlogia – Universidade de São Paulo, Instituto Butantan, Instituto de Pesquisas Tecnologicas para obtenção do título de Doutor em Biotecnologia.

Área de Concentração: Biotecnologia

Orientador: Prof. Dr. Pedro Ismael da Silva Júnior

Versão Corrigida. A versão original encontra-se disponível na Secretaria de Pós-Graduação que aloja o Programa de Pós-Graduação.

São Paulo
2020

LAURA CRISTINA LIMA DINIZ

Biological evaluation of antimicrobial peptides isolated from the hemolymph of *Triatoma infestans* (HEMIPTERA:REDUVIIDAE)

.

Thesis submitted to the Postgraduate Interunits Post-Graduation Program in Biotechnology – University of São Paulo, Butantan Institute, Institute of Technological Research to obtain the Doctor's degree in Biotechnology

Concentration area: Biotechnology

Advisor: Prof. Dr. Pedro Ismael da Silva Júnior

Corrected version. The original versionis available from the Graduate Secretariat hosting the Post-Gradute Program.

São Paulo
2020

CATALOGAÇÃO NA PUBLICAÇÃO (CIP)
Serviço de Biblioteca e informação Biomédica
do Instituto de Ciências Biomédicas da Universidade de São Paulo

Ficha Catalográfica elaborada pelo(a) autor(a)

Diniz, Laura Cristina Lima
Biological evaluation of antimicrobial peptides isolated from the hemolymph of Triatoma infestans (HEMIPTERA:REDUVIIDAE) / Laura Cristina Lima Diniz; orientador Dr.Pedro Ismael Silva Júnior. -- São Paulo, 2020.
141 p.

Tese (Doutorado)) -- Universidade de São Paulo, Instituto de Ciências Biomédicas.

1. Antimicrobianos. 2. Moléculas bioativas. 3. Triatoma infestans. 4. Sangue. 5. Peptídeos. I. Silva Júnior, Pedro Ismael , orientador. II. Título.

UNIVERSIDADE DE SÃO PAULO

Programa de Pós-Graduação Interunidades em Biotecnologia

Universidade de São Paulo, Instituto Butantan, Instituto de Pesquisas Tecnológicas

Candidato(a): Laura Cristina Lima Diniz

Titulo da Tese: Biological evaluation of antimicrobial peptides isolated from the hemolymph of Triatoma infestans (HEMIPTERA:REDUVIIDAE). Avaliação biológica de peptídeos antimicrobianos isolados da hemolinfa do *Triatoma infestans* (Hemiptera:Reduviidae).

Orientador: Dr. Pedro Ismael da Silva Junior .

A Comissão Julgadora dos trabalhos de Defesa da Tese de Doutorado, em sessão pública realizada a **...../...../.....**, considerou o(a) candidato(a):

( ) Aprovado(a) ( ) Reprovado(a)

Examinador(a): Assinatura: .....
Nome: .....
Instituição: .....

Examinador(a): Assinatura: .....
Nome: .....
Instituição: .....

Examinador(a): Assinatura: .....
Nome: .....
Instituição: .....

Examinador(a): Assinatura: .....
Nome: .....
Instituição: .....

Examinador(a): Assinatura: .....
Nome: .....
Instituição: .....

Presidente: Assinatura: .....

Nome: .....

Instituição: .....

butantan *Comissão de Ética no Uso de Animais*

São Paulo, 09 de julho de 2020
CEUAx N 3925250716

Ilmo(a). Sr(a).
Responsável: Pedro Ismael Da Silva Junior
Área: Lab. Especial De Toxicologia Aplicada
Equipe envolvida: Laura Cristina Lima Diniz - executor (instituto Butantan); Pedro Ismael Da Silva Junior (orientador)

Título do projeto: "Avaliação Biológica de Análogos de Peptídeos Antimicrobianos Presentes na Hemolinfa Triatoma infestans (HEMIPTERA: REDUVIIDAE).".

Parecer Consubstanciado da CEUA IB

A Comissão de Ética no Uso de Animais do Instituto Butantan, na reunião de 17/08/2016, **ANALISOU** e **APROVOU** o protocolo de estudo acima referenciado. A partir desta data, é dever do pesquisador:
1. Comunicar toda e qualquer alteração do protocolo.
2. Comunicar imediatamente ao Comitê qualquer evento adverso ocorrido durante o desenvolvimento do protocolo.
3. Os dados individuais de todas as etapas da pesquisa devem ser mantidos em local seguro por 5 anos para possível auditoria dos órgãos competentes.
4. **Relatórios parciais** de andamento deverão ser enviados **anualmente** à CEUA até a conclusão do protocolo.

Maria Leonor Sarno de Oliveira
Coordenador da Comissão de Ética no Uso de Animais
Instituto Butantan

Nancy Oguiura
Vice-Coordenadora da Comissão de Ética no Uso de Animais
Instituto Butantan

butantan

Comissão de Ética no Uso de Animais

CERTIFICADO

Certificamos que a proposta intitulada "AVALIAÇÃO IN VIVO DE ANÁLOGOS DE PEPTÍDEOS ANTIMICROBIANOS DO Triatoma infestans (HEMIPTERA:REDUVIIDAE) POR ENSAIO POR MICROSCOPIA INTRAVITAL E ZEBRAFISH - Ressubmissão - prazo anterior expirado e experimento ainda não realizado", protocolada sob o CEUA nº 2873120618 (ID 001315), sob a responsabilidade de **Pedro Ismael da Silva Júnior** *e equipe; Laura Cristina Lima Diniz; Mônica Valdyrce dos Anjos Lopes Ferreira* - que envolve a produção, manutenção e/ou utilização de animais pertencentes ao filo Chordata, subfilo Vertebrata (exceto o homem), para fins de pesquisa científica ou ensino - está de acordo com os preceitos da Lei 11.794 de 8 de outubro de 2008, com o Decreto 6.899 de 15 de julho de 2009, bem como com as normas editadas pelo Conselho Nacional de Controle da Experimentação Animal (CONCEA), e foi **aprovada** pela Comissão de Ética no Uso de Animais do Instituto Butantan (CEUAIB) na reunião de 20/08/2018.

We certify that the proposal "IN VIVO EVALUATION OF ANTIMICROBIAL PEPTIDES ANALOGUES FROM Triatoma infestans (HEMIPTERA:REDUVIIDAE) THROUGH INTRAVITAL MICROSCOPY AND ZEBRAFISH ASSAYS", utilizing 240 Fishes (males and females), 15 Heterogenics mice (15 males), protocol number CEUA 2873120618 (ID 001315), under the responsibility of **Pedro Ismael da Silva Júnior** *and team; Laura Cristina Lima Diniz; Mônica Valdyrce dos Anjos Lopes Ferreira* - which involves the production, maintenance and/or use of animals belonging to the phylum Chordata, subphylum Vertebrata (except human beings), for scientific research purposes or teaching - is in accordance with Law 11.794 of October 8, 2008, Decree 6899 of July 15, 2009, as well as with the rules issued by the National Council for Control of Animal Experimentation (CONCEA), and was **approved** by the Ethic Committee on Animal Use of the Butantan Institute (CEUAIB) in the meeting of 08/20/2018.

Finalidade da Proposta: Pesquisa

Vigência da Proposta: de 06/2018 a 12/2019 Área: Lab. Especial de Toxicologia Aplicada

Origem:	LETA - Plataforma Zebrafish						
Espécie:	Peixes	sexo:	Machos e Fêmeas	idade:	1 a 3 horas	N:	240
Linhagem:	Danio rerio (zebrafish)			Peso:	0 a 0000 g		
Origem:	Biotério Central						
Espécie:	Camundongos heterogênicos	sexo:	Machos	idade:	6 a 8 semanas	N:	15
Linhagem:	Swiss			Peso:	30 a 40 g		

Local do experimento: Unidade Imunorregulação do Laboratório Especial de Toxinologia Aplicada, Instituto Butantan

São Paulo, 09 de julho de 2020

Maria Leonor Sarno de Oliveira
Coordenador da Comissão de Ética no Uso de Animais
Instituto Butantan

Nancy Oguiura
Vice-Coordenadora da Comissão de Ética no Uso de Animais
Instituto Butantan

INSTITUTO FEDERAL DE EDUCAÇÃO, CIÊNCIA E TECNOLOGIA DE SÃO PAULO

PARECER CONSUBSTANCIADO DO CEP

DADOS DO PROJETO DE PESQUISA

Título da Pesquisa: AVALIAÇÃO BIOLÓGICA DE PEPTÍDEOS ANTIMICROBIANOS ISOLADOS DA HEMOLINFA DO Triatoma infestans (HEMIPTERA: REDUVIIDAE).

Pesquisador: LAURA CRISTINA LIMA DINIZ

Área Temática:

Versão: 2

CAAE: 15562219.2.0000.5473

Instituição Proponente: Instituto Butantan

Patrocinador Principal: Financiamento Próprio

DADOS DO PARECER

Número do Parecer: 3.432.972

Apresentação do Projeto:

AVALIAÇÃO BIOLÓGICA DE PEPTÍDEOS ANTIMICROBIANOS ISOLADOS DA HEMOLINFA DO Triatoma infestans (HEMIPTERA: REDUVIIDAE)

Objetivo da Pesquisa:

Objetivo Primário:

Avaliar atividades biológicas dos peptídeos análogos de Triatogenio, Triastina, Tin-TK-I e Tin-TK-II isolados durante o projeto de mestrado realizado
de 2014 a 2016 no Laboratório Especial De Toxinologia Aplicada.

Objetivo Secundário:

1) Confirmar a hipótese levantada sobre a internalização do Fibrinopeptídeo A por parte do Triatoma infestans;2) Avaliar in vitro possíveis atividades
biológicas apresentadas pelos peptídeos isolados: Atividade antiviral; Atividade antiparasítica; Citotoxicidade frente a linhagens celulares não
tumorais.

Avaliação dos Riscos e Benefícios:

O projeto não apresenta nenhum tipo de risco. Os experimentos antiparasíticos e antivirais são realizados em salas e capelas apropriadas e com
organismos atenuados (não representando risco de contaminação ou potencial patogenia)

Endereço: Rua Pedro Vicente, 625
Bairro: Canindé **CEP:** 01.109-010
UF: SP **Município:** SAO PAULO
Telefone: (11)3775-4665 **E-mail:** cep_ifsp@ifsp.edu.br

Comentários e Considerações sobre a Pesquisa:

Pesquisa relevante para produção de novos medicamentos.

Considerações sobre os Termos de apresentação obrigatória:

Estão de acordo com o solicitado pelo CEP.

Recomendações:

Não apresenta.

Conclusões ou Pendências e Lista de Inadequações:

Não apresenta pendências.

Considerações Finais a critério do CEP:

Este parecer foi elaborado baseado nos documentos abaixo relacionados:

Tipo Documento	Arquivo	Postagem	Autor	Situação
Informações Básicas do Projeto	PB_INFORMAÇÕES_BÁSICAS_DO_PROJETO_1339266.pdf	28/06/2019 17:29:10		Aceito
TCLE / Termos de Assentimento / Justificativa de Ausência	TCLE_Laura.pdf	28/06/2019 17:28:23	LAURA CRISTINA LIMA DINIZ	Aceito
Projeto Detalhado / Brochura Investigador	Brochura_Projeto_Laura_com_cronograma.pdf	03/06/2019 10:33:59	LAURA CRISTINA LIMA DINIZ	Aceito
Folha de Rosto	Folha_de_rosto_Laura.pdf	03/06/2019 10:32:28	LAURA CRISTINA LIMA DINIZ	Aceito
Declaração de Manuseio Material Biológico / Biorepositório / Biobanco	Declaracao_de_uso_de_material_biologico_Laura.pdf	03/05/2019 14:49:21	LAURA CRISTINA LIMA DINIZ	Aceito

Situação do Parecer:

Aprovado

Necessita Apreciação da CONEP:

Não

Dedication

First of all, before anything, I have to dedicate this work to both God and my Family (Márcia, Arildo, Lívia, Vinicius e Jonatan). Without any of them in my life it would have been practically impossible for me to get this far. Thank you all for the love and strength that you give me every day!! I can't express enough how much I love and care for each one of you!!

Thank you too Dr. Pedro Ismael, that chose me and guided me all of these years. You are amazing! I owe it all to you too.

To my estimate friends and colleagues from the lab, I have no words to emphasize enough how important you have been on every step of the way. Andrea, Paula, Bruna, Débora, Rosa, Paty, Norton, Rosa, André, Sandrinha and more especially to Soraia, Ivan and Thiago! I love you!

To my friends from outside of the lab that have made me laugh and believe that it would all be ok, thank you too!! Aldolfo, Tami, Mari, friends from Uberaba, SP, Geography (FFLCH - USP), DF/Manaus, RJ, OP (CP e Taberna), Paraopeba, Florianopolis, Vitória and else, I carry you inside my heart everywhere I go.

So, I dedicate this work to friends, family and colleagues, close or not, that made possible for me to conclude it.

Thank you!

Acknowledgements

I would like to thank all of the personal from the Laboratory of Applied Toxinology. Mainly to Dr. Pedro Ismael for being my mentor. Also for my friends and colleagues that walked alongside with me during the steps of the work.

To Dr. Ronaldo Zucatelli that came up to be my second mentor.

To Ivan Lavander that gave me support in several áreas, especially on my English, also Soraia and Thiago that always backed me up and helped me to think in possibilities to make this work grow.

To Abraham Omar Espinoza Culupú for the support on different experiments.

To the Funding agencies. This work was financed by the São Paulo Research Foundation (FAPESP) Grant 13/07467-1 to CeTICS-CEPID and from the Brazilian National Technological and Scientific Development Council (CNPq) Grant 142224/2016-2 and 472744/2012-7.

And also to the Butantan Institute, University of São Paulo and Interunits Post-Graduation Program, specially the staff that guided me during the entire doctorate.

“Per Ardua ad Astra;
Per Aspera ad Astra”

“Por caminhos árduos, aos astros; Das dificuldades, chega-se as estrelas”

Abstract

Diniz LCL. Biological evaluation of antimicrobial peptides isolated from the hemolymph of Triatoma infestans (HEMIPTERA:REDUVIIDAE) [Thesis]. São Paulo: Universidade de São Paulo, Instituto Butantan e Instituto de Pesquisas Tecnológicas, Instituto de Ciências Biomédicas; 2020.

Microbial resistance is a recurring problem, which dates back to the first classes of antibiotics developed, and which has become alarming due to the speed and ease of emergence of (multi)resistant organisms. Thus rises the concern with the global scenario and that comes associated with the urgent need to development of new antimicrobial drugs. Antimicrobial peptides are molecules that manage to kill microbial cells by independent mechanisms of site-specific binding, being interesting molecules alternative to commercial antibiotics. In previous works of our group, four antimicrobial peptides from the hemolymph of the hematophagous insect *Triatoma infestans* were identified as human fibrinopeptide A, Triastine (glycine-rich antimicrobial) and TRP1-TINF and TRP2-TINF (Tachykinin-Related Peptides). The work presented three aspects. First: biological screening to evaluate the aforementioned peptides as possible new drugs. Anti-parasitic and antiviral activities were evaluated, to which the molecules were not active, even at the highest concentrations (FbPA – 84 µM; Triastin – 100 µM; TRP1-TINF – 128 µM; TRP2-TINF – 164 µM). The peptides did not presented hemolysis, but showed different degrees of toxicity for VERO cells (initial concentration: 1000 µM, 43% - FbPA, 16% Triastina e TRP11-TINF e 10% - TRP2-TINF). In *in vivo* tests on intravital microscopy models, at [200 µM], FbPA did not induce changes in microcirculation, Triastine was able to interrupt blood flow without the formation of thrombi and TRP1-TINF and TRP2-TINF showed a pro-inflammatory pattern. In a zebrafish model, [200 µM], FbPA could not be tested, the Triastine peptide was lethal for 100% of the embryo sampling at 48 hours post-fertilization, TRP1-TINF was lethal for 100% of the sampling at 72 hpf and TRP2-TINF showed lethality for 35% of the sample, with the majority of other embryos having malformations. In the evaluation of the mechanism of action, the only peptide capable of interacting with DNA was FbPA [≥60µM]. In the second part, the mechanism by which a human molecule is present in the hemolymph of the insect in question was verified. The synthetic FbPA was coupled with the FITC fluorophore and was supplied together with the insect feed. The fluorescence of the hemolymph of engorged insects with marked feeding

was compared with the hemolymph of non-fed insects, showing to be significant, being possible to confirm that the presence of human FbPA in the insect's hemolymph occurs through intestinal absorption. Finally, evaluating the cryptids, several fragments with antimicrobial activity were identified in the insect's intestine, resulting from digestion of murine hemoglobin. In conclusion, the general work demonstrated that the peptides tested present interesting antimicrobial activity and are potential new drugs, but need improvements due to the general toxicity presented. Two alternative sources of antimicrobials for insects were also demonstrated, one through fragments from intestinal absorption and the other through the digestion of ingested blood.

Keywords: Antimicrobial peptides. *Triatoma infestans.* Blood.

Resumo

Diniz LCL. Avaliação biológica de peptídeos antimicrobianos isolados da hemolinfa do *Triatoma infestans* (HEMIPTERA:REDUVIIDAE) [Tese]. São Paulo: Universidade de São Paulo, Instituto Butantã e Instituto de Pesquisas Tecnológicas, Instituto de Ciências Biomédicas; 2020.

Resistência microbiana é um problema recorrente, que remonta das primeiras classes de antibióticos desenvolvidos, e que vem se tornando alarmante devido à velocidade e facilidade de surgimento de organismos (multi)resistentes. Com isso surge a preocupação com o quadro mundial e que vem associada à urgente necessidade de descoberta de novas moléculas antimicrobianas. Peptídeos antimicrobianos são moléculas que conseguem levar a morte células microbianas por mecanismos independentes de ligação sítio específicas, sendo interessantes moléculas alternativas aos antibióticos comerciais. Em trabalhos prévios do nosso grupo, foram identificados quatro peptídeos antimicrobianos da hemolinfa do inseto hematófago *Triatoma infestans*, identificados como Fibrinopeptídeo A humano, Triastina (antimicrobiano rico em glicina) e TRP1-TINF e TRP2-TINF (Peptídeos Relacionandos às Taquicininas). O trabalho apresentou três vertentes. Primeira: *screening* biológico para avaliação dos peptídeos supramencionados como possíveis novas drogas. Atividade anti parasíticas e antivirais foram avaliadas, aos quais as moléculas não se mostraram ativas, mesmo nas mais altas concentrações (FbPA – 84 µM; Triastina – 100 µM; TRP1-TINF – 128 µM; TRP2-TINF – 164 µM). Os peptídeos não apresentaram hemólise, mas apresentaram diferentes graus de toxicidade para células VERO (concentração inicial: 1000 µM, 43% - FbPA, 16% Triastina e TRP11-TINF e 10% - TRP2-TINF). Nos ensaios *in vivo* em modelos de microscopia intravital, em [200 µM], o FbPA não induziu alterações de microcirculação, Triastina foi capaz de interromper o fluxo sanguíneo sem a formação de trombos e TRP1-TINF e TRP2-TINF apresentaram um padrão pró inflamatório. Em modelo zebrafish, [200 µM], onde o FbPA não pode ser testado, o peptídeo Triastina foi letal para 100% da amostragem de embriões em 48 hpf, TRP1-TINF foi letal para 100% da amostragem em 72 hpf e TRP2-TINF apresentou letalidade para 35% da amostragem, sendo que a maioria dos embriões vivos apresentaram malformações. Na avaliação de mecanismo de ação, o único peptídeo capaz de interagir com DNA foi o FbPA [≥60µM]. Na segunda vertente foi verificado o mecanismo pelo qual uma molécula humana se encontra presente na hemolinfa

do inseto em questão. O FbPA sintético foi acoplado com o fluoróforo FITC e foi fornecido juntamente com a alimentação aos insetos. A fluorescência da hemolinfa dos insetos ingurgitados com a alimentação marcada foi comparada com a hemolinfa de insetos não alimentados, se mostrando significativa, sendo possível confirmar que a presença do FbPA humano na hemolinfa do inseto ocorre através de absorção intestinal. E finalmente, avaliando os criptídeos, foram identificados vários fragmentos com atividade antimicrobiana no intestino do inseto, provenientes de digestão da hemoglobina murina. Em conclusão o trabalho geral demonstrou que os peptídeos testados apresentam interessante atividade antimicrobiana e são potenciais novas drogas, mas necessitam de melhorias em relação a sua toxicidade. Foram demonstradas também duas fontes alternativas de antimicrobianos para insetos, sendo uma através de fragmentos provenientes de absorção intestinal e outra através da digestão do sangue ingerido.

Palavras-chave: Peptídeos antimicrobianos. *Triatoma infestans*. Sangue.

List of Figures

List of Tables

Abbreviations

°C: degrees Celsius

µg: micrograms

µL: microliter

µM: micromolar

Å: Angström

Abs: absorbance

ACN: Acetonitrile

AMP: antimicrobial peptide

AR: antimicrobial resistance

ARM: resistant microorganism

AVPs: antiviral peptides

Blast: basic local alignment search tool

CEUAIB: Ethic Committee on Animal Use of the Butantan Institute

CFU: colony-forming unit

CHIKV: Chikungunya vírus

CID: collision induced dissociation

CPE: cytopathic effects

Da: Dalton

DMSO: dimethyl sulfoxide

DNA: deoxyribonucleic acid

ESI: electrospray ionization

FA: formic acid

FA: Formic acid

FbPA: Fibrinopeptide A

FbPB: Fibrinopeptide B

FBS: fetal bovine serum

FET: Fish Embryo Acute Toxicity

FITC: Fluorescein isothiocyanate

FREP: fibrinogen-related peptides

g: gravity

GDP: Gross Domestic Product

h: hours

HBB1: hemoglobin β1 chain

HBB2: hemoglobin β2 chain

hpf: hours post-fertilization

IB: inclusion bodies

IVM: Intravital microscopy

kDa: kilodalton

L: liter

LC: liquid chromatography

LPS: lipopolysacharide

LTA: Laboratório de Toxinologia Aplicada

LTQ XL: Linear Ion Trap Mass Spectrometer

MBHAR: methylbenzhydrylamine resin

min: minute

mL: milliliter

mM: millimolar

MOI: multiplicity of infection

MTT: 3-(4,5-dimethylthiazol-2-yl)-2,5-diphenyltetrazolium bromide

OECD: Organization for Economic Cooperation and Development

PB: poor broth

PBS: Phosphate-buffered saline

PDR: penicillin drug resistant;

pH: potential of hydrogen

R: resistant;

RP-HPLC: reverse phase - high performance liquid chromatography

RP-HPLC: Reverse-phase high-performance liquid chromatography

RPMI: Roswell Park Memorial Institute

RPMI: Roswell Park Memorial Institute medium

RT: retention time

TFA: trifluoroacetic acid

XDR: extremely drug resistant

ZIKV: zika vírus

Amino acid list

A	Ala	Alanine
C	Cys	Cysteine
D	Asp	Aspartic acid
E	Glu	Glutamic acid
F	Phe	Phenylalanine
G	Gly	Glycine
H	His	Histidine
I	Ile	Isoleucine
K	Lys	Lysine
L	Leu	Leucine
M	Met	Methionine
N	Asn	Asparagine
P	Pro	Proline
Q	Gln	Glutamine
R	Arg	Arginine
S	Ser	Serine
T	Thr	Threonine
V	Val	Valine
W	Trp	Tryptophan
Y	Tyr	Tyrosine

Contents

1 Introduction

1.1 General description of antimicrobial resistance (AR)

Since the discovery of the first antibiotic, in 1928 by Alexander Fleming, and the production as a drug by Norman Heatley, Ernst Chain and Howard Florey (1), the general situation of the "modern" medicine was changed.

This new drug was more effective and presented fewer side effects then the treatments available at the time. It became possible to control and treat severe bacterial infections avoiding several deaths around the globe, to prevent infections during complex procedures such as transplantations, surgical procedures in anatomic locations, or complementing higher doses of chemotherapy (1, 2). During the World War II, for example, penicilin was successfully used to treat infections on wounded soldiers (3).

The field of research on new antibiotic drugs was initiated and in short periods of time there were several new drugs being discovered and produced. But, along with new antibiotics classes, the appearance of resistance was also reported. A review published by Bailey and Cavallitto (1948, p. 169) (4) described the antibiotics available at the time and the organisms that already presented resistance:

> The frequency with which resistant organisms are isolated from patients undergoing treatment with streptomycin is the chief defect of that antibiotic; penicillin-resistant organisms are encountered less frequently but nevertheless are an important problem in the clinical use of this antibiotic.

At that time antimicrobial resistance (AR) was recognized as a problem, but there has been ways to overcome such problem, such as new drugs being developed or the available ones could be altered, thus the problem was temporarily resolved (1). Only by the decade of 1960, the interest to study mechanisms of resistance transmission began to receive proper attention (5, 6). By the 80's, AR was perceived as a global problem due to every new drug produced in a short period, new antimicrobial resistant microorganisms (ARM) were reported (figure 1).

Misuse/overuse of antibiotics in situations like: poor quality of commercial drugs in some countries; use of antibiotics in treatments where they are not really necessary (7); extensive and indiscriminate agricultural consumption of antibiotics (8); increase in income levels of antibiotics in human health treatments (9); easy travel routes (10) are factors that accelerate the rate of emergence and spread rate of ARM (11).

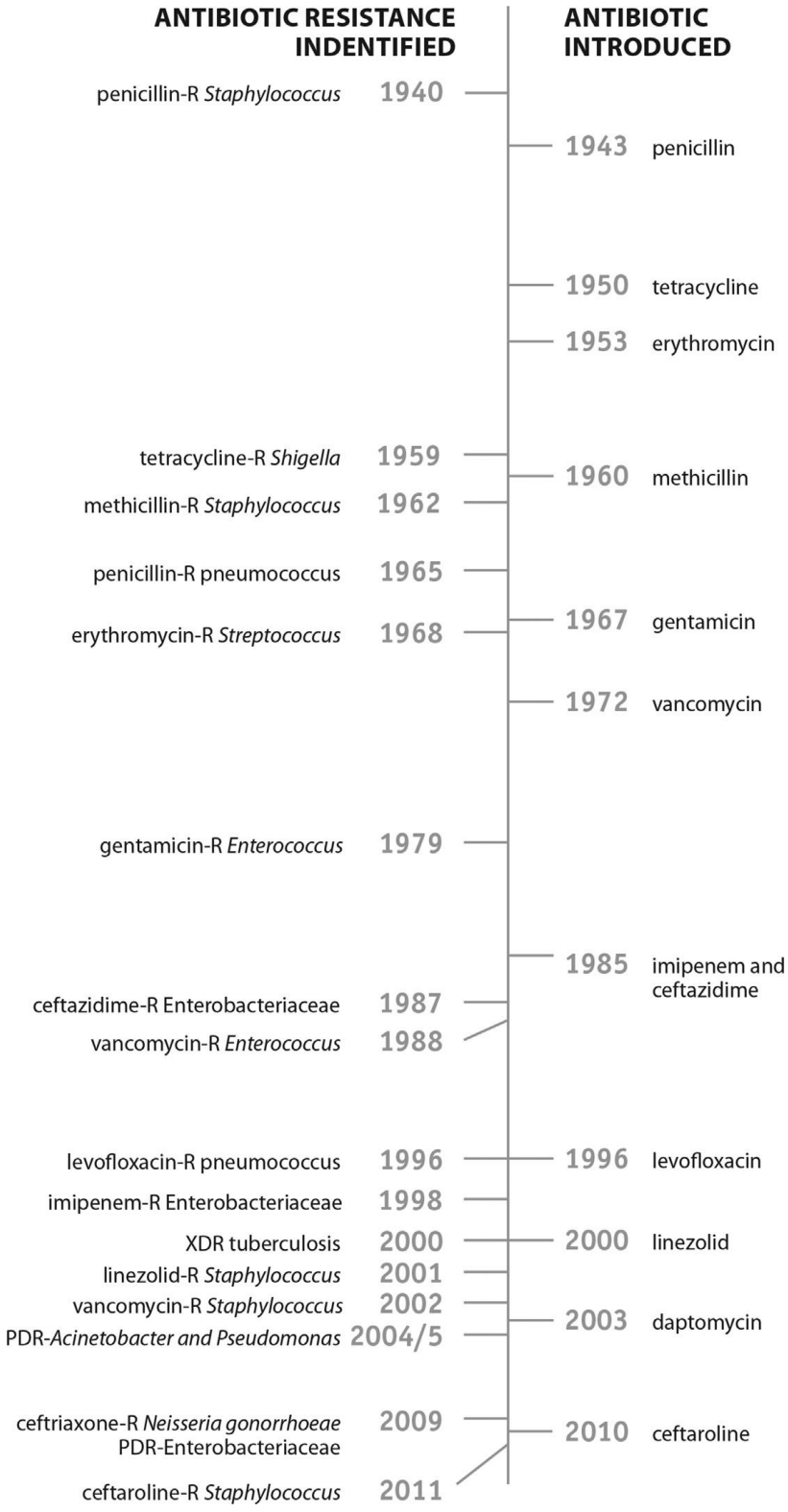

Source: Atkins and Bonomo, 2016 - NUMERO

PDR, penicillin drug resistant; R, resistant; XDR, extremely drug resistant.

Figure 1 – Timeline of antimicrobial resistance development.
Timeline demonstrating the relation between the discovery of new antibiotics and the development of antimicrobial resistance.

Nowadays several studies and reports demonstrate the global concern on the speed of emergence of resistant organisms, mainly from the year of 2000, with the description of "super-bacteria" resistant to more than one class of antibiotics (12-16).

The AR problem has evolved until a global threat. World Health Organization (2019, p. 1), in a recent report entitled "No Time to Wait: Securing the future from drug-resistant infections" (17), described the concern related to global deaths:

> Drug-resistant diseases already cause at least 700,000 deaths globally a year, including 230,000 deaths from multidrug-resistant tuberculosis, a figure that could increase to 10 million deaths globally per year by 2050 under the most alarming scenario if no action is taken. Around 2.4 million people could die in high-income countries between 2015 and 2050 without a sustained effort to contain antimicrobial resistance.

AR generates socioeconomic implications. The estimate is that, without the control of the increasing AR rate, beyond the alarming number of deaths, it will lead to a reduction of 2% to 3.5% in Gross Domestic Product (GDP) in general, or 5-7% loss in developing countries, which can correspond from 100 up to 210 trillion USD (11).

These increasin rates of AR formation implicates in a near future where there will be no drugs available to treat such infections, aggravating the overall picture. Therefore there is an urgent need to research and develop alternative drugs.

1.2 Mechanisms of antimicrobial resistance

To be able to produce new drugs that can overcome resistance, it is necessary to understand how does AR is generated.

AR is a complex concept that is built from evolutionary characteristics, genetic plasticity until biochemical pathways. It has been developed through interactions between the microorganism and the environment, where, in an attempt to survive, the organism uses genetic strategies such as mutations in genes associated to the compound-biding site and the acquisition of resistance DNA-coding, which leads to alterations on the biochemical properties on the site where the antibiotic would act (18).

Resistance can be intrinsic or induced. The intrinsic is shared within species, it is always constitutively produced and it is independent of previous exposure to antibiotics. The induced resistance is composed by DNA resistance encoding genes that are expressed only after exposure to antibiotics (19).

The alterations produced after the expression of resistance genes can be classified in

four main types (figure 2), as follows: I) changes of the target site, II) global cell adaptive processes, III) prevention to reach the antibiotic target, and IV) modifications on the antimicrobial molecule (18, 20).

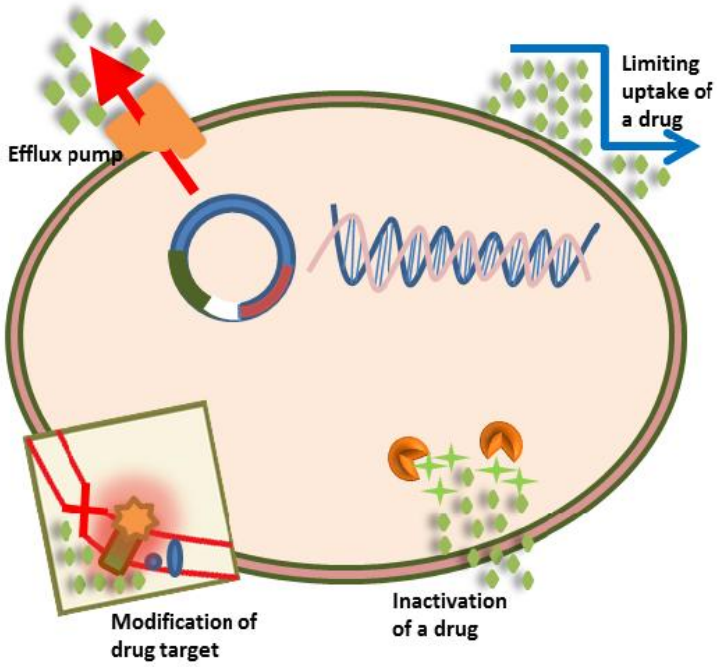

Source: Reygaert, 2018

Figure 2 – Types of antimicrobial resistance
Demonstration of the sites of alteration on the microbial cell that can generate resistance to antibiotics.

Changes of the target site

It might occur through two different mechanisms. The first is the protection of the target that avoids the interaction between the antibiotic molecule with the location on the microbial cell. The most affected drugs are tetracycline (Tet[O] and Tet[M]), fluoroquinolones (Qnr) and fusidic acid (FusC and FusB) (20, 21).

The second is by modifying the target leading to less affinity between the antibiotic and the target. It is the most common mechanism of resistance and affects almost every antibiotics families. The modifications can be: **A)** through enzymatic changes of the binding sites, for example, macrolide resistance by the methylation of the ribosome by the expression of enzymes encoded by the gene Erythromycin Ribosomal Methylation (22); **B)** target's replacement, where the organism can produce new molecules with similar function for the cell, but different structure, hindering the biding with the drug, for example, modifications on the peptidoglycan structure of enterococci that leads to vancomycin resistance; **C)** mutations in the genes that encode the target site, for example, mutation on a specific point of the DNA,

resulting on amino acid substitutions resulting on less affinity between rifamycin and bacterial DNA-dependent RNA polymerase (23);

Prevention to reach the antibiotic target

There are two main processes that can prevent the drug for reaching the target. The first mechanism is to decrease the cell permeability, which is particularly important in Gram-negative bacteria. Changes on the type and percentage of different molecules on the membrane can interfere on the penetration of toxic compounds, for example, the lipopolysaccharides (LPS) layer in Gram-negative bacteria represent a natural resistance to some large antimicrobial drugs (24). Other example is the expression of hydrophobic molecules, which affect the permeability of hydrophilic molecules that depends on porin channels to penetrate the membrane (e.g. tetraciclines, fluoroquinolones) (25).

The second mechanism is the production of machineries that remove antibiotic molecules from the intracellular environment. The first description of an efflux system was from an *Escherichia coli* that excluded tetracycline (26), and after that, several others were identified, and now there are 5 major families of efflux pumps, entitled multidrug and toxic compound extrusion family, resistance-nodulation-cell-division family, major facilitator superfamily, ATP-binding cassette family and small multidrug resistance family (27, 28).

Global cell adaptive processes

To cope with living inside other living organisms, bacterial pathogens developed mechanisms to avoid the interruption of essential cellular processes. bacteria that lack a cell wall are intrinsically resistant to drugs that has the cell wall as target, as glycopeptides for example (29).

Modifications on the antimicrobial molecule

Microorganisms can perform modification through the expression of two different types of enzimes.

They can produce enzymes that cleavages the drug, such as the enzymes that are responsible for the tetracycline degradation and the beta-lactamases that can disrupt the beta-

lactam rings on the antibiotic structure (30, 31).

Alternatively, they can produce enzymes that transfer a chemical group to the antibiotic molecule. It is an acquired form of resistance that can occur in Gram-positive and Gram-negative bacteria. One of the most common groups is the acetyl that is frequently transferred to aminoglycosides, streptogramins, fluoroquinolones and chloramphenicol (32-34).

1.3 Antimicrobial peptides (AMPs)

The ease and speed of emergence of microorganisms able to develop drug-evasion mechanisms are two of the main reasons that justify the need to research and produce new antimicrobial drugs (35-37).

Considering that, as described, every resistance mechanism depends on alterations of specific molecules of the microorganism to avoid specific drug-target interaction, a very promising class of molecules to be taken in consideration is AMPs.

Produced on the humoral portion of the innate immune system, AMPs are molecules that play important role on the elimination of the pathogens, along with other mechanisms such as melanization and clotting (38, 39).

AMPs are produced by basically every living organism, ranging from single-cells microorganisms to complex eukaryotes such as plants and mammals (40-51). AMP production can occur through different mechanisms. It occurs mainly by gene expression (52), but also by cleavage of large proteins (cryptic peptides) (53), some molecules with a variety of biological activities can also present antimicrobial potential (54-58).

Gene expression

They can be synthesized after infectious stimuli by expression of gene-enconded ribosomal pre-peptides (59), although the expression of these genes is variable on the organisms. In vertebrates, the expression of these molecules is constitutive while in insects, AMPs production is inducible by infectious/inflammatory stimuli (60).

As insects do not have immunological memory, to each new infection the activation of intracellular cascades have to be initiated again. The main pathways activated are the *Spaetzle/Toll* and the *Imd* pathways, activated by Gram-positive bacteria or fungi and by Gram-negative bacteria, respectively (61) (figure 3). Such activation occurs as a response to

the recognition of pathogens-associated molecular patterns (PAMPs) that are molecules exclusively external, allowing the distinction between self and non-self molecules. The main PAMPs recognized from Gram-negative bacteria include LPS, from Gram-positive include peptidoglycans and β-1-3-glucan from fungi (52, 61). The time of response from the activation of the cascades until the AMPs release is approximately 8 hours (62).

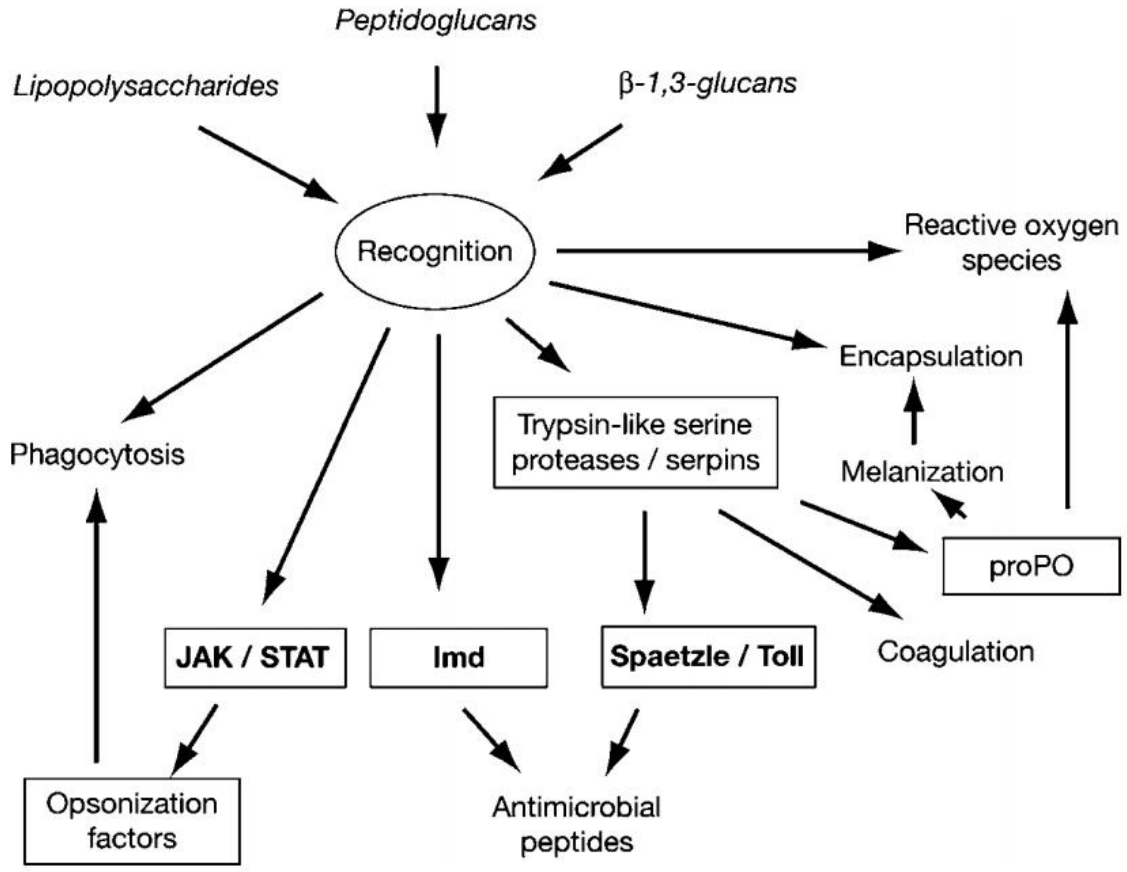

Source: Schmid-Hempel, 2005 (52)

Figure 3 – Representation of the insect pathways activated on infections.
Representation of the cascades activated by infections or lesion on insects, in a *Drosophila melanogaster* model.

Cryptic antimicrobial peptides

The cleavage of large proteins that generate bioactive peptides is a strategy developed by higher eukaryote organisms that can act as a counter-response to antimicrobial resistance mechanisms.

As mentioned previously, one bacterial resistance mechanism is the production of proteases in an attempt to cleavage antibiotic molecules, but this cleavage process forms some fragments with diverse biological activities, including antimicrobial activity, that can overcome the bacterial resistance (53).

More recently, several antimicrobial cryptic peptides have been described without direct relation to antimicrobial resistance. It has been reported that these cryptic peptides can be produced naturally during cleavage processes, generating these active peptides that can act over a broad spectrum of bacteria and fungus, representing an important AMP source (63-66).

Bioactive molecules with antimicrobial potential

While investigating the biological potential of diverse compounds, several studies discovered that such molecules present antimicrobial activity as a secondary feature (56, 67-69). It has became a common property evaluated during biological studies, and nowadays there are tools to predict if a molecule can present antimicrobial activity based mainly on the amino acid sequence (70-73).

1.4 Mechanisms of action

AMPs is a class of molecules that comprises peptides with length up to 50 amino acids, with overall positive charges (2+ to 13+) (74). Generally they contain basic and hydrophobic amino acids that are aligned in opposite surfaces of the molecule on the three dimensional structure (60, 75, 76).

Positive charges, hydrophobicity and amphipatic are three of the main characteristics that determine the mechanism of action of AMPs. Positively charged peptides tend to interact with phospholipid groups on microbial membranes, thus increasing the number of positive charges on the AMPs' sequences improves antibacterial activity (77, 78). The amino acids valine, leucine, isoleucine, alanine, methionine, phenylalanine, tyrosine and tryptophan provide hydrophobic characteristics to peptides, required to membrane penetration (79, 80). And amphipatic feature is due to the balance between cationic/hydrophilic residues and hydrophobic residues on the primary and secondary structures (mainly on α-helix), a characteristic that facilitates peptide-membrane interactions (74).

The mechanisms of action presented by AMPs have direct relations with the characteristics described above, and can be divided into two major categories (74, 81). Those directly interacting with microbial cells (membrane or intracellular) or those that can modulate the immune response (figure 4).

Direct interaction

The mechanisms of interaction can involve either membrane binding or intracellular targets.

The primary mechanism seems to be through electrostatic interaction between positive residues of the peptide and the outer surface of prokaryotic cells, which is negatively charged due to LPS or teichoic acid (82). The membrane interaction can occur with or without energy input (figure 5).

The energy independent processes (barrel-stave model, carpet model, or toroidal model) occur solely with charge interactions, where the peptides form pores on the membrane or act as a detergent recovering the membrane, leading to membrane disruption, loss of intracellular content and consequently cell death (83, 84).

The energy dependent process (macropinocytosis) is a mechanism where some of the extracellular matrix containing the AMP is trapped in a vesicle during a membrane invagination process, once inside the cell, the AMP present on the vesicle is released on the cytoplasm and exert the antimicrobial activity (82, 85).

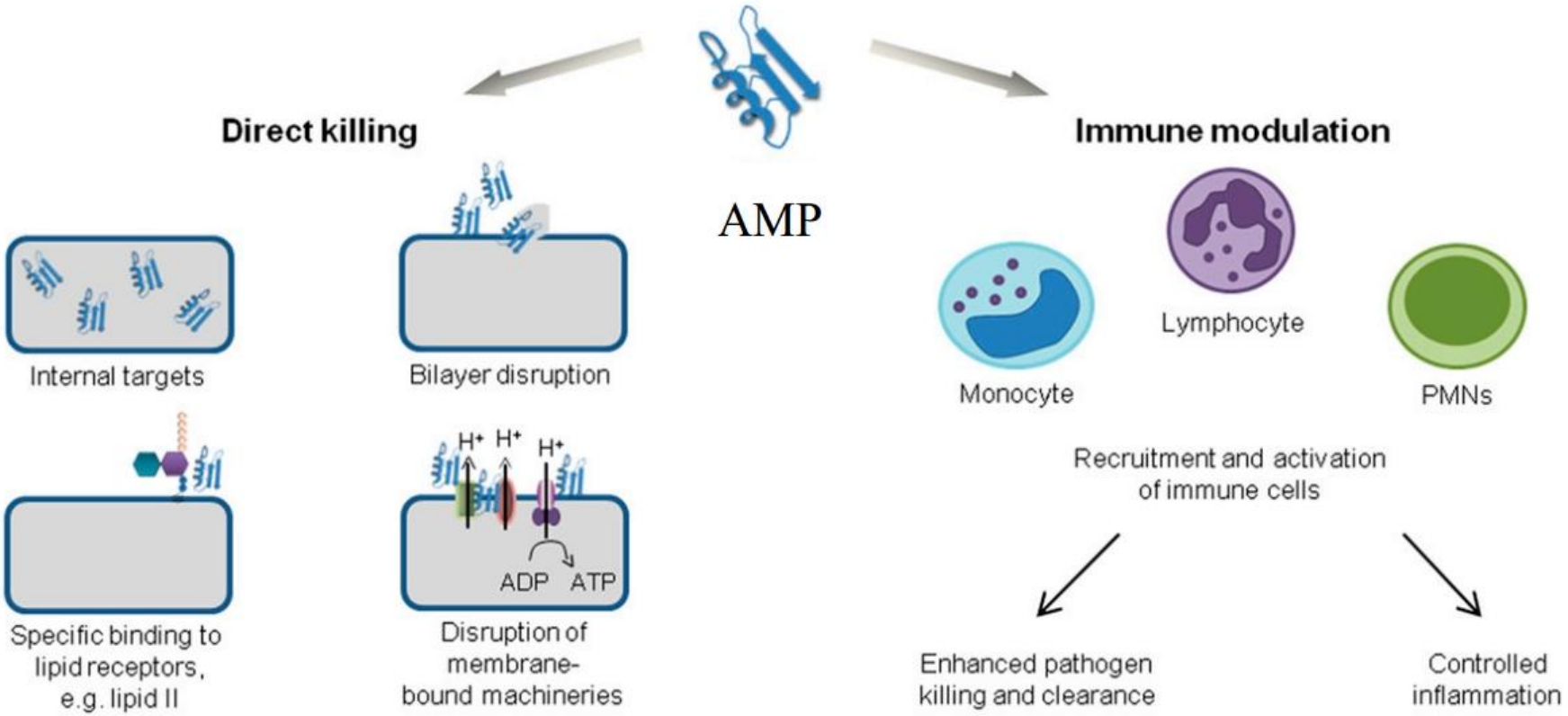

Source: Kumar et al., 2018

Figure 4 – Mechanisms of actions presented by AMPs.
AMPs can present two major mechanism to kill microbial cells. By direct killing the peptide interact directly with the membrane or intracellular pathways. By immune modulation the peptide activates and recruits cells to enhance the immune response against the pathogen.

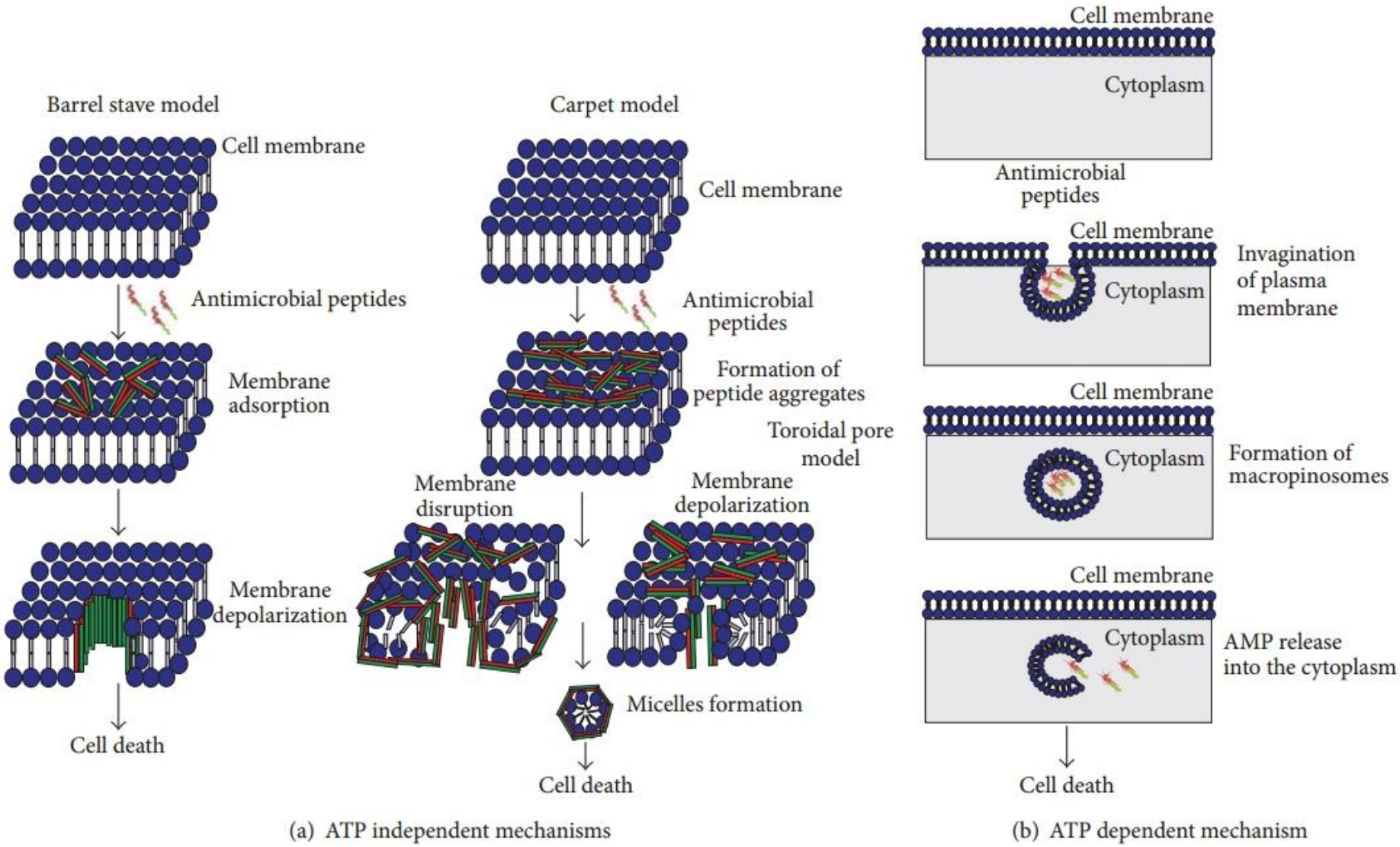

Source: Pushpanatan et al., 2013

Figure 5 – Direct killing mechanisms that occurs through membrane interaction.
Demonstration of the mechanisms of action with direct interaction with the microbial membrane. a) on the mechanisms without energy input there are the carpet, toroidal pore and barrel stave models. b) On the mechanism ATP dependent there is the macropinocytosis.

In other situations, the peptide translocates through the membrane and affects some essential cellular pathway (76, 86) (figure 6).

The presence of AMPs on the cytoplasm can affect nucleic acid biosynthesis and metabolism (e.g. buforin I, buforin II and indolicidin) (87, 88) by DNA and/or RNA affinity (89, 90), or homology to proteins that directly interacts with DNA (91, 92). AMPs can also inhibit cell division, interfering basically on every step of the process, from inhibiting DNA replication to the septation process (e.g. microcin J25, diptericin) (93, 94). They can interfere with proteases, forming noncovalent complexes inhibiting proteins such as metalloproteases (e.g. histatin 5) (95-98) or serine proteases (e.g. eNAP-2) (99, 100). Some AMPs can also bind to LPS layer on the outer membrane or during infections where these molecules, also known as bacterial endotoxins, are released to the blood, neutralizing such molecules and avoiding the evolution of the infection to a septic shock (e.g. MBI-27, MBI-28) (101-104). Interruption of the biosynthesis of cell wall is also a relevant mechanism, where the peptide interacts with some cell wall-forming lipids, inducing accumulation of the peptidoglycan precursors on the cytoplasm (e.g. some lantibiotics and some defensins) (105-109).

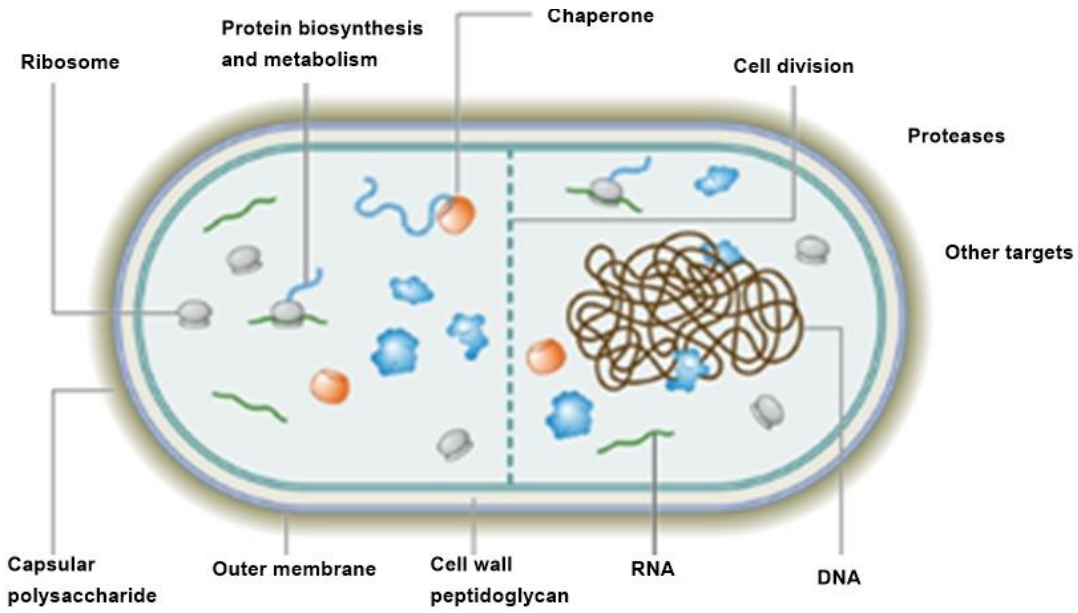

Source: adapted from Le et al., 2017

Figure 6 – Direct killing mechanisms with intracellular targets.
Description of the intracellular targets where AMPs can exert activity interfering on different pathways leading to microbial death.

Modulation of the immune response

Briefly, AMPs can act recruiting cells, such as leukocytes or dentritic cels, through chemotaxis (e.g. β defensins) (110, 111) and/or activating immune cells, potentiating the immune response, whether towards controlling the inflammation or killing the microbial. These mechanisms are not yet well understood (112).

It is important to highlight that the same AMP can have multiple mechanisms of action (74, 86). As most of the mechanisms already described do not involve specific targets and due to the ease to produce synthetic AMPs molecules, the interest on AMPs as alternative to commercial antibiotics is growing each day.

1.5 Insects' antimicrobial peptides

Bioactive molecules where discovered on insects by Stephens, 1962 (113), followed by Hink and Briggs in 1968 (114), Powning and Davidson in 1973 (115), Boman in 1974 (116) and Faye and Boman in 1975 (117). These studies represented the beginning of a growing interest on this field of study, that culminated on the characterization of the two first AMPs molecules, isolated by Steiner and group (118), entitled Cecropins as they were isolated from the moth *Hyalophora cecropia*, which became the first big AMP group to be described.

Regarding AMPs in triatomines it has been demonstrated that *T. brasiliensis and Triatoma (Meccus) pallidipennis* expresses genes for defensins (119, 120). On the salivary glands of *T. infestans* were found genes for trialisins (121), but few molecules have been identified so far.

My recent work demonstrated the isolation and characterization of four AMPs from the *T. infestans* hemolyph (42). The first molecule is a human peptide from the coagulation cascade, entitled fibrinopeptide-A (FbPA), the second is a glycine-rich peptide (Triastine) and the last two are from the tachykinin-related peptides family (TRP1-TINF and TRP2-TINF).

FbPA

This molecule is formed by the cleavage of the human fibrinogen on the last part of the clot formation pathway (122).

It has 16 amino acids (figure 7) and has α-helix secondary structure. This peptide is active against Gram-positive, yeasts, filamentous fungi but is more potent against and Gram-negative bacteria such as *Escherichia coli* and *Pseudomonas aeruginosa* (15-30 µM), and suffers degradation through aminopeptidases (42).

Triastine

It is a glycine-rich peptide from the cuticle of *T. infestans.* It has 16 amino acids (figure 8) and has helix-3_1 conformation. It is not active against Gram-positive bacteria but present activity against Gram-negative bacteria *Escherichia coli* and *Pseudomonas aeruginosa* (17-8,8 µM). It is also active against yeasts and filamentous fungi but in higher concentrations. It is a very stable peptide although it suffer degradation from carboxy and aminopeptidases (42).

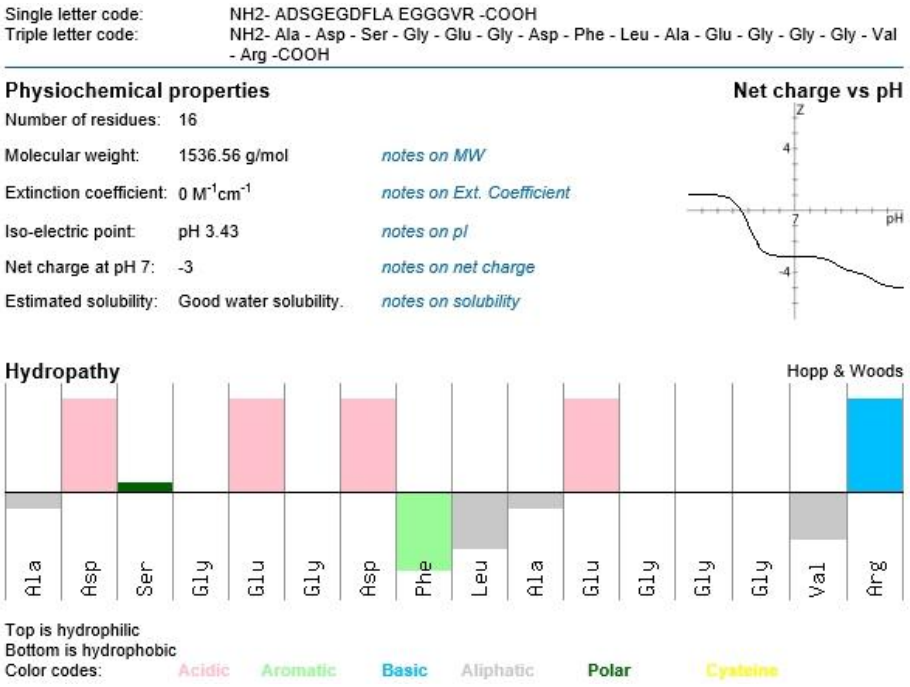

Figure 7 – Fibrinopeptide A properties calculated with pepcalc tool.
Properties of the peptide FbPA calculated with pepcalc tool (pepcalc.com). Characteristics of the amino acids, iso-electric point and net charge are demonstrated based on the peptide sequence. Information on the hydrophobicity of the peptide is also shown. The pink color corresponds to acidic amino acids, gray color

corresponds to aliphatic amino acids, light green corresponds to aromatic amino acids, dark green corresponds to polar amino acids and blue corresponds to basic amino acids.

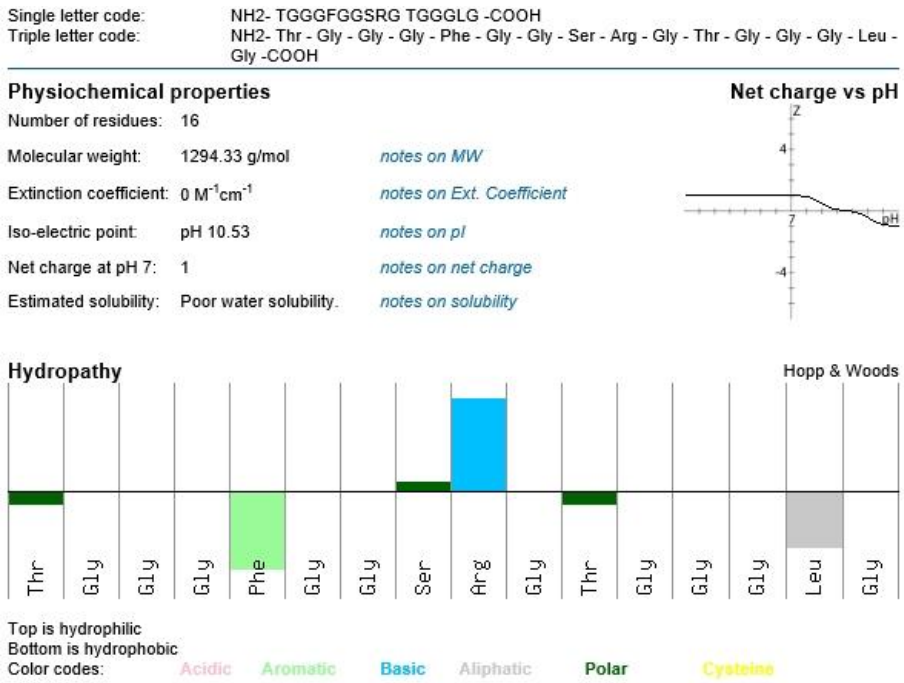

Figure 8 – Triastine properties calculated with pepcalc tool.
Properties of the peptide Triastine calculated with pepcalc tool (pepcalc.com). Characteristics of the amino acids, iso-electric point and net charge are demonstrated based on the peptide sequence. Information on the hydrophobicity of the peptide is also shown. The pink color corresponds to acidic amino acids, gray color corresponds to aliphatic amino acids, light green corresponds to aromatic amino acids, dark green corresponds to polar amino acids and blue corresponds to basic amino acids.

TRP1-TINF and TRP2-TINF

Tachykinin-related peptide is a subfamily of proteins from insects that resemble the Tachykinin family of vertebrates that have activity as neurotransmitter/neuromodulator (123).

TRP1-TINF is a random secondary structure peptide with 9 amino acid residues (figure 9). It is susceptible to aminopeptidases degradation and is active mainly against *Micrococcus luteus* (32-64 μM), but can also present activity against other classes of microorganisms.

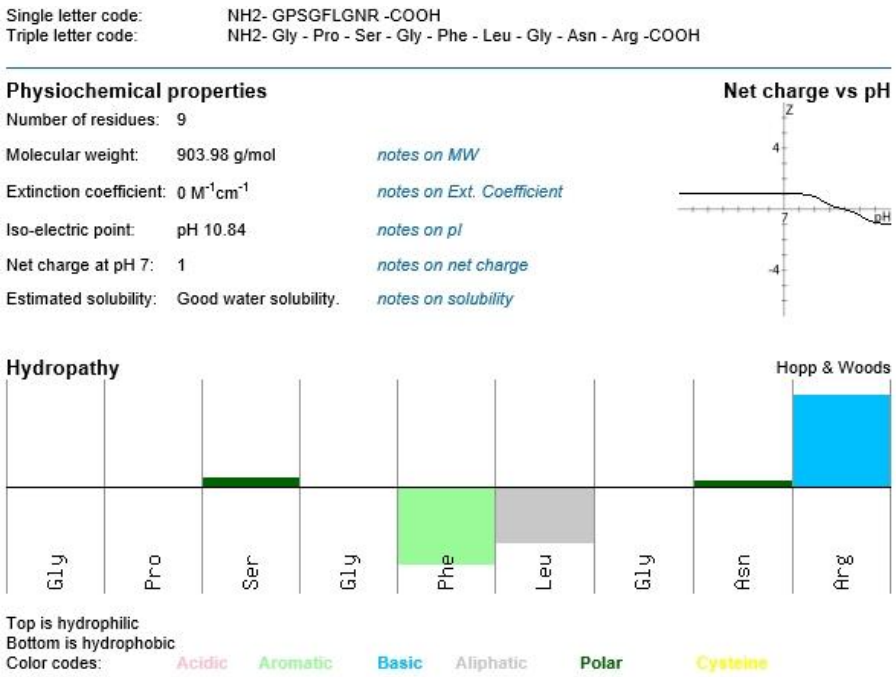

Figure 9 – TRP1-TINF properties calculated with pepcalc tool.
Properties of the peptide TRP1-TINF calculated with pepcalc tool (pepcalc.com). Characteristics of the amino acids, iso-electric point and net charge are demonstrated based on the peptide sequence. Information on the hydrophobicity of the peptide is also shown. The pink color corresponds to acidic amino acids, gray color corresponds to aliphatic amino acids, light green corresponds to aromatic amino acids, dark green corresponds to polar amino acids and blue corresponds to basic amino acids.

TRP2-TINF is a 10-amino acid peptide (figure 10) with a helix-3_1 conformation and is susceptible to carboxypeptidases degradation. It has major antimicrobial activity against both *Pseudomonas aeruginosa* and *Escherichia coli* (45-90 μM).

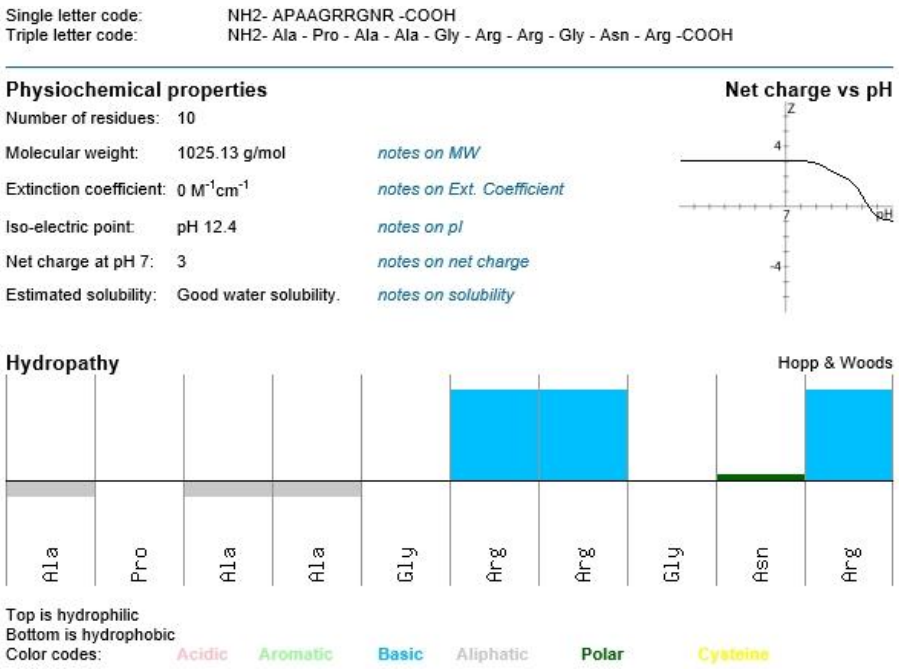

Figure 10 – TRP2-TINF properties calculated with pepcalc tool.
Properties of the peptide TRP2-TINF calculated with pepcalc tool (pepcalc.com). Characteristics of the amino

acids, iso-electric point and net charge are demonstrated based on the peptide sequence. Information on the hydrophobicity of the peptide is also shown. The pink color corresponds to acidic amino acids, gray color corresponds to aliphatic amino acids, light green corresponds to aromatic amino acids, dark green corresponds to polar amino acids and blue corresponds to basic amino acids.

These molecules were partially characterized and demonstrated a good biological potential, thus were chosen to follow screening as candidates for drug development.

1.6 Drug development

The development of new drugs is a long process that requires multiple steps. It initiates on the discovery of the active compound that involves a wide characterization of the molecule, its targets and effects. Tools for fractionation and bioinformatics have large applications at this initial stage, such as chromatography and proteomic analysis. *In vitro* assays are also applied at this stage to define the effect of the compound towards the disease of interest (124).

The secondary step is the drug development or preclinical trial, where information about toxicity, pharmacodynamics and pharmacokinetics are gathered to elucidate the potency, efficacy and safety information on the drug. Pharmacodynamics is considered on experiments that evaluate drug-target interactions (e.g. mechanism of action), pharmacokinetics is observed through absorption, distribution, metabolism and excretion of the drug. Toxicity is relatable with potency, efficacy and safety, where the information on the compound's concentration with maximum activity and lower toxicity need to be analyzed together (125). A wide diversity of *in vivo* and *in vitro* models are available nowadays and provides crucial information on the studied compound (126-128).

All of these are required for the next step entitled clinical trials, where the drug is prepared to be tested in human. Thus the preclinical trial needs to be well designed in order to obtain the maximum amount information on the new drug (125).

Taking in consideration the information described, the aim of this study was to proceed with initial experiments on the preclinical stage of the development of FbPA, Triastine, TRP1-TINF and TRP2-TINF as potential new antibiotics.

2 – Chapter 1

Biological evaluation of antimicrobial peptides isolated from the hemolymph of Triatoma infestans (HEMIPTERA:REDUVIIDAE)

2.2 Objectives

2.2.1 General objectives

Perform an evaluation on the peptides previously isolated from the *Triatoma infestans* hemolymph, in an attempt to discover other biological features that they might present.

2.2.2 Specific objectives

- Evaluate the capability of the peptides to interfere on the physiology of the parasite *Schitossoma mansoni;*
- Evaluate possible antiviral activities presented by the peptides through viral infectivity in cell cultures;
- Determine the safety concentration for each peptide by:
    - cytotoxicity
    - hemolytic assay
- Evaluate the peptides' toxicity *in vivo* models:
    - Intravital microscopy
    - Fish Embryo Acute Toxicity (FET) Test
- Determine the mechanism of action for the peptides through DNA interaction.

2.3 Materials and Methods

2.3.1 Schistosomicidal screening

Parasite

Schistosoma mansoni is a platyhelminthe of the trematoda class, and presents sexual dimorphism, where the female and male measure approximately 1.5 cm the male 1.0 cm respectively. The lifecycle depends on two different hosts, the intermediate host is the aquatic mollusk *Biomphalária glabrata* and the definitive host can be different mammalias, specially humans (129).

The life cycle of *S. mansoni* (BH strain) (130) on the Laboratory of Parasitology, on Butantan Institute, in *Biomphalaria glabrata* Say (1818) snails (Gastropoda:Planorbidae) as intermediate hosts and *Mesocricetus auratus* hamsters Waterhouse (1839) (Mammalia:Cricetidae) as definitive hosts.

To maintain the strain and to obtain the larvae for the experiments, 150 cercariae are injected on the subcutaneous tissue of the female hamsters (20-22 g). To obtain the adult worms, after 9 weeks of infection the infected females hamsters were perfused with RPIM 1640 medium (supplemented with heparin) (131). The worms were recovered through the portal and mesenteric system.

Experiment

The experiments were held in collaboration with the Laboratory of Parasitology, on Butantan Institute, under supervision of Dr. Eliana Nakano.

Adult worm pairs (male and female) obtained through perfusion, were with RPMI 1640 medium (Gibco) supplemented with 25 mM of Hepes, 200 μg/mL of streptomycin and 200 IU/mL of penicillin (Invitrogen). The coupled pairs (male and female) were then transferred to each well of a 24-well culture plate containing 2 mL of the medium supplemented calf 10% (heat inactivated), in 37 ºC and 5% CO_2. After an incubation period of 2 h, the peptides were diluted in Roswell Park Memorial Institute (RPMI) 1640 medium with 2% of dimethyl sulfoxide (DMSO) and added to the cultured worms until the final concentrations (FbPA – 84 uM; Triastine – 100 uM; TRP1-TINF – 128 uM; TRP2-TINF –

164 uM). As the negative control group for toxicity RPMI 1640 medium with 2% dimethyl sulfoxide (DMSO) was used, and there were no positive control group. The parasites were incubated for 120 h and monitored after the first 2 h and then every 24 h under an inverted microscope and stereomicroscope to assess motility, oviposition, tegument alterations, mortality rate and worm coupling. The worms were considered to be dead when no movement was observed. The experiments were carried out in three biological replicates (132, 133).

2.3.2 Cell lineage

VERO cells are a lineage initiated in 1962 by Y. Yasumura and Y. Kawakita, at Chiba University, in Chiba, Japan (134). The cells were cultivated at 37 ºC in 25 cm² plastic culture flasks in 5 mL of Leibovitz médium (L-15) supplemented with 10% inactive fetal bovine serum (FBS) from Cultilab® (Campinas, SP, Brazil).

2.3.3 Antiviral assays

Viral strains

Picornavirus – murine encephalocarditis virus, small icosahedral particles (22 to 30 nm), noneveloped, composed by single strand RNA (135);

Measle – Attenuated Edmonston strain, spherical and enveloped particle (120 to 250 nm). single-strand and negative-sense RNA (136);

Zika vírus (ZIKV) – enveloped virus with positive-sense, single-stranded RNA (137);

Chikungunya virus (CHIKV) – enveloped virus, spherical particle (70 nm), positive-sense, single-stranded RNA (138).

Picornavirus and measle viral particles are from the laboratory of Parasitology and zika and chikungunya viral particles were provided by Dr. Renato Astray from Viral Immunology Laboratory, both from Butantan Institute.

Stock solution

To maintain virus stock solutions, confluent monolayer of VERO cells was incubated

with the virus during one hour. Then 15 mL of L-15 medium were added and the flask was incubated for 5 days. After the incubation period, the supernatant was collected, separated from the residual cells and divided into aliquots in tubes and frozen in a freezer -80 ºC until use.

Infectious Dose

Confluent VERO cells were dispersed with 0.2% trypsin and diluted in L-15 medium, supplemented with 10% FBS from Cultilab® (Campinas, SP, Brazil), to a concentration of 2.0×10^4 cells/mL. 96-well plates were seeded with the cell suspension and incubated for 24 h at 37 ºC. The plates with confluent cells were then inoculated with 100 µL of the virus stock in two-fold serial dilution in triplicates. The stock solution virus was quantified by medium tissue—culture infections with 0.1 MOI (multiplicity of infection) on cell cultures. Uninfected cultures were prepared as negative control. Plate cultures were observed for cytopathic effects (CPE) daily during 2 to 5 days. Titers were provided as $TCID_{50/}$ mL (median tissue culture infectious dose) (139).

Antiviral effect

The experiments were held in collaboration with the Laboratory of Parasitology, on Butantan Institute, under supervision of Dr. Ronaldo Zucatelli Mendonça.

Vero cells were cultivated for 24 h at 37 °C until 90% confluence in 96-well plates in L-15 medium supplemented with 10% of FBS from Cultilab® (Campinas, SP, Brazil). The confluent cells were incubated for one hour with the peptides in specific concentrations and then were infected with the virus of interest in twelve two-fold serial dilutions, at an initial concentration of 10^3 for picornavirus and 10^4 for measle, ZIKV and CHIKV, and monitored for CPE daily from 2 to 5 days. The plates were stained with 0.25% crystal violet and photographed. Uninfected cultures were prepared as negative control for CPE and the control for toxicity was wells containing the peptide without virus infection. The experiments were performed in experimental and biological triplicates. The peptide concentrations were 8.4 µM, 42 µM and 84 µM for FbPA, 10 µM, 50 µM and 100 µM for Triastine, 12.8 µM, 64 µM and 128 µM for TRP1-TINF and 16.4 µM, 82 µM and 164 µM for TRP2-TINF.

2.3.4 Cytotoxic assays

Quantitative assay (MTT assay)

Cultivated VERO cells were seeded in 96-well microplate (2×10^5 cells/well) and incubated for 24 h at 37 °C until 90% confluence in L-15 medium supplemented with 10% of FBS both from Cultilab® (Campinas, SP, Brazil). The confluent cells were incubated for 24 h with the peptides in twelve two-fold serial dilutions with L-15 to give solutions with final concentrations ranging from 1.95 to 1000 µM. After the incubation time, the supernatant was discarded and 20 µL of MTT (5 mg/mL in PBS) was added to each well and allowed to react for another 4 h at 37 °C. The culture medium was removed and the formazan crystals (formed by the MTT reduction in actives mitochondria) were dissolved by adding 100 µL DMSO. Absorbance was measured in a microplate ELISA reader (1420 Multilabel Counter/Victor3, Perkin Elmer, Waltham, MA, USA) at 550 nm. Cell viability calculated by: viability (%) = (A550 of peptide-treated cells/A550 of peptide-untreated cells) × 100 (140).

Hemolytic assay

For this assay, blood type A+ from a healthy donor was used (*"Plataforma Brasil"* exemption number: 3.432.972). It was collected in the presence of 0.15 M citrate buffer (150 mM; pH 7,4) and washed three times by centrifugation (700 ×*g*, for 10 min at 4 °C) with PBS (NaCl 137 mM, KCI 2,7 mM, Na_2HPO_4 10 mM, KH_2PO_4 1,76 mM; pH 7,4). The washed erythrocytes were resuspended in phosphate buffered saline (PBS) (3% v/v). The peptides (serial two-fold dilutions in PBS) were added to 80 µL erythrocyte suspension to a final volume of 100 µL and incubated for 1 h at 37 °C. Hemoglobin release was monitored by measuring the supernatant absorbance at 405 nm with a Microplate ELISA Reader (1420 Multilabel Counter/Victor3). The hemolysis percentage was expressed in relation to a 100% lysis control (erythrocytes incubated with 0.1% Triton X-100); PBS was used as a negative control (141-143). The initial concentration of the peptides were 840 µM for FbPA, 1000 µM for Triastina, 1280 µM for TRP1-TINF and 1640 µM for TRP2-TINF.

2.3.5 *In vivo* toxicity assays

The experiments performed with living animals were registered (nº 2873120618),

evaluated and approved by the Ethic Committee on Animal Use of the Butantan Institute (CEUAIB).

The experiments were held in collaboration with the Immunoregulation Unit, Laboratory of Applied Toxinology, Brazil, on Butantan Institute, under supervision of Dr. Monica Lopes-Ferreira.

Intravital microscopy (IVM)

The appearance of changes in the microcirculatory network of cremaster muscles in the presence of the peptides was evaluated. IVM was conducted on an upright microscope (Axiolab, Carl Zeiss, Oberkochen, Germany) with a saline immersion objective (SW40/0.75 numerical aperture, Zeiss, Jena, Germany) coupled to a digital camera for image acquisition (AxioCam Icc1, Carl Zeiss, Oberkochen, Germany) using a 10/0.3 longitudinal distance objective/numeric operture and 1.6 optovar (Carl Zeiss, Oberkochen, Germany).

Cremaster Muscle Preparation

To expose the cremaster muscle, mice (swiss - male) received an intraperitoneal injection of 0.4% xylazine (Calmiun, Agner União, SP, Brazil) as a muscle relaxant and another intraperitoneal injection after 5 min, with 0.5 g/kg of ketamine and 2% xylazine (Holliday-Scott SA, Buenos Aires, Argentina) as the anesthesia. The animals were placed in a heating pad (controlled temperature 37 ºC), the scrotum was opened, the cremaster muscle was exteriorized, and to access the microcirculatory network a longitudinal incision was made on the muscle (144).

IntravitalMicroscopy (IVM) assay

With the muscle exposed, to count the number of rolling leukocytes, post-capillary venules with a specific diameter range is selected (25 to 40 μm) with Axiovision program v 4.8.2.0.

After determined the field with the venule, and after stabilization of the microcirculation, the basal number of rolling and/or adherent leukocytes in the venules were counted and considered as the control measure to rolling leukocytes. Then the topical application of 20 μL of the peptides (200 μM) was performed and the peptides' capacity to

induce mobilization of leukocytes along the vessel wall was evaluated every 10 min for 30 min, counting the number of rolling leukocytes. A rolling leukocyte was defined as a white cell that moved slower than the stream of flowing erythrocytes. The number of rolling leukocytes was quantified as the number of white cells that passed a fixed preset point during 1 min (145).

Fish Embryo Acute Toxicity (FET) Test – Toxicity in Zebrafish (Danio rerio) embryos

The experiment was performed in accordance with guideline No. 236 of the Organization for Economic Cooperation and Development (OECD) (146). Adult zebrafish (*Danio rerio*), AB strain (<18 months old) were maintained under standard laboratory conditions, in a 14h light and 10h dark cycle at a temperature of 28 °C. The peptides were diluted in E2 medium to a final concentration of 200 μM. For each peptide, three replicates were prepared on each plate (20 embryos). Viable embryos of zebrafish generated 30 minutes after fertilization were obtained and groups of five were placed to each plate of a 24 well plates (Costar® 24 Well Cell Culture Cluster, Corning Incorporated, NY, USA), containing 2 mL of the peptides' solutions. E2 medium was used as the control group. During the treatment, the development of the embryos was evaluated and mortality, defects on the morphological development or teratogenic effects were monitored for fluorescence microscopy (Leica M205C) every 24 h during 4 days (96 h after fertilization) (147). The experiments were performed in triplicates and at the end of every experiment, the zebrafish were euthanized. The statistical analyses of variances were performed through the one-way analysis of variance (ANOVA), results were significant when $p < 0.05$.

2.3.6 Mechanism of action

DNA Binding activity

To determine if the peptides were capable to act in a DNA-binding mechanism of action, a gel retardation assay was performed. Briefly, *E. coli* DH5α genomic DNA was purified using Landry's method (148), and 500 ng of DNA were incubated for an hour with 15, 30, 60, 120 and 240 μM of each peptide. After the incubation period, the content was submitted to gel electrophoresis on a 0.8% agarose gel (149).

2.4 Results

2.4.1 Schistosomicidal screening

After the 96 h incubation of the pair of parasites with the peptides FbPA at 84 µM, Triastin at 100 µM, TRP1-TINF at 128 µM, TRP2-TINF I at 164 µM, none of parasites' couples showed any alteration on the physiology. All of the worms were stayed alive, coupled and with normal motility. Thus, the peptides presented no antischistosomal activity (data not shown).

2.4.2 Antiviral assay

The experiment was held in three stages, each stage with a different peptide concentration, higher than the previous. The concentrations are listed on the section 1.3.3 (Methods – antiviral assays). Even on the highest concentration tested, the peptides were not able to inhibit the viral action of any virus over the cultured cells.

2.4.3 Cytotoxic assays

MTT assay

The cytotoxicity of the peptides was tested against VERO cell line (figure 11).

The most toxic pepetide was FbPA, which 47% toxicity was observed at the highest concentration (1000 µM). Cell viability was 53% after the incubation with 1000 µM of FbPA, but with 500 µM the cell viability was 100%, demonstrating no toxicity of the peptide at this concentration.

Triastine presented 16% toxicity in 1000 µM, with a cell viability of 84%, with 500 µM the toxicity decreased to 5% and at a concentration of 250 µM the peptide was no longer toxic, achieving a cell viability of 100%.

The peptides TRP1-TINF and TRP2-TINF also presented low levels of toxicity at 1000 µM, where TRP1-TINF was toxic to 16% of the cells and TRP2-TINF to only 10% of the cells. With a concentration of 500 µM TRP1-TINF was no longer toxic, but TRP2-TINF was toxic to 3% of the cells. TRP2-TINF toxicity decreased along with the concentration,

achieving 100% of cell viability at 62,5 µM, but as these toxicity levels represented lower than 3%, it is not relevant to the overall action of the peptide.

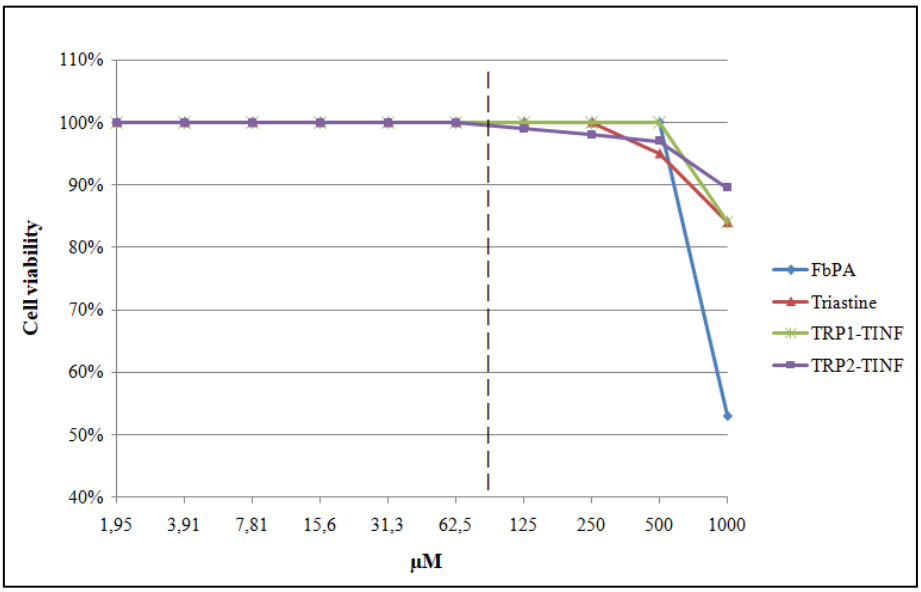

Figure 11 – Cell viability of VERO cells after 24 h incubation with the tested peptides.
Percentage of viable VERO cells after 24 h incubating with FbPA (in blue), Triastine (in red), TRP1-TINF (in green) and TRP2-TINF (in purple). The cells were incubated with the peptides in twelve two-fold serial dilutions with final concentrations ranging from 1.95 to 1000 µM. The dashed line represents the average value of the maximum concentration necessary for antimicrobial activity.

Hemolytic assay

The experiment was assessed to verify if any of the peptides had on human erythrocytes at different concentrations, but none were able to disrupt hemoglobin membranes even at the highest concentration of 1000 µM, indicating that the peptide are not hemolytic (data not shown).

2.4.4 Intravital microscopy (IVM) assay

The results summarized on the figure 12 demonstrate interesting features presented by the topic application of 200 µM of each peptide over the cremaster muscle of mice.

The FbPA induced no alterations on the microcirculation network with a concentration of 200 µM. It did not alter the diameter of the vessels or recruited leukocytes do the site.

In opposition, the peptide Triastine presented an interesting activity. After the application of 200 µM of the peptide on the surface of the muscle it impaired the blood flow without forming thrombi. Before 10 minutes from the topic application of the peptide, it had totally interrupted the blood flow on all the post-capillary vessels. As the blood flow as

interrupted, it was not possible to count the number of rolling leukocytes and that is the reason why this peptide was not included on the figure 12.

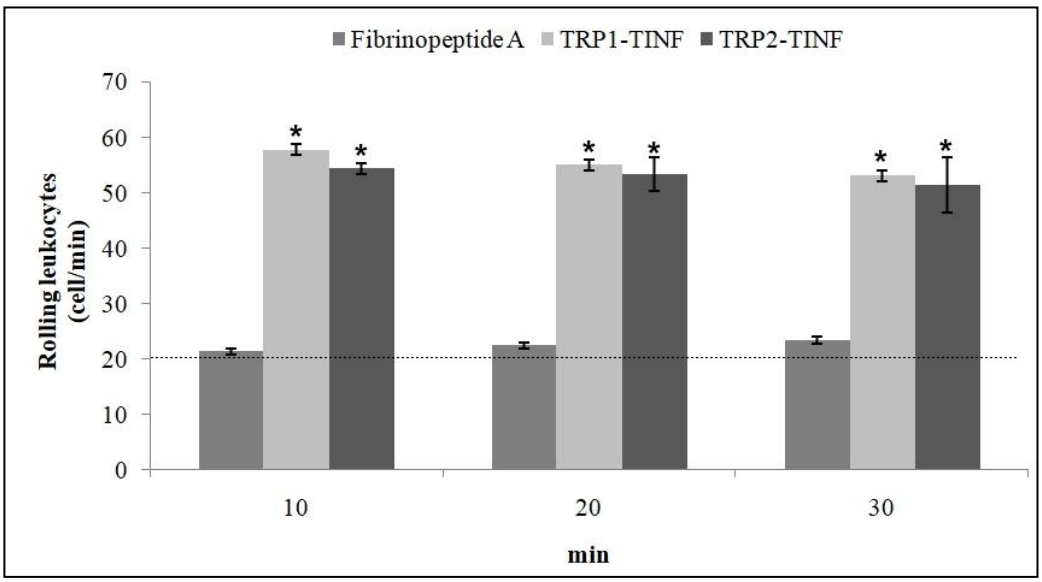

Figure 12 – Evaluation of rolling leukocytes with intravital microscopy.
The basal number of leukocytes is represented by the dashed line. Represented in shades of grey are the peptides FbPA, TRP1-TINF and TRP2-TINF after 10, 20 and 30 minutes of topic application on the cremaster muscle. (*) marks the significant results on statistic analysis ($p<0.05$).

Another interesting response was obtained after the application of the tachykinin-related peptides (TRP1-TINF and TRP2-TINF). Both peptides induced a considerable augmented number of leukocyte rolling in the venules at 10 min (over three times the basal number of leukocytes) with the topical application of 200 µM. This increased cellular mobilization characterized was maintained along the experiment, until 30 min, but it did not induced leukocytes adhesion or transmigration, which are the culmination of leukocyte recruitment (150).

2.4.5 Fish Embryo Acute Toxicity (FET) Test

To evaluate if the peptides are toxic for Zebrafish embryos at 200 µM during the stages of the development, the peptides were incubated with the embryos 30 minutes post-fertilization.

According to the embryos mortality observed daily through 96 hpf (figure 13A) it was possible to infer the peptides toxicity. Triastine was the most toxic peptide that until 24 hpf it did not interfere on the embryos development but it was lethal to 100% of the embryos on the period between 24 and 72 hpf, were several dead hatched larvae (figure 13C) and unhatched darkened embryos were observed (data not shown).

TRP1-TINF was also lethal to 100% of the sample but only 96 hpf. During the entire incubation period the mortality was comparable to the control group (incubated with E2 medium), but several malformations were visible on the embryos (data not shown).

TRP2-TINF was the least lethal peptide with mortality rates at 35%. Although the mortality was not significant in comparison with the control group ($p>0.05$), almost 40% of the embryos developed correctly (figure 13B), but the other presented late development (figure 13 D) cardiac and tail malformations, pericardial and yolk sac edema (figure 13E).

Due to the small amount of the sample, FbPA was not included on the experiment. As only one concentration was evaluated for each peptide it was not possible to determine LC_{50}.

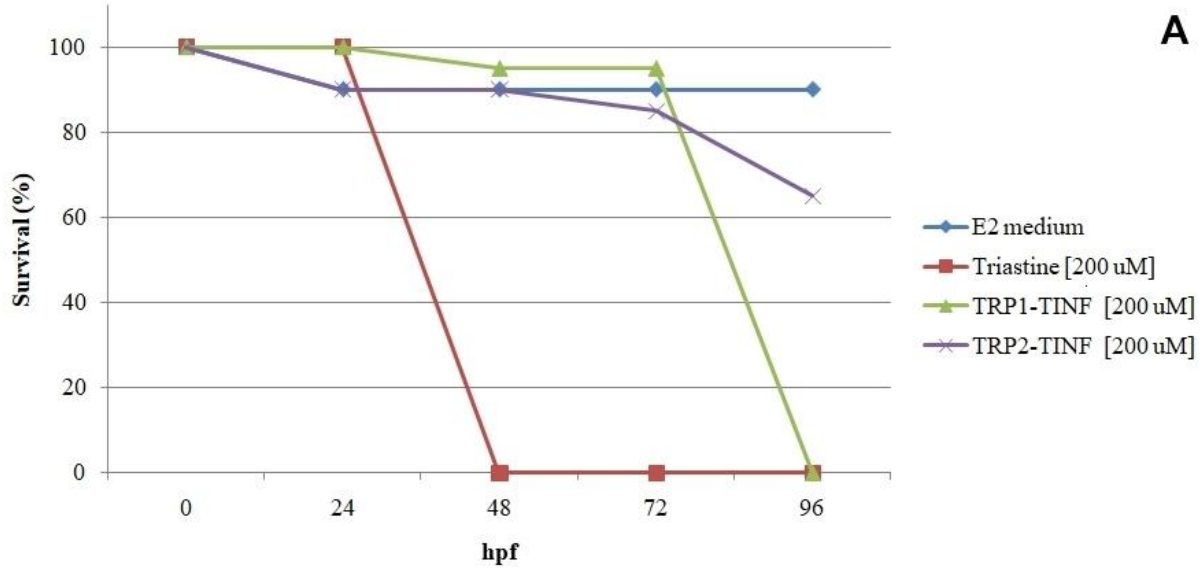

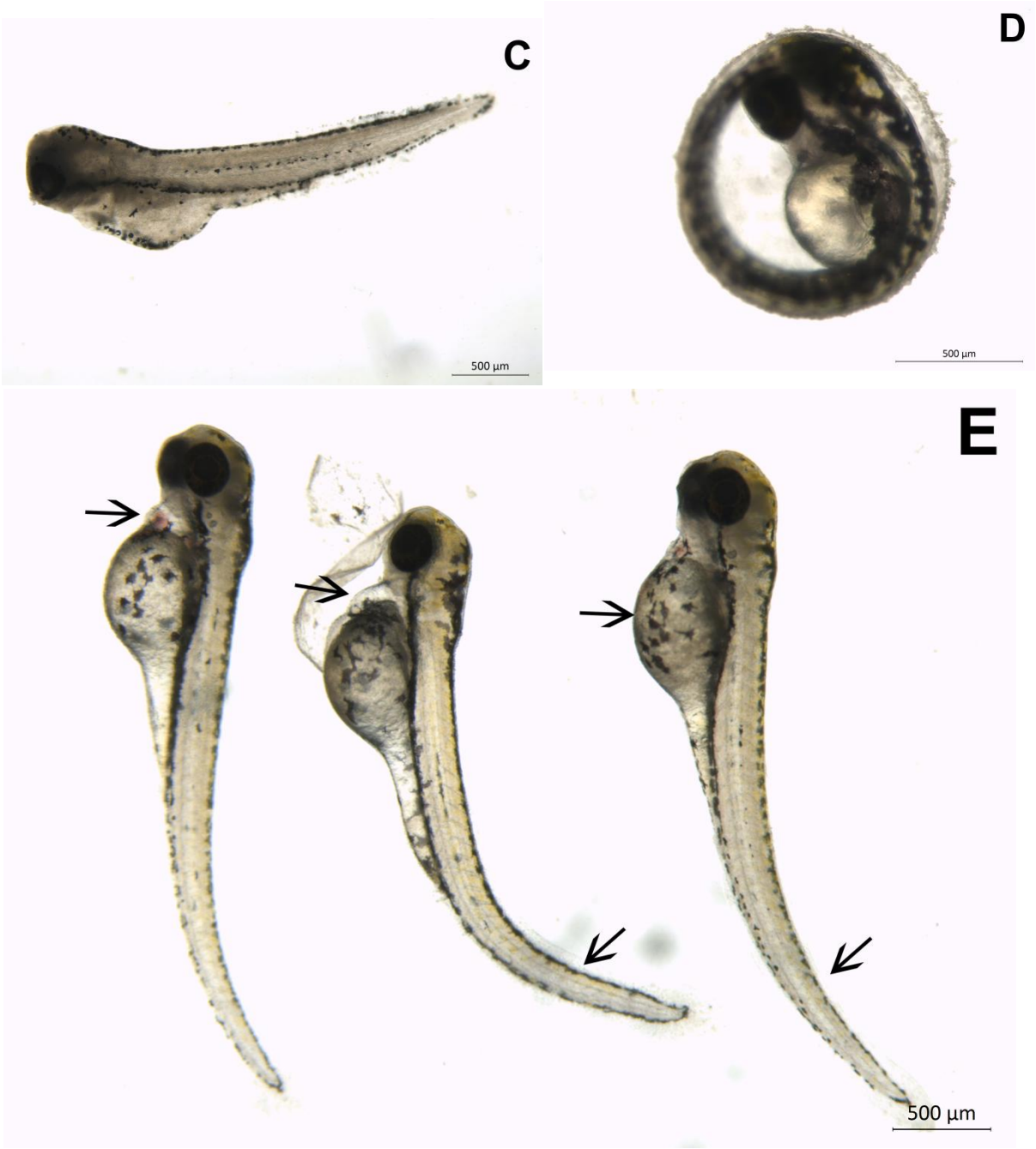

Figure 13 – Fish Embryo Acute Toxicity (FET) Test.
A) Graphical demonstration of *Danio rerio* embryos survival after 24, 48, 72 and 96 hpf incubated with the tested peptides at 200 µM. B) Healthy larvae after 96 hpf incubated with TRP2-TINF [200 µM]. C) Dead hatched larvae 96 hpf incubated with TRP1-TINF [200 µM]. D) Embryo with late development 96 hpf incubated with TRP2-TINF [200 µM]. E) Malformations on the larvae after 96 hpf incubated with TRP2-TINF [200 µM], marked with the arrows are the cardiac and tail malformations, pericardial and yolk sac edema.

2.4.6 Mechanism of action

The gel retardation assay was conducted to verify whether the peptides activity was due to DNA binding (figure 14).

Of the four peptides, only FbPA was able to interfere on the electrophoretic migration pattern of the genomic DNA at 60, 120 and 240 µM. This indicates that the antimicrobial mechanism of action of the peptide could be through DNA binding, thus inhibiting the processes involving nucleic acids (e.g. replication and transcription) (151).

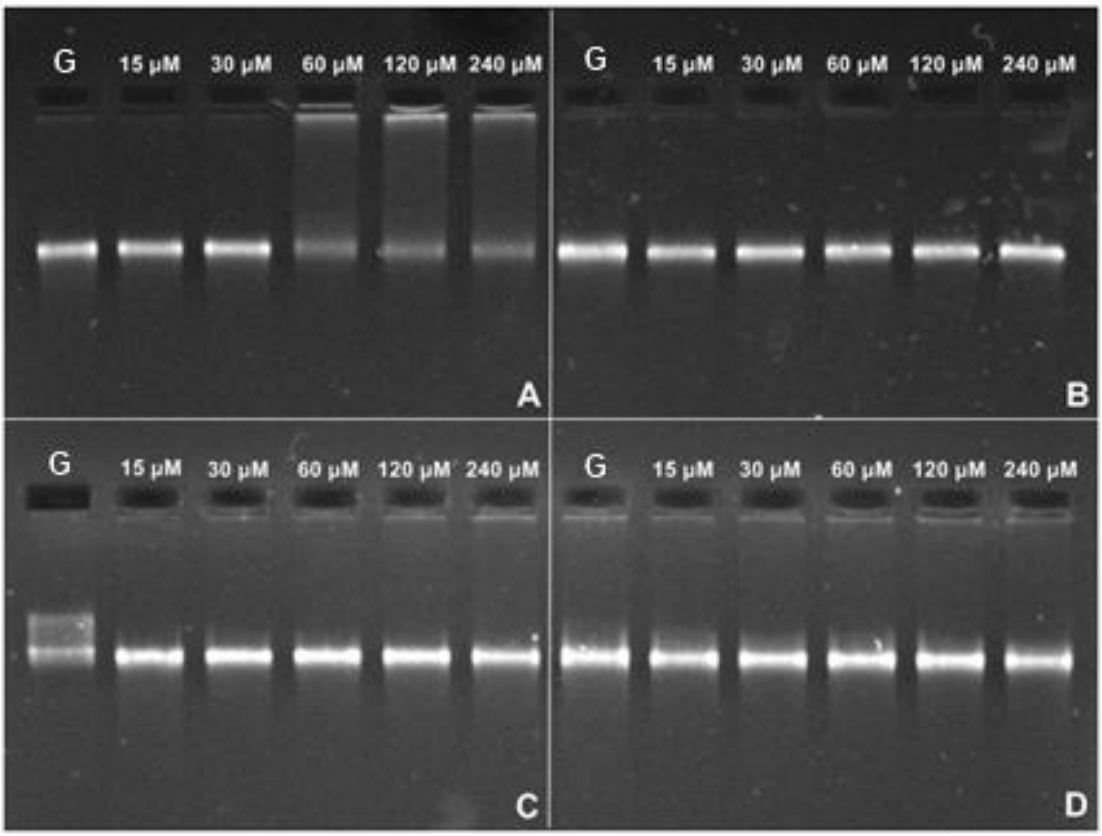

Figure 14 – DNA biding assay.
Assay to verify mechanism of action of the tested peptides. The letter G indicates the genomic DNA control without incubation with peptides. A) DNA-FbPA interaction, where the peptide interrupts the DNA migration at 60, 120 and 240 µM. B) Triastine incubated with DNA 15, 30, 60, 120 and 240 µM, the peptide was not able to interact with de bacterial DNA. C) TRP1-TINF incubated with DNA 15, 30, 60, 120 and 240 µM, the peptide was not able to interact with de bacterial DNA. D) TRP2-TINF incubated with DNA 15, 30, 60, 120 and 240 µM, the peptide was not able to interact with de bacterial DNA.

2.5 Discussion

Nowadays the drugs available for the treatment of schistosomal infections on the American and African continents are Praziquantel that is derived from a compound entitled Pyrazinoisoquinoline, and Oxamniquine, derived from 2-aminomethyltetrahydroquinoline (152).

Praziquantel is the first drug of choice on the treatment of schistosomiasis, either for individual treatment or massive infections, due to its high efficiency, low toxicity and cost (153, 154). The concern of treatments based on one drug only rises again on this case, the

appearance of resistance. Even though the dose-dependent effect is still in discussion, there have been studies associating the interaction and potentiation of effects by association with anthelmintic drugs, such as Albendazole and Mebendazole (155, 156).

As soon as the possibility of resistance is glimpsed, emerges the need of alternative drugs. New researches already have been describing good candidates to alternative medicine using methods very similar to our experiments. The drug Piplartine (157), in opposition to our peptides, were lethal to 100% of the worms after 72 h incubation with 9.5µM. There are other compounds that also presented success on the *S. mansoni* treatment, but using different approaches, like the compound vinyl sulfone cysteine protease inhibitor K11777, which was tested in murine models and was capable to obtain parasitologic cure with the absence of eggs, thus retarding egg-associated pathology in organs (158).

As our initial experiment tented the peptide in the maximum concentration allowed, there was no need to repeat the experiment with other concentrations of the peptides. Therefore, FbPA, Triastine, TRP1-TINF and TRP2-TINF are not effective to treat *Schistosoma mansoni* infections.

On the current pharmaceutical market, although there are antiviral drugs and vaccines available, there is a small number of infections and virus which they are totally effective against (159). One of the reasons is the specificity of the new drugs developed, that hinders the possibility of one drug to act over different infections. Thus, there is the necessity to develop new drugs through antiviral screenings with multiple viruses.

Measle virus has a characteristic that the non-structural proteins F and H induce cell membrane fusion. This leads to the appearance of giant and multinucleated cells (up to 50 nucleuses or more) or syncytia (160). This fusion effect happens until a maximum stage where these giant cells disrupt, resulting in leakage of intracellular content with new viral particles, reinitiating the infection process.

The other two effects induced by measle virus are correlated. The cell penetration of viral particles and the release of transcription and replication machinery on the cytoplasm induce the formation of inclusion bodies (IB) (161, 162). IB are specific spots on the cytoplasm where the transcription and replication takes place, producing new viral particles. Infected cells that present IB tends to acquire mix sizes and shapes (162).

The VERO cells on the performed experiments acquired spindle, starry or dendritic shapes, in addition to having a greater light refringence, on both infected and treated groups, demonstrating that the peptides were not effective (data not shown). All the cells on the

toxicity controls were comparable to the control cells, indicating no toxicity even after 96 h incubation at these peptides' concentrations.

Currently, the unique effective treatment for measle viruses available is vaccination. Some drugs on production stages have been described with interesting effects over viral polymerases and inhibiting cellular fusion (163-165). Recent studies focusing on AMPs with antiviral activity (now called antiviral peptides - AVPs) (166) have demonstrated that some AMPs present activity over measle virus (167, 168), but the number of these works are still very low compared with AVPs over hepatitis C, herpes or HIV (166, 167, 169, 170). Continuing, the viruses from the *Picornaviridae* family are some of the smallest particles, with non-enveloped particles with 30 nm diameter, containing single stranded RNA (171). The cytopathic effect is due to cell death induction through apoptosis. The virus uses the cell machinery to produce its own mRNA and proteins, blocking the overall cell production. This leads to formation of vacuole on the nucleus, membrane vesicles and apoptotic bodies due to alterations on membrane permeability and loss of intracellular content (171, 172).

After the incubation period, the VERO cells on the infected and treated groups of the experiment presented the alterations mentioned above, with the withered aspects due intracellular loss on both infected and treated groups, demonstrating that the peptides were not effective (data not shown). All the cells on the toxicity controls were comparable to the control cells, indicating no toxicity even after 96 h incubation at these peptides concentrations.

Even with descriptions of less complex active molecules from biological extracts (173, 174), some of the main antiviral activities against *Picornaviridae* family viruses are complex molecules such as prostaglandins, interferons and derivates (175-178).

CHIKV induces a lytic effect while ZIKV induces mainly vacuolization on the infected cells (179, 180). Studies have shown that Brazilian ZIKV strains tend to be more aggressive, with higher cytopathic effects when compared to other international strains (181), demonstrating the importance of researches for new products that can overcome this effect.

As more recent emerging viruses, most of the works regarding antiviral activities against ZIKV and CHIKV are recent descriptions of new features of known molecules (182-188), and as there is no specific treatment or vaccine, the need to identify effective compounds increases the number of researches every day.

The molecules described on previous works against measle and ZIKV viruses presented activity in concentration of approximately 5 µM (173, 184), against CHIKV in a concentration of approximately 10 µM (186) and against *Picornaviridae* family viruses

described activities in a concentration range of 40-60 µM approximately. Our samples were not effective nor at that or higher concentrations, confirming the lack of antiviral potential by the tested peptides.

All the peptides presented antimicrobial activity in a lower concentration that they presented some levels of toxicity, indicating that they are safe samples to work *in vitro* as antimicrobial agents.

Verifying the hemolytic activity is crucial while investigating new drug candidates because to achieve the action site, the drug must be carried through the circulatory system. High concentrations of the molecules need to be tested considering bioavailability so a specific concentration can arrive without degradation on the infectious site (125).

IVM was used to evaluate two connected factors. First, alterations on the microcirculatory network are observed, and second the toxicity for the cremaster muscle due to topic application of the peptides (189).

Fibrinopeptides (both A and B) are molecules formed at the last cleavage step of the clot formation pathway on the vertebrates immune system. The cleavage of a specific Arg-Gly bond at the fibrinogen C-terminus by the thrombin results in the release of FbPA and FbPB (122). Thus, as the peptide is a natural blood component on vertebrates, it was expected that it would not impact the microcirculation network.

There are three main parameters that can alter the resistance to blood flow, that are vessel diameter, blood viscosity and arterial length (190). As for the peptide Trisatine as there was no blood flow, no thrombi formed and no alterations on the diameter of the vessel or the arterial length, we cannot infer that the peptide has influence on one of these parameters.

Blood vessels are basically composed by elastic fibers, connective tissue, smooth muscle cells. The proportion of each tissue and thickness of the wall depends on the vessel. Venules are small post-capillary vessels with thin wall and sphincters between capillaries and venules (191). The blood flow on the venules are determined by the muscle contraction from both vessel smooth cells and the skeletal muscle that surrounds the vessel (191), all correlated with rigid control from the sympathetic/parasympathetic nervous system, which is responsible for the vascular tone control.

One possible effect that can justify the activity of Triastine, causing the absence of blood flow without forming thrombi, is the block of muscular contraction, leading to stiffness of the vessel, blocking the blood flow. The peptide might be interfering directly on the muscle

contraction or indirectly on the nervous signal to the muscle (192, 193).

Without further experiments it is not possible to determine the exact nature of the interaction between the peptide and the vessel environment. It is known that this peptide suffers degradation by amino and carboxypeptidases, but even with the action of two types of enzymes it is not easily degraded (42). The half-life in plasma of the peptide is approximatelly 2 h, and as the experiment had a 30 minute duration, it is still unknown if the action is reversed after the initial degradation of the peptide.

As demonstrated for the peptides TRP1-TINF and TRP2-TINF, they generate an increase on the number of rolling leukocytes. Although the level of cytokines and chemokines were not evaluated, the leukocyte recruitment is a typical response of acute inflammation that can occur within minutes apart from the initial stimuli (150, 194) via PSGL-1/L-selectin, while leukocytes adhesion occurs via β2 integrins (195). The rolling step of the leukocyte recruitment is reversible, as soon as the stimulus that induces the expression of selectin ligands (PSGL-1, L-selectin) stops, the expression stops and consequently the rolling also stops (150, 196).

As the peptides did not induce cell adhesion, it is possible that the stimulus that they represented to the tissue was comparable to an initial stimulus for acute inflammation, thus being considered as pro-inflammatory molecules.

These results are preliminary but already provided very important information regarding the four molecules, and that leads us towards new possibilities of researches.

In vivo toxicity assays are required during the screening process for new drugs. It is complementary to *in vitro* tests and represents a large step towards specific knowledge on the safe concentration for each drug tested (125).

Zebrafish (*Danio rerio*) have become a growing applicable model on biomedical research due to its transparent embryos that allows the researcher to see through every development step (197), and all in a small period of time, because within 72 h post-fertilization (hpf) the embryonic stage is already ending and starting the larval stage (198).

Since the early 70's the zebrafish (*Danio rerio*) has been used for different researches fields including neuronal cell proliferation (199), hormone interactions (200), behavioral model (201), cancer (202, 203), among others (204). A relevant field among them is the use of zebrafish as an *in vivo* model on new drug development studies, mainly for toxicity tests (128, 205-209).

Even though it has been demonstrated to be a powerful tool on these researches,

investigations on AMPs toxicity using zebrafish models are still scarce (210-214). This work is the first to use zebrafish toxicity assay on AMPs isolated from triatomines.

Results demonstrating the level of toxicity of new drugs are very important because they demonstrate that adjustments are required in order to set the levels of biological activity without interfering negatively on the organism used. The three peptides evaluated on the experiments demonstrated high levels of toxicity, indicating that they cannot be administered yet as an antimicrobial drug in living organisms. Probably will be necessary to alter the amino acid composition to obtain molecules with the same potency and lower toxicity.

Although the results presented indicates the FbPA's mechanism of action, there are no indication for the other peptides. There are complementary methodologies that can be used to determine if the mechanism of action of Triastine, TRP1-TINF and TRP2-TINF is through RNA, proteins or membrane interactions (215, 216). Diniz (2016) performed giant unilamellar vesicles assays with the four peptides, but the results obtained were inconclusive on the conditions applied on the test.

The initial studies on AMPs believed that the peptides interacted only with membrane surfaces and that they could not have intracellular targets (217), but further studies revealed that in low concentrations some peptides could not interact with membranes but still caused microbial death (76). Important discoveries on the field of AMPs' mechanism of action were made since then, which resulted on the discovery of several different mechanisms (76, 90, 91, 218).

2.6 Conclusion

In conclusion the work demonstrated that the peptides have interesting antimicrobial activity and are indeed potential new drugs, but need improvement towards the toxicity presented.

Although the peptides seemed promising for other activities, they did not present biological activities beyond the antimicrobial potential and presented different levels of toxicity, thus further studies need to be performed.

3 – Chapter 2

Human antimicrobial peptide isolated from *Triatoma infestans* hemolymph, *Trypanosoma cruzi* - transmitting vector

This chapter is a description of the study regarding the identification of the source of the human Fibrinopeptide A with antimicrobial activity isolated on the hemolymph of *Triatoma infestans*.

Paper published on Frontier in Cellular and Infection and Microbiology. doi: 0.3389/fcimb.2018.00354

3.1 Objective

The aim of this work was to determine the source of the human Fibrinopeptide A (FbPA) isolated from the Chagas disease-transmitting vector *T. infestans* haemolymph.

3.2 Materials and Methods

The experiments were performed under the exemption of the Animal Research Ethics Committee (CEUAIB—Comitê de ética no uso de animais do Instituto Butantan) n◦ I-1345/15, and approval from the "*Plataforma Brasil*", nº 3.432.972 ("*Plataforma Brasil*" is a national and unified database of research records involving human beings for the entire ethics committee system).

3.2.1 Bacterial Strains

The microorganisms *Micrococcus luteus* (strain A270), *Staphylococcus aureus* (ATCC 29213), *M. luteus* (Nalidixic resistant), *Bacillus megaterium* (ATCC 10778), *Bacillus subtilis* (ATCC 6633), *Escherichia coli* (SBS363), *Enterobacter cloacae* b-12, *Alcaligenes faecalis* (ATCC 8750), *Serratia marcescens* (ATCC 4112), *Pseudomonas aeruginosa* (ATCC 27853), *Candida parapsilosis* (IOC 4564), *Candida albicans* (IOC 4558), *Cryptococcus neoformans*, *Saccharomyces cerevisiae*, *Candida tropicalis* (IOC 4560), *Cladosporium sp*. (bread isolated), *Penicillium expansum* (bread isolated), *Aspergillus niger* (bread isolated), *Paecilomyces farinosus* (IBCB-215), and *Cladosporium herbarum* (ATCC 26362) were

obtained from the Special Laboratory of Toxinology, Butantan Institute (São Paulo, Brazil).

3.2.2 Animals

Triatoma infestans were obtained from the Ecolyzer Group Entomology Laboratory and kept alive in the vivarium of the Special Laboratory of Toxinology, Butantan Institute (São Paulo, Brazil) at 37◦C and fed every 2 weeks with human blood from a healthy volunteer donor, in the presence of citrate buffer (150 mM, pH 7,4) (219).

3.2.3 Bacteria Inoculation and Hemolymph Collection

One week after blood feeding, adult *T. infestans* were injured with needles soaked in an *E. cloacae* and *M. luteus* pool, both at logarithmic-phase growth. After 72 h, 300 μL of hemolymph was collected by excising the metathoracic legs and pressing on the abdomen of the *T. infestans* (Boman et al., 1974) (116) in the presence of phenylthiourea (PTU), to avoid the activation of the phenoloxidase cascade, and stored at −80◦C until use.

3.2.4 Sample Fractionation

Acid and Solid-Phase Extractions

To release the contents of the hemocytes, the sample was incubated in acetic acid (2 M) for 5min and centrifuged at 16.000 × g for 30min at 4◦C. The supernatant was injected into coupled Sep-Pack C18 cartridges (Waters Associates) equilibrated in 0.1% trifluoroacetic acid (TFA). The sample was eluted in three different acetonitrile (ACN) concentrations (5, 40, and 80%) and then concentrated and reconstituted in ultrapure water.

Reverse-phase high-performance liquid chromatography (RP-HPLC)

RP-HPLC separation was performed with a C18 column (Jupiter, 10 × 250mm) equilibrated with 0.05% TFA. The elution gradient for the 5% ACN fraction was 2%to 20%(v/v) of solution B (0.10% (v/v) TFA in ACN) in solution A (0.05% (v/v) TFA in water). For the 40% ACN fraction, the gradient was 2–60% of solution B in solution A, and for the

80% ACN fraction, the gradient was 20–80% of solution B in solution A.

The gradient was performed for 60 min, at a 1.5 mL/min flow rate. Effluent absorbance was monitored at 225 nm, and the fractions corresponding to absorbance peaks were hand collected, concentrated under vacuum, and reconstituted in ultrapure water.

When necessary, a second chromatographic step was performed on a VP-ODS analytic column (Shim-pack®), with a 1.0 mL/min flow rate gradient for 60 min. This was performed to guarantee sample homogeneity. The gradients for these second chromatographic stages were determined by the target molecule's elution ACN concentration, applying a gradient range variation of 10% including the percentage of the molecules elution (e.g. molecule eluted with 50% ACN, thus the gradient of the second chromatographic step 45-55% ACN).

3.2.5 Liquid Growth Inhibition Assay

The antimicrobial assay was performed against all the microorganisms listed previously on the section Bacterial Strains, using poor broth nutrient medium (PB: 1.0 g peptone in 100 mL of water containing 86 mM NaCl at pH 7.4; 217 mOsM) and Müller-Hinton medium (peptone 5.0 g/L; casein peptone 17.5 g/L; agar 15.0 g/L; Ca^{2+} 20.0–25.0 mg/L; Mg^{2+} 10.0–14.5 mg/L; pH 7.4) for bacteria and potato dextrose broth (1/2 PDB: 1.2 g potato dextrose in 100 mL of H2O at pH 5.0; 79 mOsM), and RPMI 1640 (Roswell Park Memorial Institute medium) medium with MOPS 0.165 mol/L [RPMI without bicarbonate 10.4 g/L; MOPS (3-(n-morpholino) propanesulphonic acid) 34.53 g/L; pH 7.0] at half-strength for fungi (220, 221)

Antimicrobial activity was determined using a five-fold microlitre broth dilution assay in 96-well sterile plates at a final volume of 100 μL. A mid-log-phase culture was diluted to a final concentration of 1×10^5 colony-forming units/mL. The dried fractions were dissolved in 500 μL of ultrapure water, and 20 μL of this was added to each well. We then added 80 μL of microorganism dilution. To determine the minimal inhibition concentration (MIC), the bacterial growth rates were measured after 18 h incubation. To determine the minimal bactericidal concentration (MBC), the bacterial growth rates were measured after 96 h at 595 nm (222, 223)

3.2.6 Mass Spectrometry (LC/MS)

Mass spectrometry analysis was performed on an LTQ XL (Thermo Scientific). The

equipment was previously calibrated with the following substances: caffeine (m/z 194.5), L-MRFA acetate in water (m/z 524.3), and Ultramark 1621. Ovalbumin was used as molecular weight control (43 kDa). The samples were concentrated and diluted in 15 μL 0.1% formic acid (FA). For the liquid chromatography, a C18 column (Waters) was used with an ACN gradient linear from 0 to 80% in acidic water (FA 0.1%) during 60min at a 400 nL/min flow. The spectrometer was set to a positive parameter.

3.2.7 Computational Analysis

Mass spectrometry data were analyzed with Xcalibur 5.0 (Thermo Electron, EUA) and Mascot Deamon® version 5.4.2, using Swiss-Prot and NCBInr Insects, Hemipteran, Triatomines and Fibrinogen banks for database comparison.

The homology searches for possible results were performed on the following databases: ArachnoServer Spider Toxin Database www.arachnoserver.org; The Arthropoda PartiGeneDatabases www.nematodes.org/NeglectedGenomes/; ARTHROPODA; PepBank pepbank.mgh.harvard.edu; Vector Base pepbank.mgh.harvard.edu; APD2: Antimicrobial Peptide Calculator and Predictor and BLAST (NCBI), aps.unmc.edu/AP/main.html. The data were also analyzed through PEAKS® (Bioinformatics Solutions Inc.) with Insects, Hemipteran, Triatomines, and Fibrinogen databases obtained on UniProt (www.uniprot.org, 1243446; 133071; 31334; and 12342 sequences, respectively, March 25th, 2015). The results were considered valid only when they were reproducible in a different analysis.

3.2.8 Solid-Phase Peptide Synthesis

Peptides were synthesized by the solid-phase method (224), using a methylbenzhydrylamine resin (MBHAR) and employing the t-Boc strategy. After cleaving the peptides from the resin, peptides were purified from the lyophilized crude solutions by HPLC on a C18 column. To guarantee high purity and to characterize the peptides, LC-ESI-MS equipment was used.

3.2.9 Synthetic Peptide Concentration

Peptide concentrations were determined by using the Lambert–Beer law using the molar extinction coefficient at 205 nm absorption (225), obtained using the tool available at

http://nickanthis.com/tools/a205.html.

3.2.10 Internalization Assays

Preparation of Fluorescein Conjugate

Fluorescein isothiocyanate (FITC) isomer I (Sigma-Aldrich®) was used by following the protocol provided by Sigma-Aldrich®. FITC was dissolved in dry DMSO at a concentration of 1 mg/mL and protected from light. For coupling, 150 μL of FITC solution was added, 5 μl at a time, to the synthetic FbPA solution (2mM) and kept for more than 8 h at 4◦C in the dark. Ammonium chloride was added to a final concentration of 50mM and incubated for 2 h to quench the reaction. The FITC–FbPA conjugate was then purified [Methods section: Acid and Solid Phase Extractions and Reverse Phase High-Performance Liquid Chromatography (RP-HPLC)].

Blood feeding and hemolymph extraction containing the fluorescein conjugate

After the purification, 3 mg of the conjugated FbPA were diluted in 4mL human blood and offered to the insects (219). The hemolymph from the engorged animals without bacterial challenge was collected 72 h after the blood feeding and then submitted to fluorescence measurement and purification [Methods section: Acid and Solid Phase Extractions and Reverse Phase High-Performance Liquid Chromatography (RP-HPLC)]. The hemolymph of non-fed animals was also collected for fluorescence control comparisons.

Human Fibrinopeptide A Isolation

Human blood was extracted to a final volume of 10mL and incubated at 37◦C until complete clot formation. The clot and plasma obtained were macerated in the presence of PBS and centrifuged at 16,000 × g for 5min. The supernatant was filtered with polyvinylidene difluoride (PVDF) membrane filters (Merck Millipore®, 25 mm; 0.45μm) and then purified [Methods section: Acid and Solid Phase Extractions and Reverse Phase High-Performance Liquid Chromatography (RP-HPLC)]. The fraction corresponding to the human FbPA was isolated and submitted for antimicrobial assay (Methods section: Liquid Growth Inhibition Assay).

Fluorescence Measurements

The fluorescence evaluation was performed in a Perkin Elmer® Wallac 1420 VICTOR 2™ as triplicates nine times within a 15-min gap between them. The statistical analyses of variances were performed through the one-way analysis of variance (ANOVA) (single variant); results were significant when $p < 0.05$. When necessary, Thermo Scientific Nano Drop™ fluorescence measurements were performed. Both readings used a 495 nm filter for excitation and a 520–530 nm filter for emission.

3.3 Results

3.3.1 Purification/Isolation

Acid was extracted from the total hemolymph and, subsequently, via three sequential ACN elutions leading to the separation of the main sample into three different fractions according to the ACN concentration (Methods section: Acid and Solid Phase Extractions). During the 80% ACN fraction purification via HPLC, a fraction eluted at 34.4min. A fraction eluted at 34.4 min demonstrated antimicrobial activity and was completely isolated (figures 15 A,B).

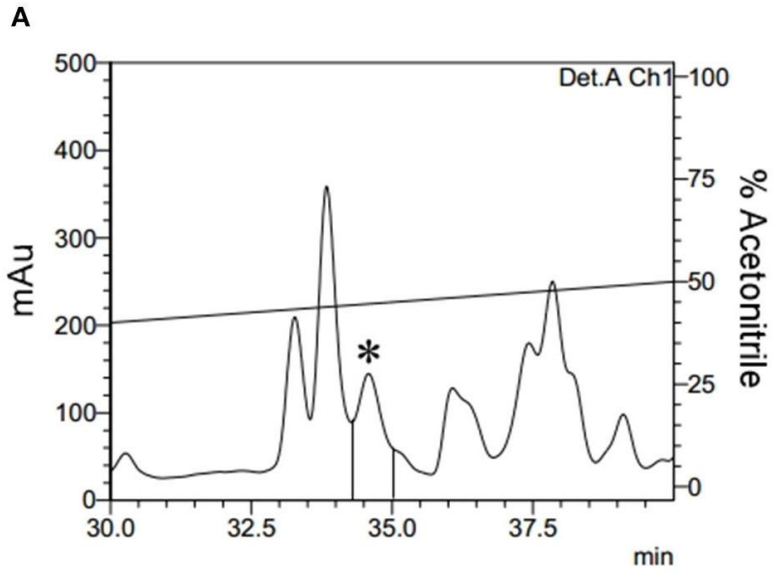

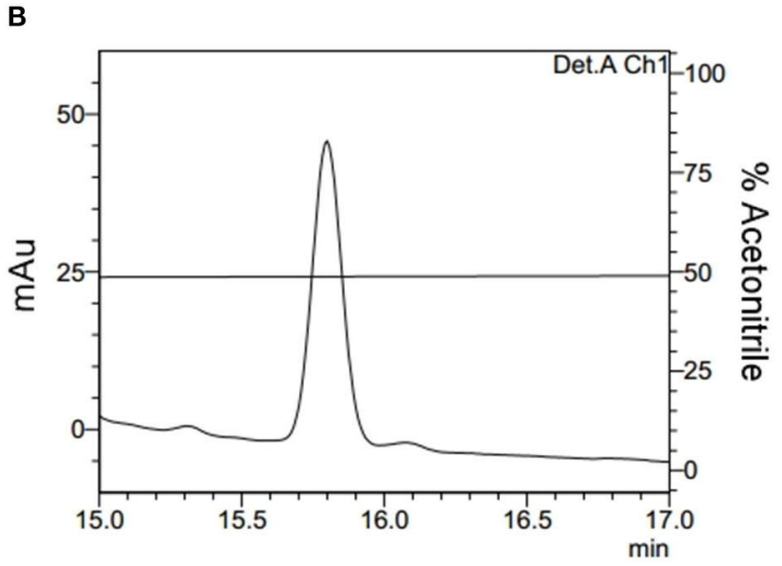

Figure 15 – Isolation of Fibrinopeptide A.
(A) The 80% ACN fraction isolated from *Triatoma infestans* hemolymph was separated by RP-HPLC using a C18 column, eluted with a linear gradient from solution A from 20 to 80% of the solution B run for 60min. The labeled fraction (*), eluted at 34.4min, exhibited antimicrobial activity and was submitted to a second chromatography step.
(B) The second RP-chromatographic step on an analytic VP-ODS column, with an ACN gradient from 47 to 57% solution B in 60min, to guarantee its homogeneity.

When analyzed using the MASCOT® software to search the Swiss-Prot database, mass spectrometry data from the isolated molecule showed high identity with the human fibrinogen alpha chain. The sequence obtained from Peaks software confirmed this result, demonstrating that the sequence obtained corresponds to the human FbPA located on the N-terminal portion of the alpha chain of human fibrinogen (Figure 16).

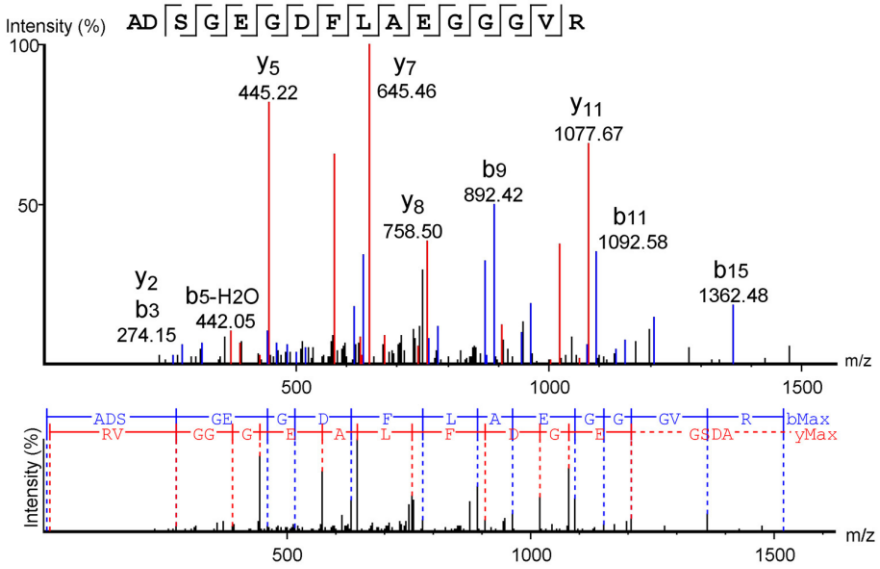

Figure 16 – Fibrinopeptide A mass spectrometry analysis.
Mass spectrometry data analysis from the software Peaks™, using the Swiss-Prot database as a comparison. The

y-series is represented in red, and the b-series in blue.

To confirm the results obtained with native human FbPA, human blood was processed (Methods section: Human Fibrinopeptide A Isolation) and the target fraction was isolated by HPLC (figure 17); this fraction also exhibited antimicrobial activity. Mass spectrometry data analysis from the isolated fraction (not shown) confirms the molecular weight present in the fraction to be equivalent to that expected for human FbPA, suggesting that the antimicrobial results are due to FbPA enrichment in this fraction.

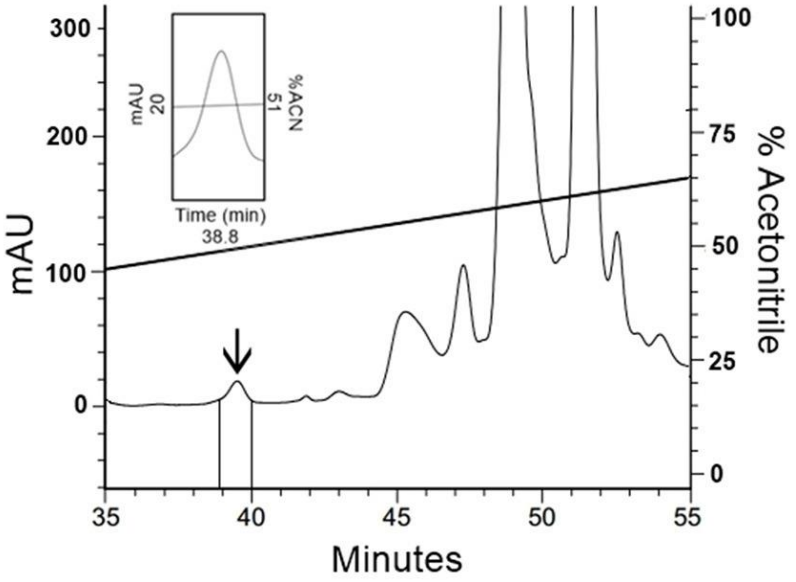

Figure 17 – Isolation of human Fibrinopeptide A.
The extract from coagulated human blood was separated by RP-HPLC using a C18 column, eluted with a linear gradient from solution A from 20 to 80% on solution B run for 60min. Expanding the chromatogram, it is possible to see the fraction labeled with an arrow, eluted at 38.8min, that corresponds to FbPA.

3.3.2 Antimicrobial Activity

The major antimicrobial activity of the human FbPA isolated from the *T. infestans* hemolymph when tested via the liquid growth inhibition assay was against *M. luteus* (A270) at 0.002– 0.005 mg/mL concentrations. Due to the small amount of the native FbPA isolated from human blood, it was tested directly against *M. luteus* and exhibited activity in the same concentration range.

FbPA was synthetized to supply the amount of native sample obtained from the HPLC purifications. As a matter of comparison, the synthetic FbPA and the FITC–FbPA conjugate were also tested against *M. luteus* (A270); the first was active at 0.06–0.12 mg/mL and the second at 0.01–0.02 mg/mL (table 1), indicating a decrease on the antimicrobial potential of

the synthetic molecules.

Table 1 | Antimicrobial activity concentrations.

Microorganism	*Micrococcus luteus* A270			
FbPA source	*T. infestans*' haemolymph	Human blood	S-FbPA	S-FbPA+FITC
Concentration (mg/mL)	0.002–0.005	0.002–0.005	0.04–0.08	0.01–0.02

Minimal interval concentration required for natural and synthetic molecules to exhibit activity against Micrococcus luteus A270. S-FbPA, the synthetic peptide; S-FbPA+FITC, the synthetic peptide–fluorescein conjugate.

The synthetized FbPA was tested with a broad range of bacterial and fungal species and showed antimicrobial activity against *Pseudomonas aeruginosa*, *Escherichia coli*, *Candida parapsilosis*, *Cryptococcus neoformans*, *Candida tropicalis*, *Paecilomyces farinosus*, *Cladosporium sp*., and *Penicillium expansum*. Only those susceptible to FbPA's antimicrobial activity are listed in the table below (table 2).

Table 2 | Synthetic fibrinopeptide A's antimicrobial activities against bacterial and fungal strains.

Microorganism	MIC μM (mg/mL)		MBC μM (mg/mL)	
MEDIA	**MH**	**PB**	**MH**	**PB**
GRAM-POSITIVE BACTERIA				
Micrococcus luteus	NA[a]	42–84 (0.04–0.08)	NA	NA
GRAM-NEGATIVE BACTERIA				
Pseudomonas aeruginosa	NA	5.2–10.5 (0.005–0.01)	NA	NA
Escherichia coli	NA	5.2–10.5 (0.005–0.01)	NA	NA
MEDIA	**RPMI**	**PDB**	**RPMI**	**PDB**
EASTS				
Candida parapsilosis	NA	42–84 (0.04–0.08)	NA	NA
Cryptococcus neoformans	NA	42–84 (0.04–0.08)	NA	NA
Candida tropicalis	NA	5.2–10.5 (0.005–0.01)	NA	5.2–10.5 (0.005–0.01)
FILAMENTOUS FUNGI				
Cladosporum sp.	42–84 (0.04–0.08)	42–84 (0.04–0.08)	NA	42–84 (0.04–0.08)
Penicilium expansum	42–84 (0.04–0.08)	42–84 (0.04–0.08)	NA	42–84 (0.04–0.08)
Paecilomyces farinosus	NA	42–84 (0.04–0.08)	NA	42–84 (0.04–0.08)

Minimal inhibition concentration (MIC) and minimal bactericidal concentration (MBC) values obtained on the

liquid growth inhibition assay. NA, not active on a concentration of 84μM. PB, poor broth nutrient medium; MH, Müller-Hinton medium. PDB, potato dextrose broth medium; and RPMI, Roswell Park Memorial Institute medium

The synthetic FbPA concentrations effective as an antimicrobial varied according to the microorganism class. The main bacteriostatic activity was against *P. aeruginosa* and *E. coli*, at 0.005–0.01 mg/mL in the PDB medium. The main fungicidal activity was against *Cladosporium sp*. and *P. expansum*, both at 0.06–0.12 mg/mL n the RPMI medium and *C. tropicalis* at 0.005–0.01 mg/mL in PDB medium. These results prove that FbPA has a potent and effective antimicrobial activity against different microorganisms.

3.3.3 Internalization Assays

After confirming that the isolated molecule had 100% homology to the human FbPA and confirming that all of the isolated and produced FbPA had similar antimicrobial activity, our next step was to verify the origin of the molecule isolated from the *T. infestans* hemolymph. To carry out this, the synthetic FbPA was coupled to a fluorescent probe (FITC) and the insects were fed with blood containing incremental amounts of the FITC–FbPA complex.

3.3.4 FITC–FbPA Coupling Confirmation

First, to verify the FITC–FbPA coupling and its fluorescence, the complex was examined via NanoDropTM scan. The conjugate presents one FITC molecule for each FbPA sequence, confirming the coupling (data not shown). The fluorescence scan shows that the complex has a significant emission.

3.3.5 Internalization

To confirm the hypothesis of FbPA internalization by the T. infestans, the insects were fed with human blood containing the fluorescent FITC–FbPA conjugate and their hemolymph was collected and analyzed.

After feeding the insects with blood containing the FITC– FbPA conjugate, the hemolymph was collected from both engorged and non-fed insects for general fluorescence evaluation, verifying if the insect was able to absorb the fluorescently labeled peptide (figure

18).

We observed the expected difference between the hemolymphs: the engorged insect's hemolymph exhibits a higher absorbance, comparable to the positive control (FITC– FbPA conjugate), while the non-fed insect's hemolymph showed no absorbance. This demonstrates that at least part of the conjugate was absorbed by the insects. Based on this, the hemolymph with fluorescence was tested by HPLC as previously described [Methods section: Reverse Phase High-Performance Liquid Chromatography (RP-HPLC)] to isolate the internalized conjugate.

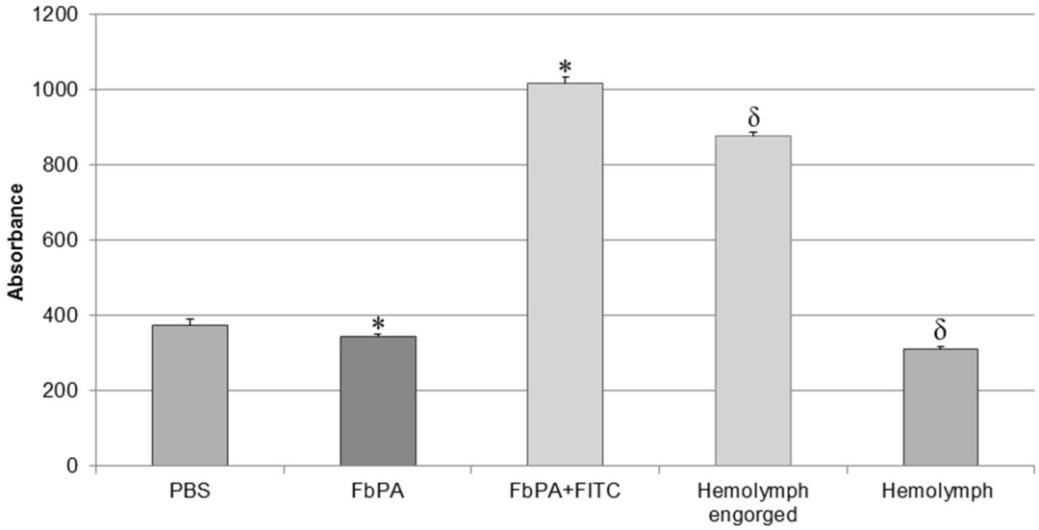

Figure 18 – Comparison of hemolymph fluorescences.
Comparison of the hemolymphs of engorged and non-fed insects. Through excitation with 495 nm, it is possible to observe the significant difference between the synthetic FbPA and the FITC–FbPA conjugate (*p = 3.84−17), as previously shown. The hemolymph of the engorged insects also has a significant difference when compared to the hemolymph of non-fed insects (_p = 1.7−21). The fluorescence evaluation was carried out in a Perkin Elmer® Wallac 1420 VICTOR 2™, as triplicates and at nine times within a 15-min gap between them. Statistical evaluations were made with the ANOVA (single variant).

Based on the fact that the initial FbPA isolated from the *T. infestans*' hemolymph was eluted in 43% ACN, the fractions eluted between 40 and 50% ACN had their fluorescence evaluated. The fraction eluted with 43% ACN exhibited the predicted fluorescence emission (figure 19). The mass spectrometry data of this fraction confirms that the material from the isolated fraction corresponds to the FITC–FbPA conjugate (data not shown).

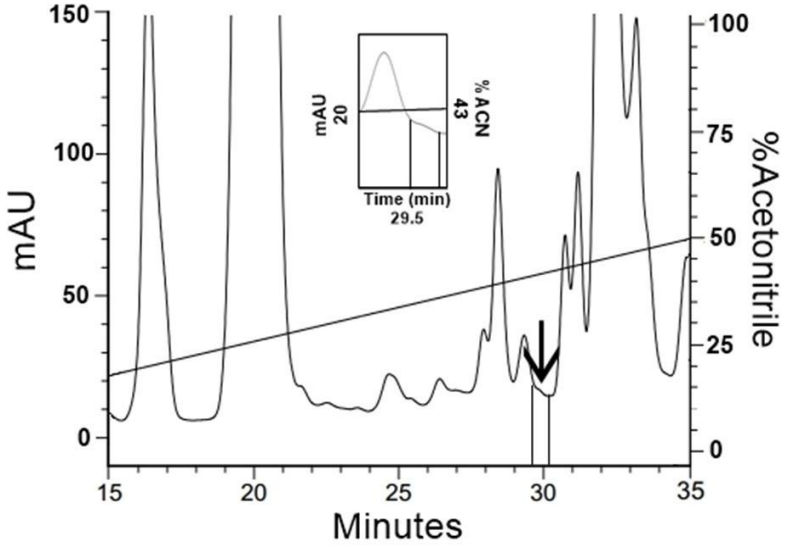

Figure 19 – Isolation of FITC–FbPA conjugate on the insects hemolymph.
The hemolymph from the engorged insects was separated by RP-HPLC using a C18 column, eluted in a linear solution A gradient from 20 to 80% on solution B for 60min. Zooming the chromatogram, it is possible to see the fraction, eluted at 29.5min in 43% ACN, that corresponds to the conjugate.

Fluorescence readings were taken via excitation with a 495 nm filter and a 520–530 nm emission filter as a method to evaluate and compare the fluorescence emissions from the isolated fraction, the FITC–FbPA conjugate, and by the synthetic FbPA (figure 20). The isolated fraction was tested via the inhibition assay (Methods section: Liquid Growth Inhibition Assay) and was active against M. luteus at 0.02 mg/mL.

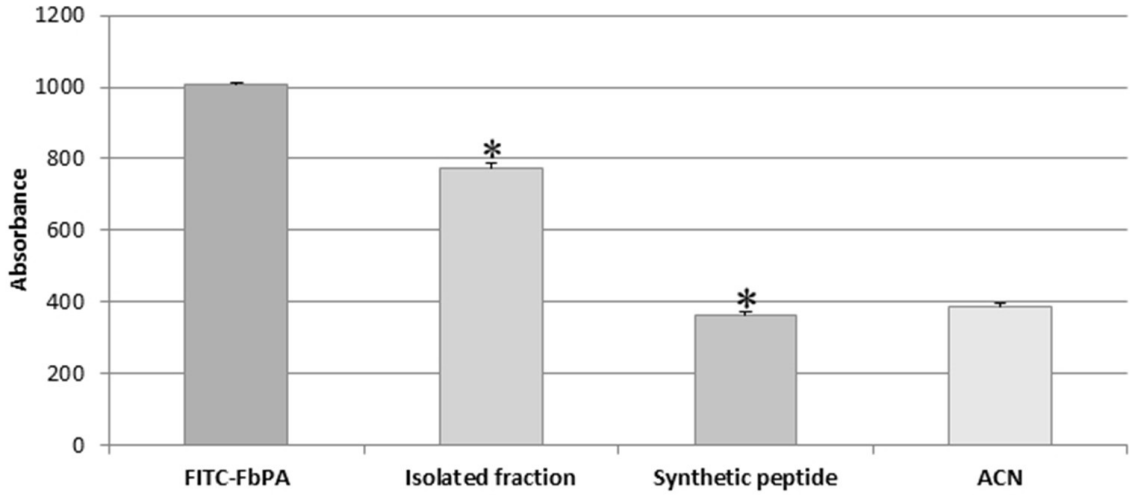

Figure 20 – Isolated fraction fluorescence evaluation.
Determination of the difference on the emitted fluorescence between the internalized fraction (FITC–FbPA conjugate) and the synthetic FbPA (*p = 1.85−15). The evaluation was performed in a Perkin Elmer® Wallac 1420 VICTOR 2TM, as triplicates and nine times within a 15-min gap between them. Statistical evaluations were made with the ANOVA (single variant).

3.5 Discussion

Although several studies have been performed aimed at a wider comprehension of the immune system of invertebrates, there are no consistent data about their adaptive immunity. It is known that there is no cell-based immunological memory, but some molecules produced by invertebrates have been described, such as molecules related to the immunoglobulin G superfamily (226). Other studies were able to demonstrate a certain specificity of the immune response in a second pathogen exposure (227-229).

As insects do not have a relevant immune memory, a rapid response mechanism is required. Therefore, AMPs play an important role on the immunological response of these animals. Commonly, AMP levels in the insect's hemolymph without bacterial or fungal contamination is low, increasing only with the stimuli of invasion/infection. As insects lack immunological memory, there is the necessity to activate intracellular pathways to induce the production of AMPs against each microorganism invasion. The main AMP production pathways activated are the Spaetzle-Toll—activated by fungi and gram-positive bacteria—and Imd—activated by gram-negative bacteria (52). Representing rapid responses, the peptide production does not exceed 8 h (62). Confirming that FbPA has antimicrobial activity represents a huge step because it reinforces the idea of evolutionary improvements of the *T. infestans* immune system.

FbPA was obtained from the *T. infestans* hemolymph inthe presence or absence of bacterial challenge and was active against several microorganisms in both cases. Thus it is possible to infer that the presence of this molecule in the insect's hemolymph is relevant to the insect's protection, whereas it is a known fact that AMPs can act in synergy and potentialize their effect over a target cell (230-235). It is still unknown whether *T. infestans* internalizes other molecules from the human blood. Diniz (42) isolated ten AMPs and identified four among them, but unlike FbPA, none of the AMPs described belonged to the blood ingested.

Few studies have been performed to identify the antimicrobial activities of fibrinopeptides. Although the work performed by Påhlman and group (236) was unable to prove FbPA's antimicrobial action, Tang and group (237) demonstrated that seven molecules derived from human platelets (including fibrinopeptides A and B) exhibited antimicrobial activity. The authors also confirmed that FbPA exhibited antimicrobial activity against *E. coli, S. aureus, C. albicans,* and *C. neoformans,* while our work demonstrated its activity against *M. luteus, P. aeruginosa, E. coli, C. parapsilosis, C. neoformans, C. tropicalis, P.*

farinosus, *Cladosporium sp*., and *P. expansum*.

The native FbPA isolated has activity at a 0.002–0.005 mg/mL concentration, while the synthetic FbPA has activity at a 0.1– 0.2 mg/mL concentration. This discrepancy can be explained by the fact that the synthetic peptide has an amide group in its C-terminal portion, whereas the original sequence has a carboxyl group in the C-terminal portion. This change to the structure may impact the peptide–microorganism interaction, leading to a higher peptide concentration required to obtain the same effect. It might also explain some differences found between our research and others demonstrating FbPA's antimicrobial activity (237).

The synthetic FbPA exhibited the strongest antifungal activity against *C. tropicalis* at 5.2–10.5μMin poor medium. Other fungi were incapable of growth after 72 h of incubation in either rich or poor medium at a higher peptide concentration (42–84μM). A common recurrent infection that affects general insect species is induced by filamentous fungi and is described in several wild insects (238-241). These results indicate resistance specificity of the peptide against these microorganisms, suggesting that FbPA might play a role to help increase the efficiency of the insect's immunological barrier when facing these infections.

The inhibition assay of the FITC–FbPA conjugate indicates that it was active against *M. luteus* at a 0.02mg/mL concentration. Although a higher concentration was necessary for it to be active, this result corroborates previous inhibition results: the native FbPA was active against the same *M. luteus* strain at 0.002 mg/mL and the synthetic variant at 0.2 mg/mL. This change might occur due to the coupling of the FITC to the peptide via its amino groups. As the sequence has three possible FITC binding sites, it could be covering one of the major active sites of the molecule, thus interfering with its action against the bacteria.

In humans, the cleavage of fibrinogen chains is via thrombin action. Thrombin cleaves a specific Arg-Gly at the C-terminus during the last part of the clot formation pathway, resulting in the release of FbPA and B (122). Similarly, invertebrates produce molecules called fibrinogen-related peptides (FREP). Components of this class have been identified in ascidians, echinoderms, annelids, arthropods, nematodes, cnidarians, and mollusks (242-245). Their function is related mainly to defense mechanisms such as agglutination and antimicrobial action (246). Although some similarities to specific portions of human fibrinogen have been identified, there are no known similarities between FREPs and human FbPA.

Considered together with the fact that the *T. infestans* feeds on human blood our results suggest that this insect can assimilate FbPA during feeding and internalize it in the midgut. In turn, it may use this peptide as an antimicrobial in its hemolymph. Similar

strategies have already been described in different invertebrates (63, 64). Beyond this capacity, some insects can absorb whole or partial molecules obtained during feeding (247). The presence of this internalization capability has been observed in *Rhodnius prolixus* (248), phylogenetically related to *T. infestans* that assimilates human hemoglobin.

The introduction of the insect proboscis into the host tissue causes local damage that activates immune responses as well as the clotting cascade, leading to thrombin activation and FbPA production (249). This pathway, however, is inhibited due to the release of thrombin inhibitors expressed within insect saliva (250). The presence of an anticoagulant buffer in the blood offered to the insects suggests that the cleavage can occur in the midgut, but this piece of information isolated does not represent a definite answer to this issue, because we analyzed only the blood with the presence of citrate buffer. It would be necessary to analyse the hemolymph of *T. infestans* after it feeds on a real organism instead of an in vitro system.

Thus, it remains to be investigated whether FbPA internalized by *T. infestans* comes from endogenous cleavage within the host or another process. Moreover, the role played by the peptide in the *T. infestans* hemolymph in vivo requires further investigation. Finally, further research is warranted as to the peptide's local action and its potential application as a therapeutic agent against infectious diseases.

3.6 Conclusion

Therefore, our results demonstrate the presence of antimicrobial active human FbPA in the hemolymph of the blood-sucking insect *T. infestans*. The hypothesis confirmed was that the presence of this molecule on the *T. infestans* hemolymph happens through intestinal absorption, through FITC–FbPA internalization experiments. This discovery allows us to confirm that blood-sucking insects can gather different molecules from various resources as an attempt to defend themselves against pathogens. These results also contribute to a wider comprehension of the insect immune system, such as its role on an evolutive scale, and the results generate some necessary information to facilitate the discovery of new sources of antimicrobial peptides.

4 – Chapter 3

Hemoglobin Reassembly of Antimicrobial Fragments from the Midgut of *Triatoma infestans*

This chapter describes the production of active antimicrobial fragments from hemoglobin digestion on the *T. infestans* digestive tract.

Paper published on Biomolecules. doi: 10.3390/biom10020261

4.1 Objective

The objective of this study was to elucidate if during the blood digestion on *T. infestans* midgut there were the production of antimicrobial peptides.

4.2 Materials and Methods

The experiments were performed under the exemption of the *Animal Research Ethics Committee* (CEUAIB – Comitê de ética no uso de animais do Instituto Butantan) nº I–1345/15.

4.2.1 Animals

Triatoma infestans were obtained from an axenic culture and kept alive in the vivarium of the Special Laboratory of Toxinology, Butantan Institute (São Paulo, Brazil) at 37 ◦C and fed every 2 weeks with murine blood.

4.2.2 Bacteria Inoculation and Intestinal Content Collection

One week after blood feeding, adult *T. infestans* were injured with needles soaked in an *Enterobacter cloacae* and *Micrococcus luteus* pool, both at logarithmic-phase growth. After 72 h, the insect's midgut was sectioned and the content were scraped and stored at −80 ◦C until use.

4.2.3 Sample Fractionation

Acid and Solid Phase Extractions

To release the contents of the blood cells, the sample was incubated in acetic acid (2 M) for 30 minutes and centrifuged at 16,000×g for 30 min at 4 ◦C. The supernatant was injected into coupled Sep-Pack C_{18} cartridges (Waters Associates) equilibrated in 0.1% trifluoroacetic acid (TFA). The sample was eluted in two different acetonitrile (ACN) concentrations (40% and 80%) and then concentrated and reconstituted in ultrapure water.

Reverse Phase High-Performance Liquid Chromatography

Reverse Phase High-Performance Liquid Chromatography (RP-HPLC) separation was performed with a VYDAC semi-preparative C_{18} column (10 × 250 mm) equilibrated with 0.046% TFA. The elution gradient for the 40% ACN fraction was 2% to 60% (v/v) of solution B (0.046% (v/v) TFA in ACN) in solution A (0.046% (v/v) TFA in water) and for the 80% ACN fraction the gradient was 20% to 80% of solution B in solution A. RP-HPLC was performed for 120 min at a 1.5 mL/min flow rate. Effluent absorbance was monitored at 225 nm, and the fractions corresponding to absorbance peaks were hand-collected, concentrated under vacuum and reconstituted in ultrapure water.

4.2.4 Liquid Growth Inhibition Assay

A liquid growth inhibition assay was used for evaluating the fractions' antibacterial activity (251, 252). The microrganisms tested were *Micrococcus luteus, Staphylococcus aureus* and *Escherichia coli*. Lyophilized fractions were suspended in 500 µL Milli-Q water; the assay was carried out using 96-well sterile plates. Twenty µL of the fractions were aliquoted into each well with 80 µL of the bacterial dilution, to 100 µL final volume. Bacteria were cultured in poor nutrient broth (PB) (1.0 g peptone in 100 mL of water containing 86 mM NaCl at pH 7.4; 217 mOsm). Exponential growth phase cultures were diluted to 5 × 104 CFU/mL (DO = 0.001) final concentration (251, 253, 254). Sterile water and PB were used as growth control, and streptomycin was used as growth inhibition control. Microtitre plates were incubated for 18 h at 30 ◦C. Microbial growth was measured by monitoring optical density at 595 nm and assays were performed in triplicate (PerkinElmer Victor 3TM 1420

multilabel counter) (45, 63, 255).

4.2.5 Mass Spectrometry (LC/MS)

Active antibacterial fractions were analyzed by mass spectrometry Liquid Chromatography – Mass spectrometry (LC-MS/MS) on a LTQ-Orbitrap Velos (Thermo Fisher Scientific, Bremen, Germany) coupled to a liquid nanochromatography system (Easy-nLCII – Thermo Fisher Scientific, Bremen, Germany). The chromatographic step involved using 5 mL of each sample automatically on a C18 pre-column (100 mm I.D. × 50 mm; Jupiter 10 mm, Phenomenex Inc., Torrance, California, United States) coupled to a C18 analytical column (75 mm I.D. × 100 mm; ACQUA 5 mm, Phenomenex Inc.). The eluate was electro-sprayed at 2 kV and 200 ◦C in positive ion mode. Mass spectra were acquired by a Fourier transform mass analyzers (FTMS); full scan (MS1) involved using 200–2,000 m/z (60,000 resolution at 400 m/z) as mass scan interval with the instrument operated in data dependent acquisition mode, the five most intense ions per scan being selected for fragmentation by collision-induced dissociation. The minimum threshold for selecting an ion for a fragmentation event (MS2) was set to 5000. The dynamic exclusion time used was 15 s, repeating at 30 s intervals.

4.2.6 Computational Analysis and Sequences Alignment

The MS/MS peak list files were submitted to an in-house version of (analyzed through) PEAKS® (Bioinformatics Solutions Inc., Waterloo, Ontario, Canada), screened against hemoglobin databases obtained on Universal Protein (UniProt) (256) and National Center for Biotechnology Information (NCBI) (257) (36,315 sequences and 5866 sequences respectively). Mass spectrometry data were also analyzed on Mascot Deamon®software, version 2.2.2, through MS/MS search using Swissprot database. The results were considered valid only when they were reproducible in a different analysis. Analysis involved 10 ppm error tolerance for precursor ions and 0.6 Da for fragment ions. Metionin oxidation was considered as a variable modification.

The alignment of the primarily peptide sequences were performed with the multiple sequence alignment program Clustal Omega (258) using default parameters. Hemoglobin sequences for comparison were obtained on UniProt using *Monodelphis domestica, Dasypus novemcinctus, Nasua* and *Sus scrofa* as key words.

The net charge at pH 7 and total charge, possible secondary structure, isoeletric point and total hydrophobic ratio were predicted through the peptide property calculator (copyright © 2015 Innovagen AB) (259), and APD3: Antimicrobial Peptide Calculator and Predictor (260).

4.2 Results

After the sample preparation, the intestinal content was submitted to an initial fractionation through Sep-Pack C18 (Material and Methods – item 2.3.1), where elutions with 40% and 80% of ACN were performed. The eluted samples were submitted to a second fractionation step in a RP-HPLC (Materials and Methods - item 2.3.2). An antimicrobial screening assay was performed with all the fractions obtained on the second fractionation step (figure 21 A).

From the 80% ACN elution, 8 fractions presented activity against *M. luteus* but they showed no similarity with any hemoglobin fragments when analyzed through mass spectrometry (data not shown). We focus only on the 40% ACN fractions. Among the 41 fractions obtained by HPLC from the 40% ACN elution, 37 presented antimicrobial activity against *Micrococcus luteus*. Thus, highlighted on the figure 21 are only the fractions selected to mass spectrometry.

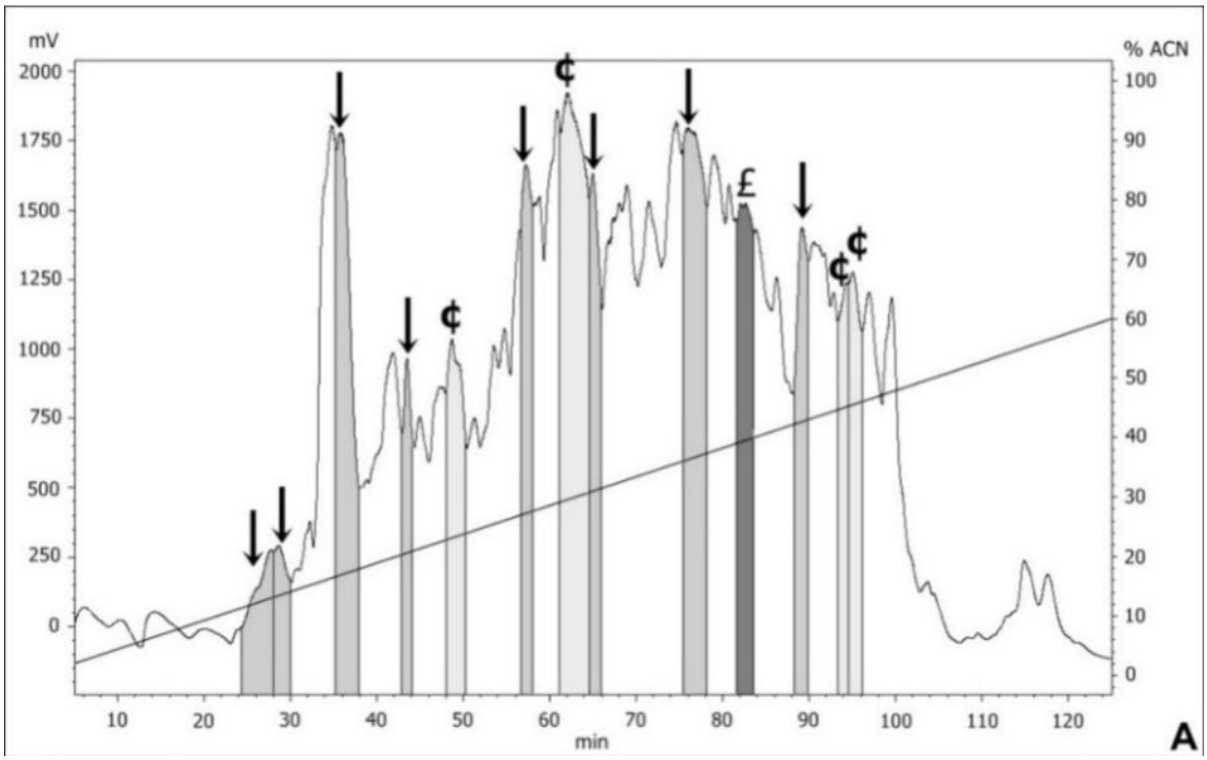

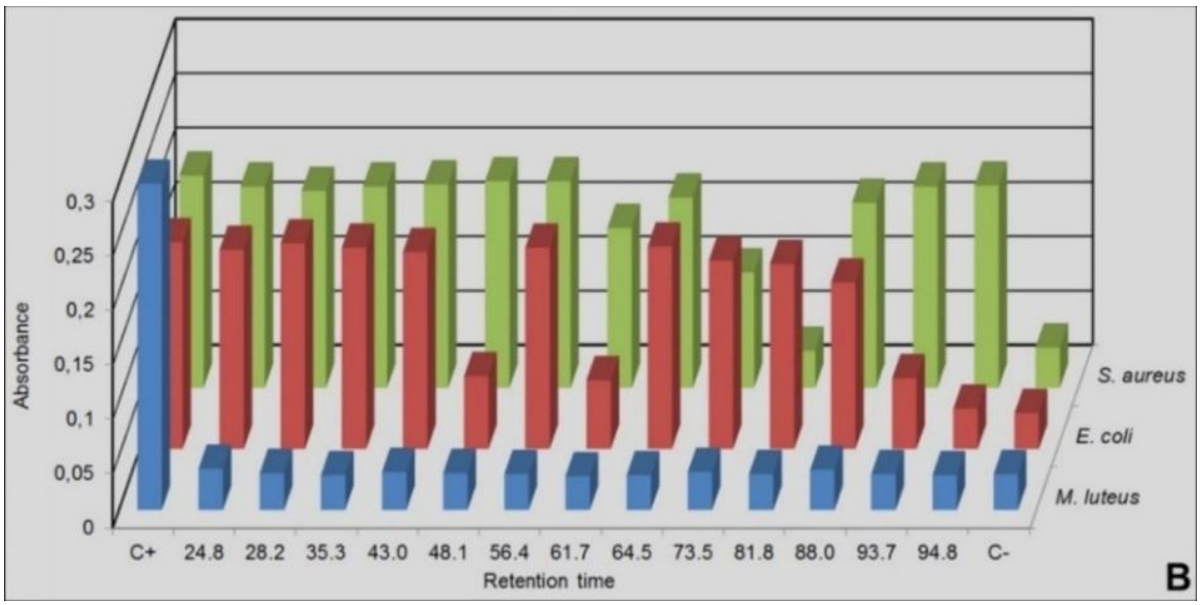

Figure 21 – RP-HPLC chromatogram and antimicrobial growth inhibition of 40% ACN Sep-Pack elution samples.

(**A**) The fractions isolated from *Triatoma infestans* intestinal content were separated by RP-HPLC using a C_{18} column, eluted with a linear gradient from solution A from 2% to 60% of the solution B run for 120 min. The labeled fractions (↓), eluted at 24.8 min, 28.2 min, 35.3 min, 43 min, 56.4 min, 64.5 min, 75.3 min and 88 min, exhibited antimicrobial activity against *Micrococcus luteus*. The labeled fraction (£) eluted at 81.8 min exhibited antimicrobial activity against *Micrococcus luteus* and *Staphylococcus aureus*. The labeled fractions (¢), eluted at 48.1 min, 61.7 min, 93.7 min and 94.8 min, presented antimicrobial activity against *M. luteus* and *Escherichia coli*. (**B**) The absorbance registered after the incubation of the RP-HPLC eluted fractions with *M. luteus, E. coli* and *S. aureus*. C+ is the positive control for bacterial growth, consisting in bacteria incubated only with PB medium. C- is the negative control for bacterial growth, consisting in bacteria incubated with PB medium in the presence of streptomycin.

Among the selected fractions, eight were active against *M. luteus* (retention time-RT of 24.8 min, 28.2 min, 35.3 min, 43 min, 56.4 min, 64.5 min, 75.3 min and 88 min), the fraction eluted in 81.8 min presented activity against *M. luteus* and *Staphylococcus aureus* and four fractions were active against *M. luteus* and *Escherichia coli* (RT 48.1 min, 61.7 min, 93.7 min and 94.8 min) (figure 22 and table 3).

Mass spectrometry data of ten fractions presented similarities to different portions of *Mus musculus* hemoglobin (Supplementary material: Figure S1 to Figure S10), three fractions with eight fragments of α chain (table 4) and 7 fractions with 24 fragments of the β chain (table 5).

Table 3 – Antimicrobial results of the HPLC-selected fractions.
The highlighted fractions obtained through HPLC with their respectively retention time and antimicrobial activity.

Chromatogram Label	Retention Time	Activity
↓	24.80	*M. luteus*
↓	28.28	*M. luteus*
↓	35.50	*M. luteus*
↓	43.00	*M. luteus*
↓	56.40	*M. luteus*
↓	64.50	*M. luteus*
↓	75.30	*M. luteus*
↓	88.80	*M. luteus*
¢	48.10	*M. luteus and E. coli*
¢	61.70	*M. luteus and E. coli*
¢	93.70	*M. luteus and E. coli*
¢	94.8	*M. luteus and E. coli*
£	81.80	*M. luteus and S. aureus*

Table 4 – Mass spectrometry data database search (α chain results).
Fraction A1 (eluted at 24.8 min) has two peptides corresponding to the fragments 2–10 and 110–117 of the hemoglobin α chain. Fraction A2 (eluted at 64.5 min) has three peptides corresponding to the fragments 45–57, 75–95 and 119–145 of the hemoglobin α chain. Fraction A3 (eluted at 81.8 min) has three peptides corresponding to the fragments 45–58, 76–104 and 106–147 of the hemoglobin α chain.

Fraction	Retention Time	Fragment
A1	24.80	VLSGEDKSN (α 2-10)
A1	24.80	LASHHPAD (α 110-117)
A2	64.50	ASFPTTKTYFPHF (α 45-57)
A2	64.50	DALASAAGHLDDLPGALSALSDLHAHKLRVD (α 75–95)
A2	64.50	LASHHPADFTPAVHASLDKFLASVST (α 119–145)
A3	81.80	ASFPTTKTYFPHFD (α 45–58)
A3	81.80	ALASAAGHLDDLPGALSALSDLHAHKLRVDPVNFKLLSH (α 76–104)
A3	81.80	LLVTLASHHPADFTPAVHASLDKFLASVSTVL (α 106–147)

Table 5 – Mass spectrometry data database search (β chain results).
Fraction B1 (eluted at 28.28 min) has two peptides corresponding to the fragments 2–10 and 56–77 of the hemoglobin β chain. Fraction B2 (eluted at 35.5 min) has five peptides corresponding to the fragments 1-10, 16–27, 49–70, 73–80 and 122–136 of the hemoglobin β chain. Fraction B3 (eluted at 43 min) has three peptides corresponding to the fragments 1–12, 58–72 and 112–129 of the hemoglobin β chain. Fraction B4 (eluted at 48.1 min) has three peptides corresponding to the fragments 2–14, 59–88 and 135–147 of the hemoglobin β chain. Fraction B5 (eluted at 56.4 min) has four peptides corresponding to the fragments 34–40, 59–71, 75–86 and 90–100 of the hemoglobin β chain. Fraction B6 (eluted at 61.7 min) has five peptides corresponding to the fragments 2–15, 21–33, 90–100, 104–110 and 131–147 of the hemoglobin β chain. Fraction B7 (eluted at 93.7 min) has two peptides corresponding to the fragments 100–107 and 112–146 of the hemoglobin β chain.

Fraction	Retention Time	Sequence
B1	28.28	HLTDAEKSA (β2_ 2-10)
B1	28.28	GDLSSASAIMGN (β2_ 46-57)

B2	35.50	VHLTDAEKSA (β2_1-10)
B2	35.50	AKVNPDEVGGEA (β2_16-27)
B2	35.50	SSASAIMGNPKVKAHGKKVITA (β2_ 49-70)
B2	35.50	EGLKNLDN (β2_73-80)
B2	35.50	FTPAAQAAFQKVVAG (β2_122-136)
B3	43.00	VHLTDAEKSAVS (β2_1-12)
B3	43.00	PKVKAHGKKVITAFN (β2_58-72)
B3	43.00	IVLGHHLGKDFTPAAQAA (β2_112-129)
B4	48.10	VHLTDAEKAAVSC (β1_ 2-14)
B4	48.10	AKVKAHGKKVITAFNDGLNHLDSLKGTFAS (β1_ 59-88)
B4	48.10	AGVATALAHKYH (β1_135-147)
B5	56.40	VVYPWTQ (β1_34-40)
B5	56.40	AKVKAHGKKVITA (β1_ 59-71)
B5	56.40	GLNHLDSLKGTF (β1_75-86)
B5	56.40	SELHCDKLHVD (β1_90-100)
B6	61.70	VHLTDAEKAAVSCL (β1_2-15)
B6	61.70	SDEVGGEALGRLL (β1_21-33)
B6	61.70	SELHCDKLHVD (β1_ 90-100)
B6	61.70	FRLLGNM β (β1_104-110)
B6	61.70	FQKVVAGVATALAHKYH (β1_131-147)
B7	93.70	PENFRLLG (β2_100-107)
B7	93.70	IVLGHHLGKDFTPAAQAAFQKVVAGVATALAHKYH (β2_112-146)

Coverage for almost the entire sequence was obtained (figures 22 and 23). There was approximately 67% coverage for all the sequences.

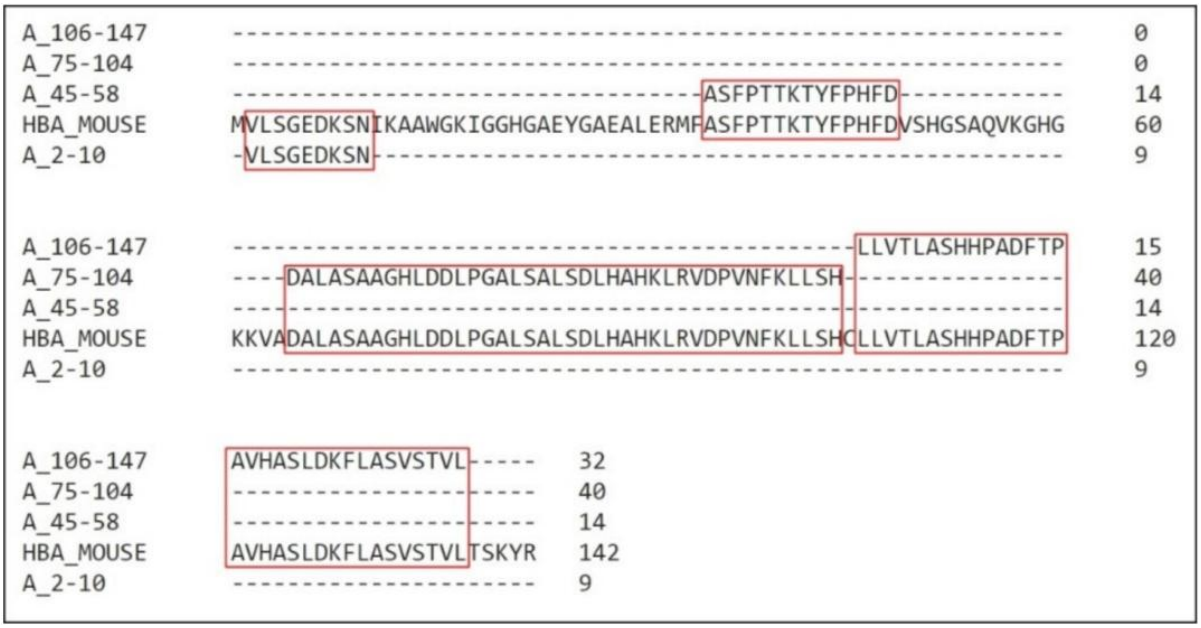

Figure 22 – Coverage of *Mus musculus* α hemoglobin sequence.
Alignment of the fragments obtained through mass spectrometry with the mouse hemoglobin α chain. Sequence compilations were performed to avoid residues repetitions. The residues coverage is highlighted in red.

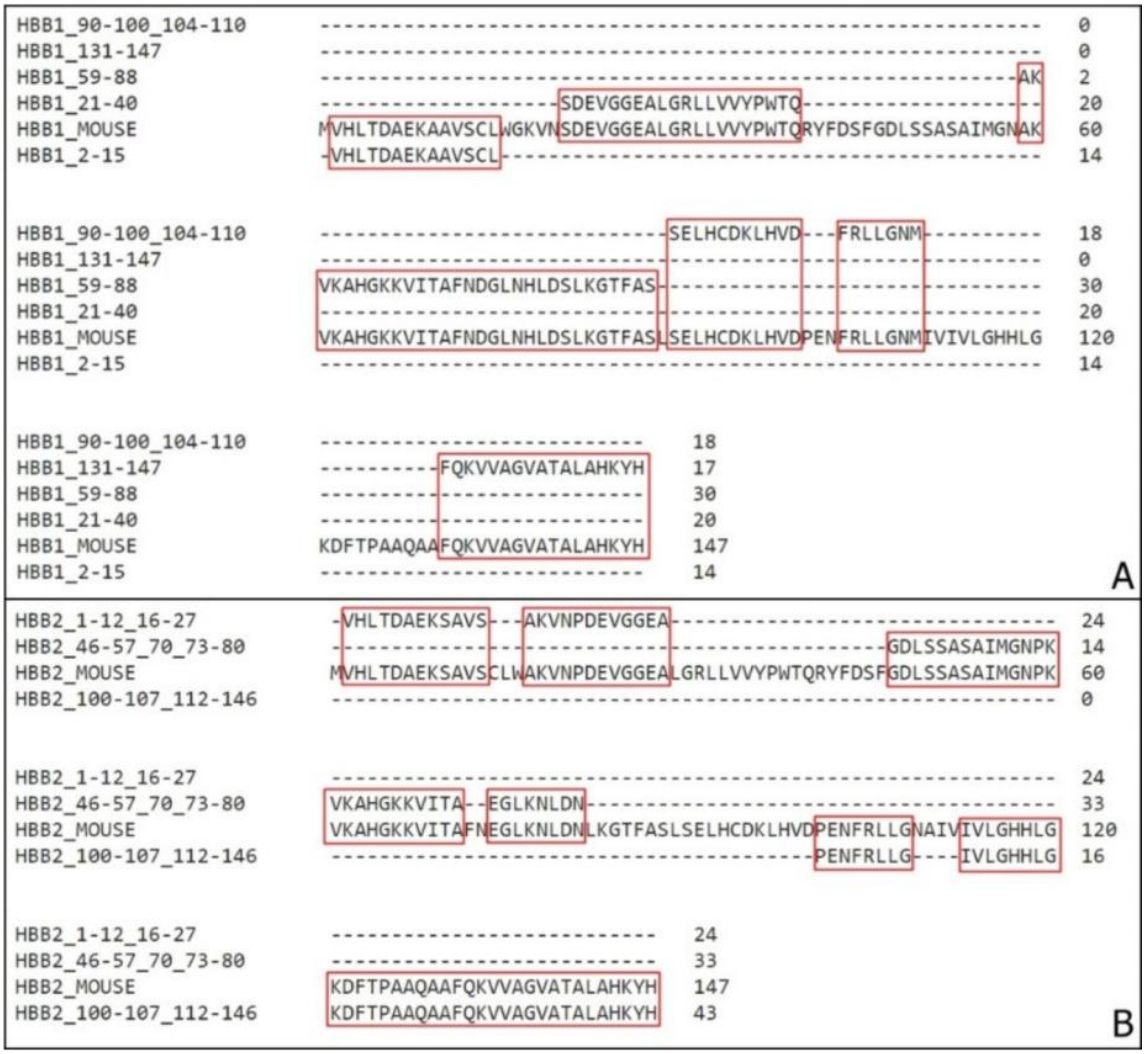

Figure 23 – Coverage of *Mus musculus* β hemoglobin sequence.
(**A**) Alignment of the fragments obtained through mass spectrometry with the mouse hemoglobin β1 chain (HBB1). (**B**) Alignment of the fragments obtained through mass spectrometry with the mouse hemoglobin β2 chain (HBB2). Sequences compilation was performed to avoid residues repetitions. Highlighted in red are the residues coverage.

As demonstrated, more than one sequence was identified on each fraction eluted on the chromatogram. Due to this information, although very unlikely, we cannot exclude the possibility that there could be additional non-Hb peptide or nonpeptide components in each fraction that could contribute to the activity.

To determine which sequence may be the responsible for the main antimicrobial activity, other purifications steps would be required. With further analysis, the fragments with higher score were defined (Table 6 and Supplementary Material Figure S11 to Figure S20) and aligned with the complete hemoglobin α and β chain sequences (Figure 24). This result provides more confidence to which fragment present in the sample is the one responsible for the antimicrobial activity. As the aim of the work was to perform a general screening, all the sequences are registered.

Table 6 – Sequences with highest score.
On the hemoglobin α chain, three fragments are the most confident sequence. Fraction A1 (eluted at 24.8 min) has the fragment from the amino acid 2 to 10, Fraction A2 (eluted at 64.5 min) and Fraction A3 (eluted at 81.8 min) have the fragment from the amino acid 77 to 95. On the hemoglobin β chain, the most confident sequence on the Fraction B1 (eluted at 28.28 min) is the fragments from the amino acid 2 to 10, on the Fraction B2 (eluted at 35.5 min) is the fragment from the amino acid 1 to 10, on the Fraction B3 (eluted at 43 min) is the fragments 1–12, 58–72 and 112–129 of the hemoglobin β chain. Fraction B4 (eluted at 48.1 min) has three peptides corresponding to the fragments 2–14, 59–88 and 135–147 of the hemoglobin β chain. Fraction B5 (eluted at 56.4min) has four peptides corresponding to the fragments 34–40, 59–71, 75–86 and 90–100 of the hemoglobin β chain. Fraction B6 (eluted at 61.7 min) has five peptides corresponding to the fragments 2–15, 21–33, 90–100, 104–110 and 131–147 of the hemoglobin β chain. Fraction B7 (eluted at 93.7 min) has two peptides corresponding to the fragments 100–107 and 112–146 of the hemoglobin βchain.

Fraction	Retention Time	Fragment
A1	24.80	VLSGEDKSN (α 2–10)
A2	64.50	LPGALSALSDLHAHKLRVD (α 77–95)
A3	81.80	LPGALSALSDLHAHKLRVD (α 77–95)
B1	28.28	HLTDAEKSA (β2_ 2–10)
B2	35.50	VHLTDAEKSA (β2_1–10)
B3	43.00	AKVKAHGKKVITAFND (β1_59–74)
B4	48.10	AKVKAHGKKVITAFNDGLN (β1_ 59–77)
B5	56.40	GLNHLDSLKG (β1_75–84)
B6	61.70	FQKVVAGVATALAHKYH (β1_131–147)
B7	93.70	TPAAQAAFQKVVAGVATALAHKYH (β2_123–147)

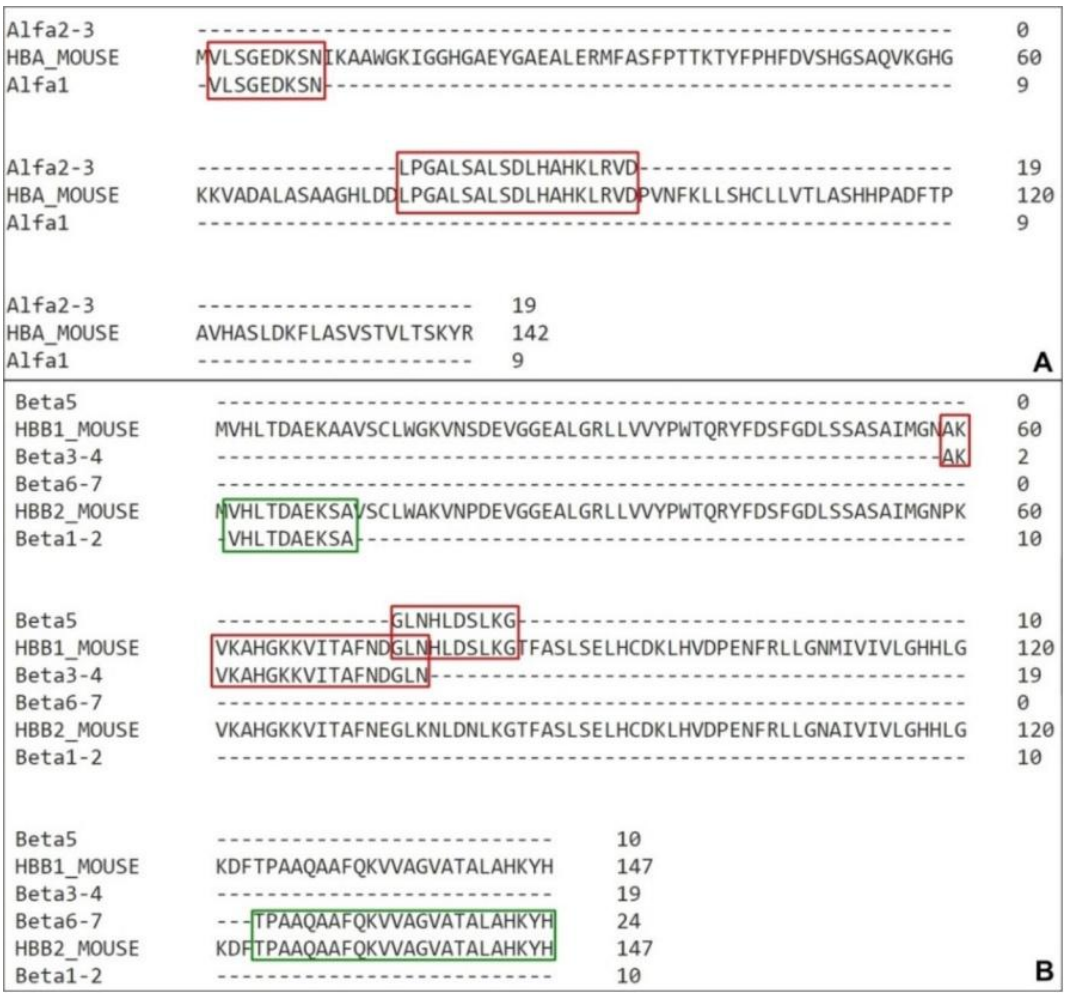

Figure 24 – Coverage of *Mus musculus* hemoglobin sequences with high confidence active molecules.
(**A**) Alignment of the highest-score fragments obtained through mass spectrometry with the mouse hemoglobin α chain. (**B**) Alignment of the highest score fragments obtained through mass spectrometry with the mouse

hemoglobin β1 and β2 chain (HBB1 and HBB2, red and green respectively). Sequences compilation was performed to avoid residues repetitions. The residues coverage is highlighted in red and green.

4.4 Discussion

Hence this result represents a very important conclusion because it is the first description of a Hemiptera being capable of produce hemoglobin fragments on the intestinal content that can have other biological function for its own benefit, beyond nutrition.

These insects have a continuous digestion system. It consists, initially, in the storage of the ingested blood in the anterior midgut (distensible stomach) where it remains undigested, with only lysis of erythrocytes and water absorption takes place (261, 262). Then small portions of blood are passed through other digestive and absorptive regions on the mid- and hindgut (263, 264).

As previously described by Albritton (265) and Altman and Dittmer (266), with little variation among vertebrate species, whole blood is contained by 80% of water, approximately (corresponding to 94% of the plasma alone). As their mobility is compromised by the volume of blood ingested, and considering that insects do not require this amount of water, its necessary to have a very efficient absorption mechanism and excretion system associated (263).

Along with the water loss, one of the most important process during blood digestion takes place, lysis of erythrocytes also initiates inside the midgut. Red blood cells represent most part of the protein content on the blood, while the plasma alone has a total of 7.41 g of proteins in 100 mL, red blood cells have a total of 36.8 g/100 mL (263).

Due to different pH among insect groups, there are adaptations in the digestive enzymes. Hemipterans have acidic midgut contents, with pH decreasing toward the posterior region (267). The first active degrading molecule in the anterior midgut, as described in *Rhodnius prolixus*, is one haemolisyn small basic peptide (262).

Corresponding to the pH alterations through the gut, triatomines have cathepsins as their principal protein degrading enzyme on the posterior midgut (263, 268-270). Cathepsins belong to the cysteine protease class and have an optimum activity in pH 5 (271), acting especially in the posterior midgut lumen (272).

After the initial degradation by hemolysins and cathepsins, the generated hemoglobin fragments reach the perimicrovillar spaces where they are cleaved into dipeptides by aminopeptidases and then absorbed (267, 273, 274).

It has been described that when cleaved, hemoglobin produces several bioactive

peptides (65, 275-278). Antimicrobial peptides (AMPs) are generally small molecules, with under than 50 amino acid residues, and normally have high hydrophobicity and amphipathic features. Cationic charges are one chemical property is the most common AMPs mode of action that can indicate interaction with anionic membranes (279-281).

The amino acid residue position on the α-helix formation is also essential for membrane interaction, because it allows the peptide to penetrate lipid membranes. This amphipathic characteristic is observed in all the sequences with alpha-helix conformation predicted (Table 7).

In 2000, a human hemoglobin fragments with antimicrobial peptides were gathered as a unique family entitled hemocidins (282). Beyond human fragments, bovine and rabbit hemoglobin antimicrobial peptides were also reported (64, 283, 284). As these peptides can have different hemoglobin sources, and as this work were developed using mouse, sequence comparison between these species is required (Figure 25).

Table 7 – Fragments chemical properties.
Chemical features of the fragments with alpha-helix predicted structure. H.R. stands for hydrophobic residue. α stands for alpha chain, β1 stands for beta-1 chain and β2 stands for beta-2 chain.

Fraction	Fragment	Charge pH 7	Total Hydrophobic Ratio	Same Surface brk H.R.*
A2	α 75-95	-2.7	48%	12
A2	α 119-145	-0.7	46%	8
A3	α 76-104	-0.6	48%	14
A3	α 106-147	-0.7	53%	14
B1	β2_2-10	-0.9	33%	3
B1	β2_46-57	-1	41%	4
B2	β2_1-10	-0.9	40%	3
B2	β2_49-70	4.1	40%	6
B2	β2_73-80	-1	25%	2
B2	β2_122-136	1	60%	6
B3	β2_1-12	-0.9	41%	3
B3	β2_58-72	4.1	40%	4
B3	β2_112-129	0.2	50%	6
B4	β1_2-14	-1	53%	4
B4	β1_59-88	3.2	40%	8
B4	β1_135-147	1.2	50%	4
B5	β1_59-71	4.1	46%	3
B5	β1_75-86	0.1	33%	4
B6	β1_2-15	-1	57%	6
B6	β1_21-33	-2	38%	3
B6	β1_104-110	1	57%	3
B6	β1_131-147	2.2	52%	6
B7	β2_100-107	0	37%	2
B7	β2_112-146	2.4	51%	14

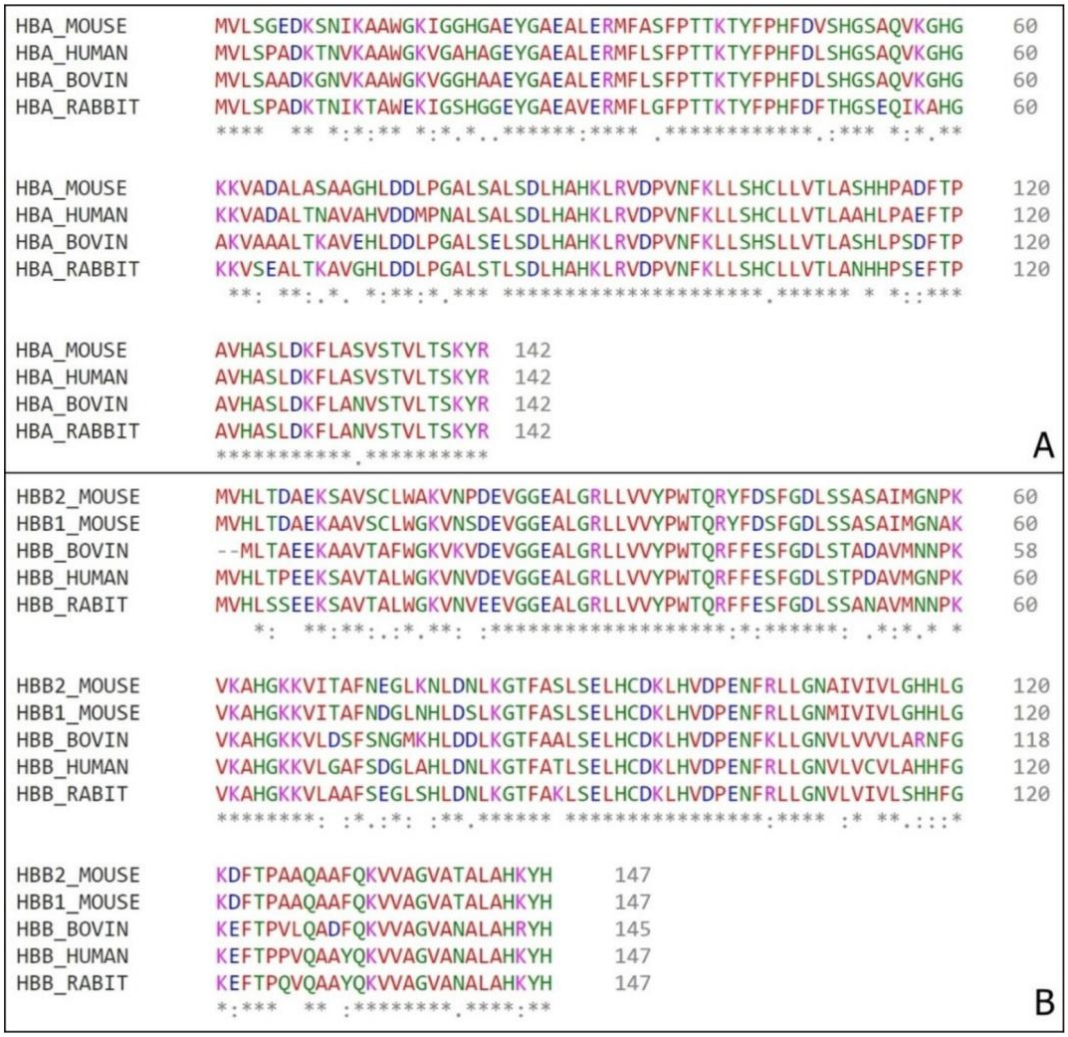

Figure 25 – Hemoglobin sequences alignment.
(**A**) Alpha chains amino acid comparison from mouse (*Mus musculus)* tag HBA_MOUSE, bovine (*Bos Taurus*) tag HBA_BOVINE, human (*Homo sapiens*) tag HBA_HUMAN and rabbit (*Oryctolagus cuniculus*) tag HBA_RABBIT. (**B**) Beta chains amino acid comparison from mouse (*Mus musculus)* tags HBB1_MOUSE and HBB2_MOUSE for β1 chain and β2 chain respectively, bovine (*Bos Taurus*) tag HBB_BOVINE, human (*Homo sapiens*) tag HBB_HUMAN and rabbit (*Oryctolagus cuniculus*) tag HBB_RABBIT. (*) – position with a single and fully conserved amino acid residue; (:) – position with amino acid residues conserved between groups of strong similar properties; (.) – position with amino acid residues conserved between groups of weakly similar properties.

The comparison among the hemoglobin chains from different organisms indicate that the sequences are highly conserved, thus there is a probability that the bioactive regions already described in other animals are also highly conserved on the murine protein.

In spite of previous descriptions of antimicrobial fragments from human hemoglobin (280, 281, 285, 286), bovine hemoglobin (287-289), comparisons between Cow, Reindeer, Sheep and Pig hemoglobins (289-291), we focus on the peptides obtained from in vivo cleavage on insects' midgut. The described sequences correspond to fractions of alpha chain from cattle and rabbit. They are the α33-61 (64), α98-114 (284) and α1–11/3–19 (283).

Interestingly, among the eight α fragments isolated on our work, fraction A1 2–10 is

partially homologous to both sequences α1–11 and α3–19 (283), A2 45-57 and A3 45–58 are fully inserted on the α33-61 (64) and Hb98–114 (284) shares approximately five residues with A3 106-147, A1 110–117 and A2 119–145 (figure 26).

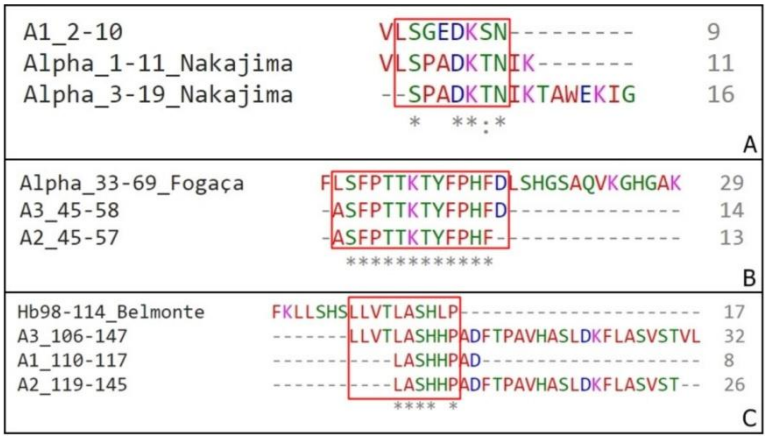

Figure 26 – Sequences homology between α chain fragments.
(**A**) Alignment of Nakajima's fragments (Alpha_1–11 and Alpha_3–19) with A1 2–10 isolated on this work. (**B**) Alignment of Fogaça's fragment (Alpha_33–69) with A2 45–57 and A3 45–58, both isolated on this work. (**C**) Alignment of Belmonte's fragments (Hb98-114) with A3 106–147, A1 110–117 and A2 119–145 isolated on this work. (*) – position with a single and fully conserved amino acid residue; (:) – position with amino acid residues conserved between groups of strong similar properties

The presence of a smaller fragment inside sequences such as the examples A and B (figure 26) can indicate the main portion responsible for the peptide antimicrobial activity.

The first important result is the fact that several sequences observed on this work are located on the middle alpha chain sequence, has antimicrobial activity and does not correspond to any of the four sequences identified previously. Examples are A2 α75–95 and A3 α76–104, active against *M. luteus* and *S. aureus*, that are both large sequences and has no amino acid residues overlap. Both A3 106–147 and A2 119–145 are other meaningful examples. Representing a large N-terminal portion of the hemoglobin molecule, it is a fragment that is generated by cathepsins activity on the midgut lumen (274). This can indicate a different cleavage site between mouse and bovine sequences, or that after the posterior gut digestion, during the aminopeptidases fragmentation, these sequences can form smaller inactive peptides, justifying the lack of identification of these peptides on other studies performed so far.

The Hb98–114 (284) has a specific cytotoxicity against different fungi, the α 1–32/3–32 (283) is active against *S. aureus* and the α 33–61 (64) is active against *M. luteus*. This predilection for Gram-positive bacteria is also observed here. Although the peptides of the murine α-chain identified here haven't been tested against any fungi strains, all presented some toxicity against *M. luteus* and/or *S. aureus*, and not against *E. coli*.

A second relevant result it is the description of the production of active beta-chains fragments from murine hemoglobin inside a hematophagous insect midgut. Among the fragments, the sequences inside B4, B6 and B7 HPLC fractions, corresponding to most of Beta1 chain and to the final portion of Beta2 chain are active against *E. coli*. This is an interesting result due to the restriction of Gram-negative activity to fragments from beta chains.

Due to the fact of the high chains coverage, it was to expect that most part of the fragments here analyzed were compatible with the fragments already described, but our work showed the opposite. The four biggest sequences of α chain presents few or none overlap with the referred before. And as already mentioned it is the first description of an in vivo β chain fragmentation by the insect.

Diniz and group (292) described a similar event in 2018 where the insect is capable not only to cleavage the protein, but to internalize the fragment produced and use it as a protective factor inside its hemolymph. This fact reinforces the importance of the work, describing the intense bioactive peptide production by the digestion and their importance as a protective factor for the insect against several occasionally pathogens ingested during the blood-feeding.

Triatomines are insects of socioeconomic importance regarding the role on Chagas disease transmission. The insect contamination occurs when the ingested blood contains trypomastigotes forms of *Trypanossoma cruzi* (293). Some wild animals are natural reservoirs of the parasite and consequentially are directly connected to the insect contamination with *T. cruzi*. Those natural reservoirs include several species form different taxon and a variety species of triatomines can be infected with *T. cruzi.* Thus, to compare a possible antimicrobial production from other natural reservoir animals, comparisons of hemoglobin sequences were performed (figure 27).

Representative organisms from different orders were selected and had their hemoglobin α and β chains compared with *Mus musculus*. The sequences selected belong to the opossum *Monodelphis domestica* (order Marsupialia), the armadillo *Dasypus novemcinctus* (order Xenarthra), the coati *Nasua nasua* (order Carnivora) and the pig *Sus scrofa* (order Artiodactyla). They represent four of the most common intermediate hosts of Chagas' disease in Brazil and some of the main natural blood source for triatomines.

All the sequences have high similarity, containing over an average 70% homology, with almost every position with a conserved amino acid or amino acids residues conserved between groups of strong similar properties.

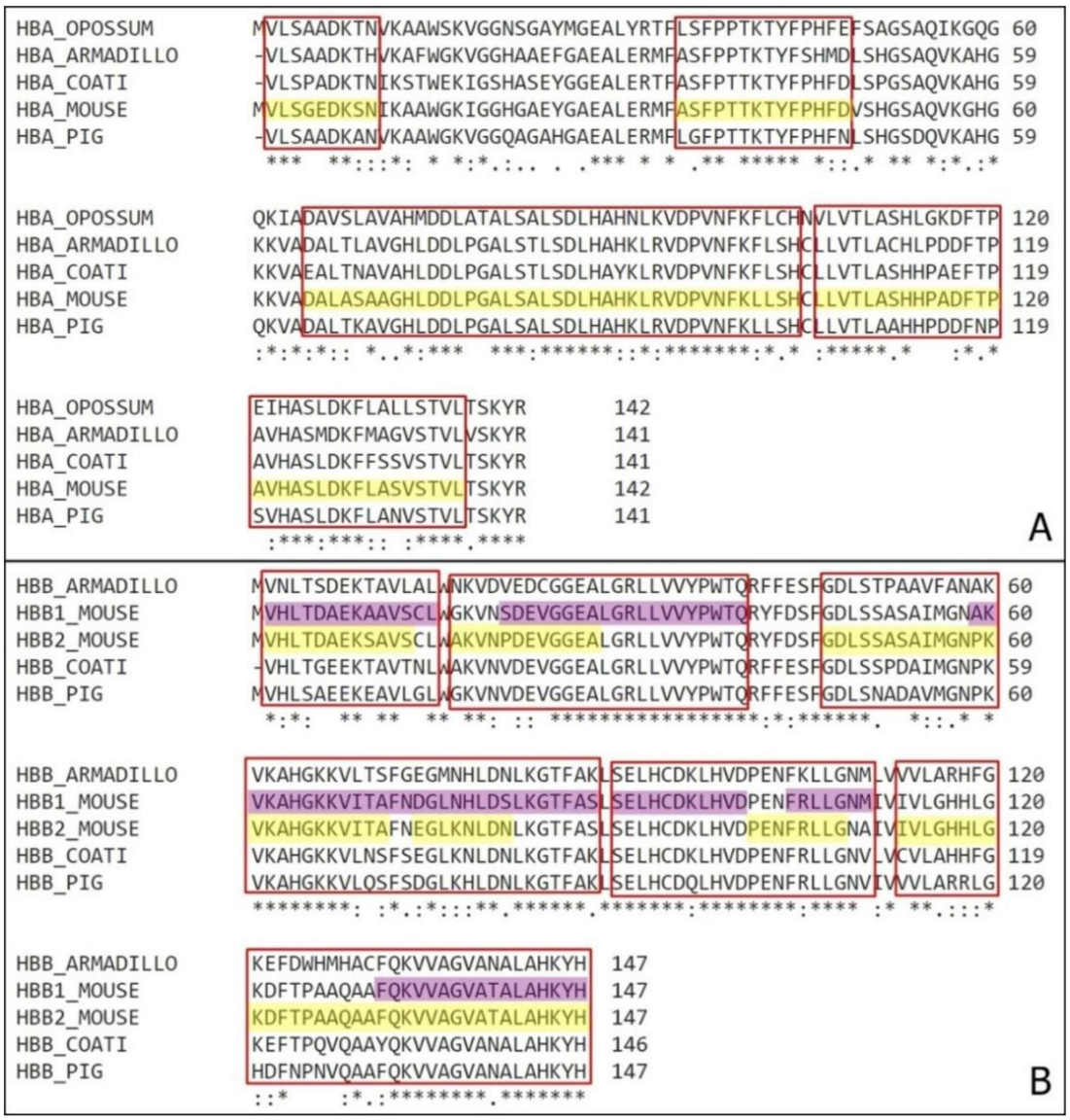

Figure 27 – Natural reservoirs organisms' hemoglobin comparison.
(A) Comparison of α hemoglobin subunit from *Mus musculus* (HBA_MOUSE) with *Monodelphis domestica* (HBA_OPOSSUM), *Dasypus novemcinctus* (HBA_ARMADILLO), *Nasua nasua* (HBA_COATI) and *Sus scrofa* (HBA_PIG). Highlighted in yellow are the antimicrobial fragments identified on this work, and marked on red are the correspondent sequences on the other animals. (B) Comparison of β hemoglobin subunit from *Mus musculus* (HBA_MOUSE) with *Dasypus novemcinctus* (HBA_ARMADILLO), *Nasua nasua* (HBA_COATI) and *Sus scrofa* (HBA_PIG). Highlighted in yellow are the antimicrobial fragments of β1 chain and in purple are the fragments of β2 chain identified on this work, and marked on red are the correspondent sequences on the other animals. (*) – position with a single and fully conserved amino acid residue; (:) – position with amino acid residues conserved between groups of strong similar properties; (.) – position with amino acid residues conserved between groups of weakly similar properties.

Considering their highly evolved digestive system, the digestion happens in a very specific way, independent of the species, we can infer that when feeding on other wild animals besides mouse, triatomines (especially *T. infestans*) can also produce the same antimicrobial fragments.

4.6 Conclusion

This work is the first description that *T. infestans* digestion is able to produce several antimicrobial peptides from different hemoglobin chains. On these experiments the insects were fed with murine blood, but as Hb sequences on different species are highly conserved, there is a great probability that this production can occur on every host that the insect might feed on.

References[1]

1. Landecker H. Antibiotic Resistance and the Biology of History. Body & Society. 2015;22(4):19-52.
2. Watkins RR, Bonomo RA. Overview: Global and Local Impact of Antibiotic Resistance. Infectious Disease Clinics of North America. 2016;30(2):313-22.
3. Sengupta S, Chattopadhyay MK, Grossart H-P. The multifaceted roles of antibiotics and antibiotic resistance in nature. Front Microbiol. 2013;4:47-.
4. Bailey JH, Cavallito CJ. ANTIBIOTICS. Annual Review of Microbiology. 1948;2(1):143-82.
5. Podolsky SH, Bud R, Gradmann C, Hobaek B, Kirchhelle C, Mitvedt T, et al. History Teaches Us That Confronting Antibiotic Resistance Requires Stronger Global Collective Action. The Journal of Law, Medicine & Ethics. 2015;43(S3):27-32.
6. Podolsky SH. The evolving response to antibiotic resistance (1945–2018). Palgrave Communications. 2018;4(1):124.
7. Chokshi A, Sifri Z, Cennimo D, Horng H. Global contributors to antibiotic resistance. Journal of Global Infectious Diseases. 2019;11(1):36-42.
8. Jonas OBI, Alec; Berther, Franck C.J.; Le Gall; Francois G.; Marquez, Patricio. Drug-resistant infections: a threat to our economic future: final report. . Washington, D.C.: World Bank Group, 2017.
9. Klein EY, Van Boeckel TP, Martinez EM, Pant S, Gandra S, Levin SA, et al. Global increase and geographic convergence in antibiotic consumption between 2000 and 2015. Proceedings of the National Academy of Sciences. 2018;115(15):E3463-E70.
10. Castro-Sánchez E, Moore LSP, Husson F, Holmes AH. What are the factors driving antimicrobial resistance? Perspectives from a public event in London, England. BMC Infectious Diseases. 2016;16(1):465.
11. Dadgostar P. Antimicrobial Resistance: Implications and Costs. Infection and drug resistance. 2019;12:3903-10.
12. Neves PR, Mamizuka EM, Levy CE, Lincopan N. Pseudomonas aeruginosa multirresistente: um problema endêmico no Brasil. Jornal Brasileiro de Patologia e Medicina Laboratorial. 2011;47:409-20.
13. Zanol FM, Picoli SU, Morsch F. Detecção fenotípica de metalobetalactamase em isolados clínicos de Pseudomonas aeruginosa de hospitais de Caxias do Sul. Jornal Brasileiro de Patologia e Medicina Laboratorial. 2010;46:309-14.
14. Figueiredo DQd, Castro LFS, Santos KRN, Teixeira LM, Mondino SSBd. Detecção de metalo-beta-lactamases em amostras hospitalares de Pseudomonas aeruginosa e Acinetobacter baumannii. Jornal Brasileiro de Patologia e Medicina Laboratorial. 2009;45:177-84.
15. Santos Filho L, Santos IB, Assis AMLd, Xavier DE. Determinação da produção de metalo-b-lactamases em amostras de Pseudomonas aeruginosa isoladas em João Pessoa, Paraíba. Jornal Brasileiro de Patologia e Medicina Laboratorial. 2002;38:291-6.
16. Tavares W. Bactérias gram-positivas problemas: resistência do estafilococo, do enterococo e do pneumococo aos antimicrobianos. Revista da Sociedade Brasileira de Medicina Tropical. 2000;33:281-301.
17. WHO WHO-. NO TIME TO WAIT: SECURING THE FUTURE FROM DRUG-RESISTANT INFECTIONS. In: IACG ICGoAR-, editor. 2019. p. 28.
18. Munita JM, Arias CA. Mechanisms of Antibiotic Resistance. Microbiol Spectr. 2016;4(2):10.1128/microbiolspec.VMBF-0016-2015.
19. Martinez JL. General principles of antibiotic resistance in bacteria. Drug discovery today Technologies. 2014;11:33-9.
20. Reygaert WC. An overview of the antimicrobial resistance mechanisms of bacteria. AIMS Microbiol. 2018;4(3):482-501.

1- According to the Vancouver style

21. Dönhöfer A, Franckenberg S, Wickles S, Berninghausen O, Beckmann R, Wilson DN. Structural basis for TetM-mediated tetracycline resistance. Proceedings of the National Academy of Sciences. 2012;109(42):16900.
22. Leclercq R. Mechanisms of resistance to macrolides and lincosamides: nature of the resistance elements and their clinical implications. Clin Infect Dis. 2002;34(4):482-92.
23. Floss HG, Yu TW. Rifamycin-mode of action, resistance, and biosynthesis. Chemical reviews. 2005;105(2):621-32.
24. Blair JM, Smith HE, Ricci V, Lawler AJ, Thompson LJ, Piddock LJ. Expression of homologous RND efflux pump genes is dependent upon AcrB expression: implications for efflux and virulence inhibitor design. J Antimicrob Chemother. 2015;70(2):424-31.
25. Pages JM, James CE, Winterhalter M. The porin and the permeating antibiotic: a selective diffusion barrier in Gram-negative bacteria. Nat Rev Microbiol. 2008;6(12):893-903.
26. McMurry L, Petrucci RE, Jr., Levy SB. Active efflux of tetracycline encoded by four genetically different tetracycline resistance determinants in Escherichia coli. Proc Natl Acad Sci U S A. 1980;77(7):3974-7.
27. Piddock LJ. Multidrug-resistance efflux pumps - not just for resistance. Nat Rev Microbiol. 2006;4(8):629-36.
28. Piddock LJ. Clinically relevant chromosomally encoded multidrug resistance efflux pumps in bacteria. Clinical microbiology reviews. 2006;19(2):382-402.
29. Bebear CM, Pereyre S. Mechanisms of drug resistance in Mycoplasma pneumoniae. Curr Drug Targets Infect Disord. 2005;5(3):263-71.
30. Kumar S, Mukherjee MM, Varela MF. Modulation of Bacterial Multidrug Resistance Efflux Pumps of the Major Facilitator Superfamily. Int J Bacteriol. 2013;2013.
31. Blair JM, Webber MA, Baylay AJ, Ogbolu DO, Piddock LJ. Molecular mechanisms of antibiotic resistance. Nat Rev Microbiol. 2015;13(1):42-51.
32. Ramirez MS, Tolmasky ME. Aminoglycoside modifying enzymes. Drug Resist Updat. 2010;13(6):151-71.
33. Robicsek A, Strahilevitz J, Jacoby GA, Macielag M, Abbanat D, Park CH, et al. Fluoroquinolone-modifying enzyme: a new adaptation of a common aminoglycoside acetyltransferase. Nat Med. 2006;12(1):83-8.
34. Schwarz S, Kehrenberg C, Doublet B, Cloeckaert A. Molecular basis of bacterial resistance to chloramphenicol and florfenicol. FEMS Microbiol Rev. 2004;28(5):519-42.
35. Brito MAd, Cordeiro BC. Necessidade de novos antibióticos. Jornal Brasileiro de Patologia e Medicina Laboratorial. 2012;48:247-9.
36. Santos NdQ. A resistência bacteriana no contexto da infecção hospitalar. Texto & Contexto - Enfermagem. 2004;13:64-70.
37. Ferreira LLM, Carvalho ES, Berezin EN, Brandileone MC. Colonização e resistência antimicrobiana de Streptococcus pneumoniae isolado em nasofaringe de crianças com rinofaringite aguda. Jornal de Pediatria. 2001;77:227-34.
38. Riera Romo M, Pérez-Martínez D, Castillo Ferrer C. Innate immunity in vertebrates: an overview. Immunology. 2016;148(2):125-39.
39. Sheehan G, Garvey A, Croke M, Kavanagh K. Innate humoral immune defences in mammals and insects: The same, with differences ? Virulence. 2018;9(1):1625-39.
40. Hassan M, Kjos M, Nes IF, Diep DB, Lotfipour F. Natural antimicrobial peptides from bacteria: characteristics and potential applications to fight against antibiotic resistance. J Appl Microbiol. 2012;113(4):723-36.
41. Chung CR, Jhong JH, Wang Z, Chen S, Wan Y, Horng JT, et al. Characterization and Identification of Natural Antimicrobial Peptides on Different Organisms. International journal of molecular sciences. 2020;21(3).

42. Diniz LCL. Identificação e Caracterização de Peptídeos Antimicrobianos da Hemolinfa de Triatoma infestans (Hemiptera: Revuviidae). [Dissertation]: Universidade de São Paulo/Instituto Butantan.; 2016.
43. de Jesus Oliveira T, Oliveira UCd, da Silva Junior PI. Serrulin: A Glycine-Rich Bioactive Peptide from the Hemolymph of the Yellow Tityus serrulatus Scorpion. Toxins (Basel). 2019;11(9):517.
44. Nascimento S, Martins L, Oliveira U, Moraes R, Mendonça R, da Silva Junior P. A new lysozyme found in the haemolymph from pupae of Lonomia obliqua (Lepidoptera: Saturniidae). Trends in Entomology. 2016.
45. Silva PI, Jr., Daffre S, Bulet P. Isolation and characterization of gomesin, an 18-residue cysteine-rich defense peptide from the spider Acanthoscurria gomesiana hemocytes with sequence similarities to horseshoe crab antimicrobial peptides of the tachyplesin family. J Biol Chem. 2000;275(43):33464-70.
46. Wang X, Wang G. Insights into Antimicrobial Peptides from Spiders and Scorpions. Protein and peptide letters. 2016;23(8):707-21.
47. Bertrand B, Munoz-Garay C. Marine Antimicrobial Peptides: A Promising Source of New Generation Antibiotics and Other Bio-active Molecules. International Journal of Peptide Research and Therapeutics. 2019;25(4):1441-50.
48. Tam JP, Wang S, Wong KH, Tan WL. Antimicrobial Peptides from Plants. Pharmaceuticals (Basel). 2015;8(4):711-57.
49. Díaz-Roa A, Patarroyo MA, Bello FJ, Da Silva PI. Sarconesin: Sarconesiopsis magellanica Blowfly Larval Excretions and Secretions With Antibacterial Properties. Front Microbiol. 2018;9(2249).
50. Chaparro-Aguirre E, Segura-Ramírez PJ, Alves FL, Riske KA, Miranda A, Silva Júnior PI. Antimicrobial activity and mechanism of action of a novel peptide present in the ecdysis process of centipede Scolopendra subspinipes subspinipes. Scientific Reports. 2019;9(1):13631.
51. Segura-Ramírez PJ, Silva Júnior PI. Loxosceles gaucho Spider Venom: An Untapped Source of Antimicrobial Agents. Toxins (Basel). 2018;10(12):522.
52. Schmid-Hempel P. Evolutionary ecology of insect immune defenses. Annu Rev Entomol. 2005;50:529-51.
53. Pizzo E, Cafaro V, Di Donato A, Notomista E. Cryptic Antimicrobial Peptides: Identification Methods and Current Knowledge of their Immunomodulatory Properties. Current pharmaceutical design. 2018;24(10):1054-66.
54. El Karim IA, Linden GJ, Orr DF, Lundy FT. Antimicrobial activity of neuropeptides against a range of micro-organisms from skin, oral, respiratory and gastrointestinal tract sites. J Neuroimmunol. 2008;200(1-2):11-6.
55. Sung WS, Park SH, Lee DG. Antimicrobial effect and membrane-active mechanism of Urechistachykinins, neuropeptides derived from Urechis unicinctus. FEBS Lett. 2008;582(16):2463-6.
56. Abreu TF, Sumitomo BN, Nishiyama MY, Jr., Oliveira UC, Souza GH, Kitano ES, et al. Peptidomics of Acanthoscurria gomesiana spider venom reveals new toxins with potential antimicrobial activity. J Proteomics. 2017;151:232-42.
57. Candido-Ferreira IL, Kronenberger T, Sayegh RSR, Batista IdFC, da Silva Junior PI. Evidence of an Antimicrobial Peptide Signature Encrypted in HECT E3 Ubiquitin Ligases. Frontiers in immunology. 2017;7:664-.
58. Sutti R, Rosa BB, Wunderlich B, da Silva Junior PI, Rocha EST. Antimicrobial activity of the toxin VdTX-I from the spider Vitalius dubius (Araneae, Theraphosidae). Biochemistry and biophysics reports. 2015;4:324-8.
59. Suda S, Field D, Barron N. Antimicrobial Peptide Production and Purification.

Methods Mol Biol. 2017;1485:401-10.
60. Jenssen H, Hamill P, Hancock REW. Peptide Antimicrobial Agents. Clinical microbiology reviews. 2006;19(3):491-511.
61. Rosales C. Cellular and Molecular Mechanisms of Insect Immunity. In: Shields VDC, editor. Insect Physiology and Ecology. Mexico City, Mexico: Universidad Nacional Autónoma de México; 2017. p. 179-212.
62. Dunn PE. Biochemical Aspects of Insect Immunology. Annual Review of Entomology. 1986;31(1):321-39.
63. Riciluca KC, Sayegh RS, Melo RL, Silva PI, Jr. Rondonin an antifungal peptide from spider (Acanthoscurria rondoniae) haemolymph. Results Immunol. 2012;2:66-71.
64. Fogaça AC, da Silva PI, Miranda MT, Bianchi AG, Miranda A, Ribolla PE, et al. Antimicrobial activity of a bovine hemoglobin fragment in the tick Boophilus microplus. J Biol Chem. 1999;274(36):25330-4.
65. Lantz I, Glamsta EL, Talback L, Nyberg F. Hemorphins derived from hemoglobin have an inhibitory action on angiotensin converting enzyme activity. FEBS Lett. 1991;287(1-2):39-41.
66. Gaglione R. Crytic antimicrobial peptides hidden in protein precursors: identification of novel bioactive molecules. Italy: Università degli Studi di Napoli Federico II; 2017.
67. Berger A, Tran AH, Dedier H, Gardam MA, Paige CJ. Antimicrobial properties of hemokinin-1 against strains of Pseudomonas aeruginosa. Life Sci. 2009;85(19-20):700-3.
68. Ali SM, Siddiqui R, Khan NA. Antimicrobial discovery from natural and unusual sources. Journal of Pharmacy and Pharmacology. 2018;70(10):1287-300.
69. Chellat MF, Riedl R. Pseudouridimycin: The First Nucleoside Analogue That Selectively Inhibits Bacterial RNA Polymerase. Angew Chem Int Ed Engl. 2017;56(43):13184-6.
70. Bhadra P, Yan J, Li J, Fong S, Siu SWI. AmPEP: Sequence-based prediction of antimicrobial peptides using distribution patterns of amino acid properties and random forest. Scientific Reports. 2018;8(1):1697.
71. Pirtskhalava M GA, Cruz P, Griggs HL, Squires RB, Hurt DE, Grigolava M, Chubinidze M, Gogoladze G, Vishnepolsky B, Alekseev V, Rosenthal A, and Tartakovsky M. DBAASP v.2: an Enhanced Database of Structure and Antimicrobial/Cytotoxic Activity of Natural and Synthetic Peptides. Nucleic Acids Research. 2016;44(D1):D1104-D12.
72. Vishnepolsky B, Gabrielian A, Rosenthal A, Hurt DE, Tartakovsky M, Managadze G, et al. Predictive Model of Linear Antimicrobial Peptides Active against Gram-Negative Bacteria. Journal of chemical information and modeling. 2018;58(5):1141-51.
73. Vishnepolsky B, Pirtskhalava M. Prediction of linear cationic antimicrobial peptides based on characteristics responsible for their interaction with the membranes. Journal of chemical information and modeling. 2014;54(5):1512-23.
74. Kumar P, Kizhakkedathu JN, Straus SK. Antimicrobial Peptides: Diversity, Mechanism of Action and Strategies to Improve the Activity and Biocompatibility In Vivo. Biomolecules. 2018;8(1):4.
75. Zhang L-j, Gallo RL. Antimicrobial peptides. Current Biology. 2016;26(1):R14-R9.
76. Brogden KA. Antimicrobial peptides: pore formers or metabolic inhibitors in bacteria? Nat Rev Microbiol. 2005;3(3):238-50.
77. Hong SY, Park TG, Lee KH. The effect of charge increase on the specificity and activity of a short antimicrobial peptide. Peptides. 2001;22(10):1669-74.
78. Gagnon M-C, Strandberg E, Grau-Campistany A, Wadhwani P, Reichert J, Bürck J, et al. Influence of the Length and Charge on the Activity of α-Helical Amphipathic Antimicrobial Peptides. Biochemistry. 2017;56.
79. Yin LM, Edwards MA, Li J, Yip CM, Deber CM. Roles of hydrophobicity and charge

distribution of cationic antimicrobial peptides in peptide-membrane interactions. J Biol Chem. 2012;287(10):7738-45.
80. Chen Y, Guarnieri MT, Vasil AI, Vasil ML, Mant CT, Hodges RS. Role of peptide hydrophobicity in the mechanism of action of alpha-helical antimicrobial peptides. Antimicrob Agents Chemother. 2007;51(4):1398-406.
81. Ulm H, Wilmes M, Shai Y, Sahl H-G. Antimicrobial Host Defensins – Specific Antibiotic Activities and Innate Defense Modulation. Frontiers in Immunology. 2012;3(249).
82. Pushpanathan M, Gunasekaran P, Rajendhran J. Antimicrobial peptides: versatile biological properties. Int J Pept. 2013;2013:675391-.
83. Zhang L, Rozek A, Hancock RE. Interaction of cationic antimicrobial peptides with model membranes. J Biol Chem. 2001;276(38):35714-22.
84. Oren Z, Shai Y. Mode of action of linear amphipathic alpha-helical antimicrobial peptides. Biopolymers. 1998;47(6):451-63.
85. Madani F, Lindberg S, Langel U, Futaki S, Graslund A. Mechanisms of cellular uptake of cell-penetrating peptides. J Biophys. 2011;2011:414729.
86. Le C-F, Fang C-M, Sekaran SD. Intracellular Targeting Mechanisms by Antimicrobial Peptides. Antimicrobial Agents and Chemotherapy. 2017;61(4):e02340-16.
87. Park CB, Kim MS, Kim SC. A novel antimicrobial peptide from Bufo bufo gargarizans. Biochem Biophys Res Commun. 1996;218(1):408-13.
88. Selsted ME, Novotny MJ, Morris WL, Tang YQ, Smith W, Cullor JS. Indolicidin, a novel bactericidal tridecapeptide amide from neutrophils. J Biol Chem. 1992;267(7):4292-5.
89. Marchand C, Krajewski K, Lee H-F, Antony S, Johnson AA, Amin R, et al. Covalent binding of the natural antimicrobial peptide indolicidin to DNA abasic sites. Nucleic acids research. 2006;34(18):5157-65.
90. Subbalakshmi C, Sitaram N. Mechanism of antimicrobial action of indolicidin. FEMS Microbiol Lett. 1998;160(1):91-6.
91. Park CB, Kim HS, Kim SC. Mechanism of action of the antimicrobial peptide buforin II: buforin II kills microorganisms by penetrating the cell membrane and inhibiting cellular functions. Biochem Biophys Res Commun. 1998;244(1):253-7.
92. Park CB, Yi KS, Matsuzaki K, Kim MS, Kim SC. Structure-activity analysis of buforin II, a histone H2A-derived antimicrobial peptide: the proline hinge is responsible for the cell-penetrating ability of buforin II. Proc Natl Acad Sci U S A. 2000;97(15):8245-50.
93. Salomon RA, Farias RN. Microcin 25, a novel antimicrobial peptide produced by Escherichia coli. J Bacteriol. 1992;174(22):7428-35.
94. Ishikawa M, Kubo T, Natori S. Purification and characterization of a diptericin homologue from Sarcophaga peregrina (flesh fly). Biochem J. 1992;287 (Pt 2):573-8.
95. Gusman H, Grogan J, Kagan HM, Troxler RF, Oppenheim FG. Salivary histatin 5 is a potent competitive inhibitor of the cysteine proteinase clostripain. FEBS Lett. 2001;489(1):97-100.
96. Gusman H, Lendenmann U, Grogan J, Troxler RF, Oppenheim FG. Is salivary histatin 5 a metallopeptide? Biochim Biophys Acta. 2001;1545(1-2):86-95.
97. Gusman H, Travis J, Helmerhorst EJ, Potempa J, Troxler RF, Oppenheim FG. Salivary histatin 5 is an inhibitor of both host and bacterial enzymes implicated in periodontal disease. Infect Immun. 2001;69(3):1402-8.
98. MacKay BJ, Denepitiya L, Iacono VJ, Krost SB, Pollock JJ. Growth-inhibitory and bactericidal effects of human parotid salivary histidine-rich polypeptides on Streptococcus mutans. Infect Immun. 1984;44(3):695-701.
99. Couto MA, Harwig SS, Cullor JS, Hughes JP, Lehrer RI. eNAP-2, a novel cysteine-rich bactericidal peptide from equine leukocytes. Infection and immunity. 1992;60(12):5042-7.

100. Couto MA, Harwig SS, Lehrer RI. Selective inhibition of microbial serine proteases by eNAP-2, an antimicrobial peptide from equine neutrophils. Infect Immun. 1993;61(7):2991-4.
101. Piers KL, Brown MH, Hancock RE. Improvement of outer membrane-permeabilizing and lipopolysaccharide-binding activities of an antimicrobial cationic peptide by C-terminal modification. Antimicrob Agents Chemother. 1994;38(10):2311-6.
102. Piers KL, Hancock RE. The interaction of a recombinant cecropin/melittin hybrid peptide with the outer membrane of Pseudomonas aeruginosa. Mol Microbiol. 1994;12(6):951-8.
103. Esmon CT. Regulation of blood coagulation. Biochim Biophys Acta. 2000;1477(1-2):349-60.
104. Bernard GR, Vincent JL, Laterre PF, LaRosa SP, Dhainaut JF, Lopez-Rodriguez A, et al. Efficacy and safety of recombinant human activated protein C for severe sepsis. N Engl J Med. 2001;344(10):699-709.
105. Brotz H, Bierbaum G, Leopold K, Reynolds PE, Sahl HG. The lantibiotic mersacidin inhibits peptidoglycan synthesis by targeting lipid II. Antimicrob Agents Chemother. 1998;42(1):154-60.
106. Brotz H, Bierbaum G, Reynolds PE, Sahl HG. The lantibiotic mersacidin inhibits peptidoglycan biosynthesis at the level of transglycosylation. Eur J Biochem. 1997;246(1):193-9.
107. Breukink E, de Kruijff B. Lipid II as a target for antibiotics. Nat Rev Drug Discov. 2006;5(4):321-32.
108. Hasper HE, Kramer NE, Smith JL, Hillman JD, Zachariah C, Kuipers OP, et al. An alternative bactericidal mechanism of action for lantibiotic peptides that target lipid II. Science. 2006;313(5793):1636-7.
109. Essig A, Hofmann D, Munch D, Gayathri S, Kunzler M, Kallio PT, et al. Copsin, a novel peptide-based fungal antibiotic interfering with the peptidoglycan synthesis. J Biol Chem. 2014;289(50):34953-64.
110. Niyonsaba F, Iwabuchi K, Someya A, Hirata M, Matsuda H, Ogawa H, et al. A cathelicidin family of human antibacterial peptide LL-37 induces mast cell chemotaxis. Immunology. 2002;106(1):20-6.
111. Garcia JR, Jaumann F, Schulz S, Krause A, Rodriguez-Jimenez J, Forssmann U, et al. Identification of a novel, multifunctional beta-defensin (human beta-defensin 3) with specific antimicrobial activity. Its interaction with plasma membranes of Xenopus oocytes and the induction of macrophage chemoattraction. Cell Tissue Res. 2001;306(2):257-64.
112. Hilchie AL, Wuerth K, Hancock RE. Immune modulation by multifaceted cationic host defense (antimicrobial) peptides. Nat Chem Biol. 2013;9(12):761-8.
113. Stephens JM. BACTERICIDAL ACTIVITY OF THE BLOOD OF ACTIVELY IMMUNIZED WAX MOTH LARVAE. Canadian Journal of Microbiology. 1962;8(4):491-9.
114. Hink WF, Briggs, J.D. Bactericidal factors in hemolymph from normal and immune wax moth larvae, *Galleria mellonella*. Journal of Insect Physiology 1968;14(7):10.
115. Powning RF, Davidson WJ. Studies on insect bacteriolytic enzymes. I. Lysozyme in haemolymph of Galleria mellonella and Bombyx mori. Comparative biochemistry and physiology B, Comparative biochemistry. 1973;45(3):669-86.
116. Boman HG, Nilsson-Faye I, Paul K, Rasmuson T. Insect immunity. I. Characteristics of an inducible cell-free antibacterial reaction in hemolymph of Samia cynthia pupae. Infect Immun. 1974;10(1):136-45.
117. Faye I, Pye A, Rasmuson T, Boman HG, Boman IA. Insect immunity. 11. Simultaneous induction of antibacterial activity and selection synthesis of some hemolymph proteins in diapausing pupae of Hyalophora cecropia and Samia cynthia. Infect Immun.

1975;12(6):1426-38.
118. Steiner H, Hultmark D, Engström A, Bennich H, Boman HG. Sequence and specificity of two antibacterial proteins involved in insect immunity. Nature. 1981;292(5820):246-8.
119. Díaz-Garrido P, Sepúlveda-Robles O, Martínez-Martínez I, Espinoza B. Variability of defensin genes from a Mexican endemic Triatominae: Triatoma (Meccus) pallidipennis (Hemiptera: Reduviidae). Bioscience reports. 2018;38(5):BSR20180988.
120. Waniek PJ, Castro HC, Sathler PC, Miceli L, Jansen AM, Araujo CA. Two novel defensin-encoding genes of the Chagas disease vector Triatoma brasiliensis (Reduviidae, Triatominae): gene expression and peptide-structure modeling. J Insect Physiol. 2009;55(9):840-8.
121. Assumpção TCF, Francischetti IMB, Andersen JF, Schwarz A, Santana JM, Ribeiro JMC. An insight into the sialome of the blood-sucking bug Triatoma infestans, a vector of Chagas' disease. Insect biochemistry and molecular biology. 2008;38(2):213-32.
122. Riedel T, Suttnar J, Brynda E, Houska M, Medved L, Dyr JE. Fibrinopeptides A and B release in the process of surface fibrin formation. Blood. 2011;117(5):1700-6.
123. Vanden Broeck J, Torfs H, Poels J, Van Poyer W, Swinnen E, Ferket K, et al. Tachykinin-like peptides and their receptors. A review. Ann N Y Acad Sci. 1999;897:374-87.
124. Ng R. Chapter 2: DRUG DISCOVERY: SMALL MOLECULE DRUGS. Drugs: From Discovery to Approval. Second edition ed. Hoboken, NJ, USA: John Wiley & Sons, Inc.; 2008.
125. Ng R. Chapter 5: Drug development and preclinical studies. Drugs: From Discovery to Approval
Hoboken, NJ, USA: John Wiley & Sons, Inc; 2008.
126. Romanha AJ, Castro SLd, Soeiro MdNC, Lannes-Vieira J, Ribeiro I, Talvani A, et al. In vitro and in vivo experimental models for drug screening and development for Chagas disease. Memórias do Instituto Oswaldo Cruz. 2010;105:233-8.
127. Breyer MD, Look AT, Cifra A. From bench to patient: model systems in drug discovery. Disease Models & Mechanisms. 2015;8(10):1171.
128. Cassar S, Adatto I, Freeman JL, Gamse JT, Iturria I, Lawrence C, et al. Use of Zebrafish in Drug Discovery Toxicology. Chem Res Toxicol. 2020;33(1):95-118.
129. Doughty BL. Schistosomes and other Trematodes. In: Baron S, editor. Medical Microbiology. 4 ed. Galveston, Texas: University of Texas Medical Branch at Galveston; 1996.
130. Samboon LL. 1. Descriptions of some New Species of Animal Parasites. Proceedings of the Zoological Society of London. 1907;77(2):282-3.
131. Smithers SR, Terry RJ. The infection of laboratory hosts with cercariae of Schistosoma mansoni and the recovery of the adult worms. Parasitology. 1965;55(4):695-700.
132. Xiao S-H, Keiser J, Chollet J, Utzinger J, Dong Y, Endriss Y, et al. In vitro and in vivo activities of synthetic trioxolanes against major human schistosome species. Antimicrobial agents and chemotherapy. 2007;51(4):1440-5.
133. Stein EM, Machado LP, Roffato HK, Miyasato PA, Nakano E, Colepicolo P, et al. Antischistosomal activity from Brazilian marine algae. Revista Brasileira de Farmacognosia. 2015;25:663-7.
134. Ammerman NC, Beier-Sexton M, Azad AF. Growth and maintenance of Vero cell lines. Curr Protoc Microbiol. 2008;Appendix 4:Appendix-4E.
135. Yin-Murphy M. AJW. Picornaviruses. In: Baron S, editor. Medical Microbiology. Galveston (TX): University of Texas Medical Branch at Galveston; 1996.
136. Enders G. Paramyxoviruses. In: Baron S, editor. Medical Microbiology. 4 ed. Galveston (TX): University of Texas Medical Branch at Galveston; 1996.
137. Abushouk AI, Negida A, Ahmed H. An updated review of Zika virus. Journal of

Clinical Virology. 2016;84:53-8.
138. Cunha RVd, Trinta KS. Chikungunya virus: clinical aspects and treatment - A Review. Memórias do Instituto Oswaldo Cruz. 2017;112:523-31.
139. Reed LJ, Muench H. A SIMPLE METHOD OF ESTIMATING FIFTY PER CENT ENDPOINTS12. American Journal of Epidemiology. 1938;27(3):493-7.
140. Sayegh RS, Batista IF, Melo RL, Riske KA, Daffre S, Montich G, et al. Longipin: An Amyloid Antimicrobial Peptide from the Harvestman Acutisoma longipes (Arachnida: Opiliones) with Preferential Affinity for Anionic Vesicles. PLoS One. 2016;11(12):e0167953.
141. Hao G, Shi YH, Tang YL, Le GW. The membrane action mechanism of analogs of the antimicrobial peptide Buforin 2. Peptides. 2009;30(8):1421-7.
142. Nan YH, Bang JK, Jacob B, Park IS, Shin SY. Prokaryotic selectivity and LPS-neutralizing activity of short antimicrobial peptides designed from the human antimicrobial peptide LL-37. Peptides. 2012;35(2):239-47.
143. Chaparro E, da Silva PIJ. Lacrain: the first antimicrobial peptide from the body extract of the Brazilian centipede Scolopendra viridicornis. Int J Antimicrob Agents. 2016;48(3):277-85.
144. Lopes-Ferreira M, Moura-da-Silva AM, Piran-Soares AA, Angulo Y, Lomonte B, Gutiérrez JM, et al. Hemostatic effects induced by Thalassophryne nattereri fish venom: a model of endothelium-mediated blood flow impairment. Toxicon. 2002;40(8):1141-147.
145. Lopes-Ferreira M, martins Gomes E, Bruni F, Ferreira M, Charvet P, Lima C. First report of Interruption of mast cell degranulation and endothelial cells activation by anti-inflammatory drugs controlling the acute response provoked by Pseudoplatystoma fasciatum fish venom. Toxicon : official journal of the International Society on Toxinology. 2014;90.
146. Busquet F, halder, Braunbeck T, gourmelon, Lillicrap A, Kleensang A, et al. OECD GUIDELINES FOR THE TESTING OF CHEMICALS 236 - Fish Embryo Acute Toxicity (FET) Test. The OECD observer Organisation for Economic Co-operation and Development. 2013.
147. Kimmel CB, Ballard WW, Kimmel SR, Ullmann B, Schilling TF. Stages of embryonic development of the zebrafish. Developmental dynamics : an official publication of the American Association of Anatomists. 1995;203(3):253-310.
148. Landry BS, Dextraze L, Boivin G. Random amplified polymorphic DNA markers for DNA fingerprinting and genetic variability assessment of minute parasitic wasp species (Hymenoptera: Mymaridae and Trichogrammatidae) used in biological control programs of phytophagous insects. Genome. 1993;36(3):580-7.
149. Yang N, Liu X, Teng D, Li Z, Wang X, Mao R, et al. Antibacterial and detoxifying activity of NZ17074 analogues with multi-layers of selective antimicrobial actions against Escherichia coli and Salmonella enteritidis. Sci Rep. 2017;7(1):3392.
150. Leick M, Azcutia V, Newton G, Luscinskas FW. Leukocyte recruitment in inflammation: basic concepts and new mechanistic insights based on new models and microscopic imaging technologies. Cell and tissue research. 2014;355(3):647-56.
151. Corrêa JAF, Evangelista AG, Nazareth TdM, Luciano FB. Fundamentals on the molecular mechanism of action of antimicrobial peptides. Materialia. 2019;8:100494.
152. Ferrari MLA, Coelho PMZ, Antunes CMF, Tavares CAP, da Cunha AS. Efficacy of oxamniquine and praziquantel in the treatment of Schistosoma mansoni infection: a controlled trial. Bulletin of the World Health Organization. 2003;81(3):190-6.
153. Caffrey CR. Chemotherapy of schistosomiasis: present and future. Curr Opin Chem Biol. 2007;11(4):433-9.
154. Doenhoff MJ, Pica-Mattoccia L. Praziquantel for the treatment of schistosomiasis: its use for control in areas with endemic disease and prospects for drug resistance. Expert Rev Anti Infect Ther. 2006;4(2):199-210.

155. Lima RM, Ferreira MA, de Jesus Ponte Carvalho TM, Dumet Fernandes BJ, Takayanagui OM, Garcia HH, et al. Albendazole-praziquantel interaction in healthy volunteers: kinetic disposition, metabolism and enantioselectivity. Br J Clin Pharmacol. 2011;71(4):528-35.
156. Na-Bangchang K, Kietinun S, Pawa KK, Hanpitakpong W, Na-Bangchang C, Lazdins J. Assessments of pharmacokinetic drug interactions and tolerability of albendazole, praziquantel and ivermectin combinations. Trans R Soc Trop Med Hyg. 2006;100(4):335-45.
157. Moraes J, Nascimento C, Lopes PO, Nakano E, Yamaguchi LF, Kato MJ, et al. Schistosoma mansoni: In vitro schistosomicidal activity of piplartine. Exp Parasitol. 2011;127(2):357-64.
158. Abdulla MH, Lim KC, Sajid M, McKerrow JH, Caffrey CR. Schistosomiasis mansoni: novel chemotherapy using a cysteine protease inhibitor. PLoS Med. 2007;4(1):e14.
159. Coen DM, Richman DD. Antiviral agents. 2013.
160. Cattaneo R, McChesney M. Measles Virus. In: Mahy BWJ, Van Regenmortel MHV, editors. Encyclopedia of Virology (Third Edition). Oxford: Academic Press; 2008. p. 285-91.
161. Griffin DE, Lin W-H, Pan C-H. Measles virus, immune control, and persistence. FEMS microbiology reviews. 2012;36(3):649-62.
162. Zhou Y, Su JM, Samuel CE, Ma D. Measles Virus Forms Inclusion Bodies with Properties of Liquid Organelles. Journal of Virology. 2019;93(21):e00948-19.
163. Mathieu C, Huey D, Jurgens E, Welsch JC, DeVito I, Talekar A, et al. Prevention of measles virus infection by intranasal delivery of fusion inhibitor peptides. J Virol. 2015;89(2):1143-55.
164. Welsch JC, Talekar A, Mathieu C, Pessi A, Moscona A, Horvat B, et al. Fatal measles virus infection prevented by brain-penetrant fusion inhibitors. J Virol. 2013;87(24):13785-94.
165. Sun A, Chandrakumar N, Yoon JJ, Plemper RK, Snyder JP. Non-nucleoside inhibitors of the measles virus RNA-dependent RNA polymerase complex activity: Synthesis and in vitro evaluation. Bioorg Med Chem Lett. 2007;17(18):5199-203.
166. Vilas Boas LCP, Campos ML, Berlanda RLA, de Carvalho Neves N, Franco OL. Antiviral peptides as promising therapeutic drugs. Cell Mol Life Sci. 2019;76(18):3525-42.
167. Mata ÉCGd, Mourão CBF, Rangel M, Schwartz EF. Antiviral activity of animal venom peptides and related compounds. Journal of Venomous Animals and Toxins including Tropical Diseases. 2017;23.
168. Li Q, Zhao Z, Zhou D, Chen Y, Hong W, Cao L, et al. Virucidal activity of a scorpion venom peptide variant mucroporin-M1 against measles, SARS-CoV and influenza H5N1 viruses. Peptides. 2011;32(7):1518-25.
169. Carriel-Gomes MC, Kratz JM, Barracco MA, Bachére E, Barardi CR, Simões CM. In vitro antiviral activity of antimicrobial peptides against herpes simplex virus 1, adenovirus, and rotavirus. Mem Inst Oswaldo Cruz. 2007;102(4):469-72.
170. Wang W, Owen SM, Rudolph DL, Cole AM, Hong T, Waring AJ, et al. Activity of alpha- and theta-defensins against primary isolates of HIV-1. J Immunol. 2004;173(1):515-20.
171. Racaniello VR. Picornaviridae: The viruses and their replication. In: A. G, D..E., Lamb, R..A. et al., editor. Fields Virology. 5 ed. Philadelphia: Wolters Klewer / Lippincott Williams & Wilkins.; 2007.
172. Ryu W-S. Chapter 11 - Picornavirus. In: Ryu W-S, editor. Molecular Virology of Human Pathogenic Viruses. Boston: Academic Press; 2017. p. 153-64.
173. Müller C, Schulte FW, Lange-Grünweller K, Obermann W, Madhugiri R, Pleschka S, et al. Broad-spectrum antiviral activity of the eIF4A inhibitor silvestrol against corona- and picornaviruses. Antiviral Research. 2018;150:123-9.
174. Choi H-J. Evaluation of Antiviral Activity of Zanthoxylum Species Against

Picornaviruses. Osong Public Health and Research Perspectives. 2016;7(6):400-3.
175. Ankel H, Mittnacht S, Jacobsen H. Antiviral activity of prostaglandin A on encephalomyocarditis virus-infected cells: a unique effect unrelated to interferon. J Gen Virol. 1985;66 (Pt 11):2355-64.
176. Kawamoto S, Oritani K, Asada H, Takahashi I, Ishikawa J, Yoshida H, et al. Antiviral activity of limitin against encephalomyocarditis virus, herpes simplex virus, and mouse hepatitis virus: diverse requirements by limitin and alpha interferon for interferon regulatory factor 1. J Virol. 2003;77(17):9622-31.
177. Mayer IA, Verma A, Grumbach IM, Uddin S, Lekmine F, Ravandi F, et al. The p38 MAPK pathway mediates the growth inhibitory effects of interferon-alpha in BCR-ABL-expressing cells. J Biol Chem. 2001;276(30):28570-7.
178. Stebbing N, Weck PK, Fenno JT, Estell DA, Rinderknecht E. Antiviral effects of bacteria-derived human leukocyte interferons against encephalomyocarditis virus infection of squirrel monkeys. Brief report. Arch Virol. 1983;76(4):365-72.
179. Monel B, Compton AA, Bruel T, Amraoui S, Burlaud-Gaillard J, Roy N, et al. Zika virus induces massive cytoplasmic vacuolization and paraptosis-like death in infected cells. The EMBO Journal. 2017;36(12):1653-68.
180. Li Y-G, Siripanyaphinyo U, Tumkosit U, Noranate N, A-Nuegoonpipat A, Tao R, et al. Chikungunya Virus Induces a More Moderate Cytopathic Effect in Mosquito Cells than in Mammalian Cells. Intervirology. 2012;56.
181. Alpuche-Lazcano SP, McCullogh CR, Del Corpo O, Rance E, Scarborough RJ, Mouland AJ, et al. Higher Cytopathic Effects of a Zika Virus Brazilian Isolate from Bahia Compared to a Canadian-Imported Thai Strain. Viruses. 2018;10(2):53.
182. Chen H, Lao Z, Xu J, Li Z, Long H, Li D, et al. Antiviral activity of lycorine against Zika virus in vivo and in vitro. Virology. 2020;546:88-97.
183. Quintana VM, Selisko B, Brunetti JE, Eydoux C, Guillemot JC, Canard B, et al. Antiviral activity of the natural alkaloid anisomycin against dengue and Zika viruses. Antiviral Research. 2020;176:104749.
184. Ferreira FL, Hauck MS, Duarte LP, Magalhães JCd, Silva LSMd, Pimenta LPS, et al. Zika Virus Activity of the Leaf and Branch Extracts of Tontelea micrantha and Its Hexane Extracts Phytochemical Study. Journal of the Brazilian Chemical Society. 2019;30:793-803.
185. Lani R, Hassandarvish P, Shu M-H, Phoon WH, Chu JJH, Higgs S, et al. Antiviral activity of selected flavonoids against Chikungunya virus. Antiviral Research. 2016;133:50-61.
186. Troost B, Mulder LM, Diosa-Toro M, van de Pol D, Rodenhuis-Zybert IA, Smit JM. Tomatidine, a natural steroidal alkaloid shows antiviral activity towards chikungunya virus in vitro. Scientific Reports. 2020;10(1):6364.
187. Hitakarun A, Khongwichit S, Wikan N, Roytrakul S, Yoksan S, Rajakam S, et al. Evaluation of the antiviral activity of orlistat (tetrahydrolipstatin) against dengue virus, Japanese encephalitis virus, Zika virus and chikungunya virus. Scientific Reports. 2020;10(1):1499.
188. Loe MWC, Lee RCH, Chu JJH. Antiviral activity of the FDA-approved drug candesartan cilexetil against Zika virus infection. Antiviral Res. 2019;172:104637.
189. Weigert R, Sramkova M, Parente L, Amornphimoltham P, Masedunskas A. Intravital microscopy: a novel tool to study cell biology in living animals. Histochemistry and cell biology. 2010;133(5):481-91.
190. Touyz RM, Alves-Lopes R, Rios FJ, Camargo LL, Anagnostopoulou A, Arner A, et al. Vascular smooth muscle contraction in hypertension. Cardiovascular research. 2018;114(4):529-39.
191. Tucker WD AY, Mahajan K. Anatomy, Blood Vessels. Treasure Island (FL):

StatPearls Publishing: StatPearls [Internet]; 2020 [Available from: https://www.ncbi.nlm.nih.gov/books/NBK470401/.
192. Welsh DG, Tran CHT, Hald BO, Sancho M. The Conducted Vasomotor Response: Function, Biophysical Basis, and Pharmacological Control. Annual review of pharmacology and toxicology. 2018;58:391-410.
193. Brozovich FV, Nicholson CJ, Degen CV, Gao YZ, Aggarwal M, Morgan KG. Mechanisms of Vascular Smooth Muscle Contraction and the Basis for Pharmacologic Treatment of Smooth Muscle Disorders. Pharmacol Rev. 2016;68(2):476-532.
194. Kumar VA, AK.; Fausto, N.; Aster, J. . Robbins and Cotran: Pathologic Basis of Disease. Philadelphia: Elservier; 2010.
195. von Andrian UH, Chambers JD, McEvoy LM, Bargatze RF, Arfors KE, Butcher EC. Two-step model of leukocyte-endothelial cell interaction in inflammation: distinct roles for LECAM-1 and the leukocyte beta 2 integrins in vivo. Proc Natl Acad Sci U S A. 1991;88(17):7538-42.
196. Chen L, Deng H, Cui H, Fang J, Zuo Z, Deng J, et al. Inflammatory responses and inflammation-associated diseases in organs. Oncotarget. 2017;9(6):7204-18.
197. Teame T, Zhang Z, Ran C, Zhang H, Yang Y, Ding Q, et al. The use of zebrafish (Danio rerio) as biomedical models. Animal Frontiers. 2019;9(3):68-77.
198. Meyers JR. Zebrafish: Development of a Vertebrate Model Organism. Current Protocols Essential Laboratory Techniques. 2018;16(1):e19.
199. Lindsey BW, Kaslin J. Optical Projection Tomography as a Novel Method to Visualize and Quantitate Whole-Brain Patterns of Cell Proliferation in the Adult Zebrafish Brain. Zebrafish. 2017;14(6):574-7.
200. Siegenthaler PF, Bain P, Riva F, Fent K. Effects of antiandrogenic progestins, chlormadinone and cyproterone acetate, and the estrogen 17α-ethinylestradiol (EE2), and their mixtures: Transactivation with human and rainbowfish hormone receptors and transcriptional effects in zebrafish (Danio rerio) eleuthero-embryos. Aquatic toxicology (Amsterdam, Netherlands). 2017;182:142-62.
201. Fulcher N, Tran S, Shams S, Chatterjee D, Gerlai R. Neurochemical and Behavioral Responses to Unpredictable Chronic Mild Stress Following Developmental Isolation: The Zebrafish as a Model for Major Depression. Zebrafish. 2017;14(1):23-34.
202. Fazio M, Avagyan S, van Rooijen E, Mannherz W, Kaufman CK, Lobbardi R, et al. Efficient Transduction of Zebrafish Melanoma Cell Lines and Embryos Using Lentiviral Vectors. Zebrafish. 2017;14(4):379-82.
203. Schultz LE, Solin SL, Wierson WA, Lovan JM, Syrkin-Nikolau J, Lincow DE, et al. Vascular Endothelial Growth Factor A and Leptin Expression Associated with Ectopic Proliferation and Retinal Dysplasia in Zebrafish Optic Pathway Tumors. Zebrafish. 2017;14(4):343-56.
204. Tavares B, Santos Lopes S. The importance of Zebrafish in biomedical research. Acta Med Port. 2013;26(5):583-92.
205. Thompson F, de Oliveira BC, Cordeiro MC, Masi BP, Rangel TP, Paz P, et al. Severe impacts of the Brumadinho dam failure (Minas Gerais, Brazil) on the water quality of the Paraopeba River. Science of The Total Environment. 2020;705:135914.
206. Tesolin G, Marson M, Jonsson C, Nogueira A, Franco DAs, Almeida S, et al. Avaliação da toxicidade de herbicidas usados em cana-de-açúcar para o Paulistinha (Danio rerio). O Mundo da Saúde 1980-3990. 2014;38:86-97.
207. MacRae CA, Peterson RT. Zebrafish as tools for drug discovery. Nature Reviews Drug Discovery. 2015;14(10):721-31.
208. Vaz RL, Outeiro TF, Ferreira JJ. Zebrafish as an Animal Model for Drug Discovery in Parkinson's Disease and Other Movement Disorders: A Systematic Review. Frontiers in

Neurology. 2018;9(347).
209. Alafiatayo AA, Lai K-S, Syahida A, Mahmood M, Shaharuddin NA. Phytochemical Evaluation, Embryotoxicity, and Teratogenic Effects of Curcuma longa Extract on Zebrafish (Danio rerio). Evidence-Based Complementary and Alternative Medicine. 2019;2019:3807207.
210. Price RL, Bugeon L, Mostowy S, Makendi C, Wren BW, Williams HD, et al. In vitro and in vivo properties of the bovine antimicrobial peptide, Bactenecin 5. PLOS ONE. 2019;14(1):e0210508.
211. Morash MG, Douglas SE, Robotham A, Ridley CM, Gallant JW, Soanes KH. The zebrafish embryo as a tool for screening and characterizing pleurocidin host-defense peptides as anti-cancer agents. Disease Models & Mechanisms. 2011;4(5):622-33.
212. Maharajan K, Muthulakshmi S, Nataraj B, Ramesh M, Kadirvelu K. Toxicity assessment of pyriproxyfen in vertebrate model zebrafish embryos (Danio rerio): A multi biomarker study. Aquatic toxicology (Amsterdam, Netherlands). 2018;196:132-45.
213. Cebrian R, Rodriguez-Cabezas ME, Martin-Escolano R, Rubino S, Garrido-Barros M, Montalban-Lopez M, et al. Preclinical studies of toxicity and safety of the AS-48 bacteriocin. J Adv Res. 2019;20:129-39.
214. Vicentin MCG. Estudo de peptídeos antimicrobianos contra Candida albicans e avaliação da segurança em modelo Zebrafish (Danio rerio). Araraquara: UNIVERSIDADE ESTADUAL PAULISTA JÚLIO DE MESQUITA FILHO; 2019.
215. Shi W, Li C, Li M, Zong X, Han D, Chen Y. Antimicrobial peptide melittin against Xanthomonas oryzae pv. oryzae, the bacterial leaf blight pathogen in rice. Appl Microbiol Biotechnol. 2016;100(11):5059-67.
216. Díaz-Roa A, Espinoza-Culupú A, Torres-García O, Borges MM, Avino IN, Alves FL, et al. Sarconesin II, a New Antimicrobial Peptide Isolated from Sarconesiopsis magellanica Excretions and Secretions. Molecules. 2019;24(11).
217. Epand RM, Vogel HJ. Diversity of antimicrobial peptides and their mechanisms of action. Biochimica et Biophysica Acta (BBA) - Biomembranes. 1999;1462(1):11-28.
218. Boman HG, Agerberth B, Boman A. Mechanisms of action on Escherichia coli of cecropin P1 and PR-39, two antibacterial peptides from pig intestine. Infect Immun. 1993;61(7):2978-84.
219. Martins LPA, Castanho REP, Da Rosa JA, Tokumo MO, De Godoy CAP, Rosa RM. Estudo comparativo entre duas técnicas de xenodiagnóstico artificial aplicado empacientes chagásicos cronicos. Revista de Patologia Tropical. 2001;30(1):8.
220. Bulet P, Dimarcq JL, Hetru C, Lagueux M, Charlet M, Hegy G, et al. A novel inducible antibacterial peptide of Drosophila carries an O-glycosylated substitution. J Biol Chem. 1993;268(20):14893-7.
221. Wayne PA. Reference for Broth Dilution Antifungal Susceptibility Testing of Yeasts; Approved Standard - M27-A3. Clinical and Laboratory Standards Institute
2008.
222. Hancock RE. Modifies MIC Method for Cationic Antimicrobial Peptides: University of British Columbia; 1999 [Available from: http://cmdr.ubc.ca/bobh/method/modified-mic-method-for-cationic-antimicrobial-peptides/.
223. Yamamoto LG. Inhibitory and Bactericidal Principles (MIC & MBC). Case Based Pediatrics For Medical Students and Residents. University of Hawaii John A. Burns School of Medicine2003.
224. Miranda A, Koerber SC, Gulyas J, Lahrichi SL, Craig AG, Corrigan A, et al. Conformationally restricted competitive antagonists of human/rat corticotropin-releasing factor. J Med Chem. 1994;37(10):1450-9.
225. Anthis NJ, Clore GM. Sequence-specific determination of protein and peptide

concentrations by absorbance at 205 nm. Protein Sci. 2013;22(6):851-8.
226. Watson FL, Püttmann-Holgado R, Thomas F, Lamar DL, Hughes M, Kondo M, et al. Extensive diversity of Ig-superfamily proteins in the immune system of insects. Science. 2005;309(5742):1874-8.
227. Kurtz J, Franz K. Innate defence: evidence for memory in invertebrate immunity. Nature. 2003;425(6953):37-8.
228. Little TJ, Hultmark D, Read AF. Invertebrate immunity and the limits of mechanistic immunology. Nat Immunol. 2005;6(7):651-4.
229. Sadd BM, Schmid-Hempel P. Insect immunity shows specificity in protection upon secondary pathogen exposure. Curr Biol. 2006;16(12):1206-10.
230. Aaron SD, Ferris W, Henry DA, Speert DP, Macdonald NE. Multiple combination bactericidal antibiotic testing for patients with cystic fibrosis infected with Burkholderia cepacia. Am J Respir Crit Care Med. 2000;161(4 Pt 1):1206-12.
231. Yan H, Hancock RE. Synergistic interactions between mammalian antimicrobial defense peptides. Antimicrob Agents Chemother. 2001;45(5):1558-60.
232. Tamma PD, Cosgrove SE, Maragakis LL. Combination therapy for treatment of infections with gram-negative bacteria. Clinical microbiology reviews. 2012;25(3):450-70.
233. Doern CD. When does 2 plus 2 equal 5? A review of antimicrobial synergy testing. J Clin Microbiol. 2014;52(12):4124-8.
234. Nuding S, Frasch T, Schaller M, Stange EF, Zabel LT. Synergistic effects of antimicrobial peptides and antibiotics against Clostridium difficile. Antimicrob Agents Chemother. 2014;58(10):5719-25.
235. Zerweck J, Strandberg E, Kukharenko O, Reichert J, Bürck J, Wadhwani P, et al. Molecular mechanism of synergy between the antimicrobial peptides PGLa and magainin 2. Sci Rep. 2017;7(1):13153.
236. Påhlman LI, Mörgelin M, Kasetty G, Olin AI, Schmidtchen A, Herwald H. Antimicrobial activity of fibrinogen and fibrinogen-derived peptides--a novel link between coagulation and innate immunity. Thromb Haemost. 2013;109(5):930-9.
237. Tang YQ, Yeaman MR, Selsted ME. Antimicrobial peptides from human platelets. Infect Immun. 2002;70(12):6524-33.
238. Pagnocca F, Masiulionis V, Rodrigues A. Specialized Fungal Parasites and Opportunistic Fungi in Gardens of Attine Ants. Psyche. 2012;2012.
239. Biedermann PH, Klepzig KD, Taborsky M, Six DL. Abundance and dynamics of filamentous fungi in the complex ambrosia gardens of the primitively eusocial beetle Xyleborinus saxesenii Ratzeburg (Coleoptera: Curculionidae, Scolytinae). FEMS Microbiol Ecol. 2013;83(3):711-23.
240. Bateman C, Kendra P, Rabaglia R, Hulcr J. Fungal symbionts in three exotic ambrosia beetles, Xylosandrus amputatus, Xyleborinus andrewesi, and Dryoxylon onoharaense (Coleoptera: Curculionidae: Scolytinae: Xyleborini) in Florida. Symbiosis. 2015;66.
241. Moubasher A, Abdel-Sater MA, Soliman Z. Yeasts and filamentous fungi inhabiting guts of three insect species in Assiut, Egypt. Mycosphere. 2017;8:1297-316.
242. Wang X, Zhao Q, Christensen BM. Identification and characterization of the fibrinogen-like domain of fibrinogen-related proteins in the mosquito, Anopheles gambiae, and the fruitfly, Drosophila melanogaster, genomes. BMC Genomics. 2005;6:114.
243. Fan C, Zhang S, Li L, Chao Y. Fibrinogen-related protein from amphioxus Branchiostoma belcheri is a multivalent pattern recognition receptor with a bacteriolytic activity. Mol Immunol. 2008;45(12):3338-46.
244. Sterba J, Dupejova J, Fiser M, Vancova M, Grubhoffer L. Fibrinogen-related proteins in ixodid ticks. Parasit Vectors. 2011;4:127.
245. Chai YM, Zhu Q, Yu SS, Zhao XF, Wang JX. A novel protein with a fibrinogen-like

domain involved in the innate immune response of Marsupenaeus japonicus. Fish Shellfish Immunol. 2012;32(2):307-15.
246. Hanington PC, Zhang SM. The primary role of fibrinogen-related proteins in invertebrates is defense, not coagulation. J Innate Immun. 2011;3(1):17-27.
247. Jeffers LA, Michael Roe R. The movement of proteins across the insect and tick digestive system. J Insect Physiol. 2008;54(2):319-32.
248. Wigglesworth VB. The fate of haemoglobin in Rhodnius prolixus (Hemiptera) and other blood-sucking arthropods. Proceedings of the Royal Society of London Series B - Biological Sciences. 1943;131(865):313-39.
249. Scheraga HA. The thrombin-fibrinogen interaction. Biophys Chem. 2004;112(2-3):117-30.
250. Zavalova LL, Basanova AV, Baskova IP. Fibrinogen-fibrin system regulators from bloodsuckers. Biochemistry (Mosc). 2002;67(1):135-42.
251. Bulet P. Strategies for the discovery, isolation, and characterization of natural bioactive peptides from the immune system of invertebrates. Methods Mol Biol. 2008;494:9-29.
252. Wiegand I, Hilpert K, Hancock RE. Agar and broth dilution methods to determine the minimal inhibitory concentration (MIC) of antimicrobial substances. Nat Protoc. 2008;3(2):163-75.
253. Hetru C, Bulet P. Strategies for the isolation and characterization of antimicrobial peptides of invertebrates. Methods Mol Biol. 1997;78:35-49.
254. Poppel AK, Vogel H, Wiesner J, Vilcinskas A. Antimicrobial peptides expressed in medicinal maggots of the blow fly Lucilia sericata show combinatorial activity against bacteria. Antimicrob Agents Chemother. 2015;59(5):2508-14.
255. Lorenzini DM, da Silva PI, Jr., Fogaca AC, Bulet P, Daffre S. Acanthoscurrin: a novel glycine-rich antimicrobial peptide constitutively expressed in the hemocytes of the spider Acanthoscurria gomesiana. Dev Comp Immunol. 2003;27(9):781-91.
256. Universal Protein [Available from: www.uniprot.org
257. National Center for Biotechnology Information [Available from: www.ncbi.nlm.nih.gov
258. Sievers F, Wilm A, Dineen D, Gibson TJ, Karplus K, Li W, et al. Fast, scalable generation of high-quality protein multiple sequence alignments using Clustal Omega. Mol Syst Biol. 2011;7:539.
259. Peptide Property Calculator [Available from: http://pepcalc.com/
260. Wang G, Li X, Wang Z. APD3: the antimicrobial peptide database as a tool for research and education. Nucleic Acids Res. 2016;44(D1):D1087-93.
261. Michael Barrett F. Absorption of fluid from the anterior midgut in Rhodnius. Journal of Insect Physiology. 1982;28(4):335-41.
262. Azambuja Pd, Guimarães JA, Garcia ES. Haemolytic factor from the crop of Rhodnius prolixus: Evidence and partial characterization. Journal of Insect Physiology. 1983;29(11):833-7.
263. Lehane MJ. Managing the blood meal. In: Lehane MJ, editor. The Biology of Blood-Sucking in Insects. 2 ed. Cambridge: Cambridge University Press; 2005. p. 84-115.
264. Schaub GA. Kissing Bugs. In: Mehlhorn H, editor. Encyclopedia of Parasitology. Berlin, Heidelberg: Springer Berlin Heidelberg; 2008. p. 684-.
265. Albritton EC. Standard Values in Blood. Journal of the American Pharmaceutical Association. 1953;42(5):326-.
266. Altman PL, Katz DD. Blood and other body fluids. Washington: Federation of American Societies for Experimental Biology; 1961.
267. Terra WR, Ferreira C. Insect digestive enzymes: properties, compartmentalization and

function. Comparative Biochemistry and Physiology Part B: Comparative Biochemistry. 1994;109(1):1-62.
268. Terra WR, Ferreira C, Garcia ES. Origin, distribution, properties and functions of the major Rhodnius prolixus midgut hydrolases. Insect Biochemistry. 1988;18(5):423-34.
269. Lopez-Ordoñez T, Rodriguez MH, Hernández-Hernández FD. Characterization of a cDNA encoding a cathepsin L-like protein of Rhodnius prolixus. Insect Mol Biol. 2001;10(5):505-11.
270. Kollien AH, Waniek PJ, Nisbet AJ, Billingsley PF, Schaub GA. Activity and sequence characterization of two cysteine proteases in the digestive tract of the reduviid bug Triatoma infestans. Insect Mol Biol. 2004;13(6):569-79.
271. Barrett AJR, N.D.; Wössner, J.F. . Handbook of Proteolytic Enzymes. 2 ed. London, UK: Elsevier; 2004.
272. Balczun C, Pausch J, Schaub G. Blood digestion in triatomines - a review. Mitteilungen der Deutschen Gesellschaft für Allgemeine und Angewandte Entomologie. 2012;18:331-4.
273. Billingsley PF, Downe AER. Cellular localisation of aminopeptidase in the midgut of Rhodnius prolixus Stål (Hemiptera:Reduviidae) during blood digestion. Cell and Tissue Research. 1985;241(2):421-8.
274. Ferreira C, Ribeiro AF, Garcia ES, Terra WR. Digestive enzymes trapped between and associated with the double plasma membranes of Rhodnius prolixus posterior midgut cells. Insect Biochemistry. 1988;18(6):521-30.
275. Brantl V, Gramsch C, Lottspeich F, Mertz R, Jaeger KH, Herz A. Novel opioid peptides derived from hemoglobin: hemorphins. Eur J Pharmacol. 1986;125(2):309-10.
276. Glamsta EL, Marklund A, Hellman U, Wernstedt C, Terenius L, Nyberg F. Isolation and characterization of a hemoglobin-derived opioid peptide from the human pituitary gland. Regul Pept. 1991;34(3):169-79.
277. Glamsta EL, Meyerson B, Silberring J, Terenius L, Nyberg F. Isolation of a hemoglobin-derived opioid peptide from cerebrospinal fluid of patients with cerebrovascular bleedings. Biochem Biophys Res Commun. 1992;184(2):1060-6.
278. Erchegyi J, Kastin AJ, Zadina JE, Qiu XD. Isolation of a heptapeptide Val-Val-Tyr-Pro-Trp-Thr-Gln (valorphin) with some opiate activity. Int J Pept Protein Res. 1992;39(6):477-84.
279. Mihajlovic M, Lazaridis T. Antimicrobial peptides bind more strongly to membrane pores. Biochim Biophys Acta. 2010;1798(8):1494-502.
280. Powers JP, Hancock RE. The relationship between peptide structure and antibacterial activity. Peptides. 2003;24(11):1681-91.
281. Liepke C, Baxmann S, Heine C, Breithaupt N, Standker L, Forssmann WG. Human hemoglobin-derived peptides exhibit antimicrobial activity: a class of host defense peptides. J Chromatogr B Analyt Technol Biomed Life Sci. 2003;791(1-2):345-56.
282. Mak P, Wojcik K, Silberring J, Dubin A. Antimicrobial peptides derived from heme-containing proteins: hemocidins. Antonie Van Leeuwenhoek. 2000;77(3):197-207.
283. Nakajima Y, Ogihara K, Taylor D, Yamakawa M. Antibacterial hemoglobin fragments from the midgut of the soft tick, Ornithodoros moubata (Acari: Argasidae). J Med Entomol. 2003;40(1):78-81.
284. Belmonte R, Cruz CE, Pires JR, Daffre S. Purification and characterization of Hb 98-114: a novel hemoglobin-derived antimicrobial peptide from the midgut of Rhipicephalus (Boophilus) microplus. Peptides. 2012;37(1):120-7.
285. Catiau L, Traisnel J, Chihib NE, Le Flem G, Blanpain A, Melnyk O, et al. RYH: a minimal peptidic sequence obtained from beta-chain hemoglobin exhibiting an antimicrobial activity. Peptides. 2011;32(7):1463-8.

286. Catiau L, Traisnel J, Delval-Dubois V, Chihib NE, Guillochon D, Nedjar-Arroume N. Minimal antimicrobial peptidic sequence from hemoglobin alpha-chain: KYR. Peptides. 2011;32(4):633-8.
287. Froidevaux R, Krier F, Nedjar-Arroume N, Vercaigne-Marko D, Kosciarz E, Ruckebusch C, et al. Antibacterial activity of a pepsin-derived bovine hemoglobin fragment. FEBS Lett. 2001;491(1-2):159-63.
288. Daoud R, Dubois V, Bors-Dodita L, Nedjar-Arroume N, Krier F, Chihib NE, et al. New antibacterial peptide derived from bovine hemoglobin. Peptides. 2005;26(5):713-9.
289. Bah CS, Carne A, McConnell MA, Mros S, Bekhit Ael D. Production of bioactive peptide hydrolysates from deer, sheep, pig and cattle red blood cell fractions using plant and fungal protease preparations. Food Chem. 2016;202:458-66.
290. Nedjar-Arroume N, Dubois-Delval V, Miloudi K, Daoud R, Krier F, Kouach M, et al. Isolation and characterization of four antibacterial peptides from bovine hemoglobin. Peptides. 2006;27(9):2082-9.
291. Hu J, Xu M, Hang B, Wang L, Wang Q, Chen J, et al. Isolation and characterization of an antimicrobial peptide from bovine hemoglobin α-subunit. World Journal of Microbiology and Biotechnology. 2011;27:767-71.
292. Diniz LCL, Miranda A, da Silva PI, Jr. Human Antimicrobial Peptide Isolated From Triatoma infestans Haemolymph, Trypanosoma cruzi-Transmitting Vector. Front Cell Infect Microbiol. 2018;8:354.
293. Roque ALRJ, A.M. Reservatórios do Trypanosoma cruzi e sua relação com os vetores. In: Galvão C, editor. Vetores da doença de Chagas no Brasil Curitiba, Brazil: Sociedade Brasileira de Zoologia; 2014. p. 76-88.

Attachment - Lecture

3rd Global Congress on Antibiotics 2020
Antibiotics, Antimicrobials & Resistance
June 15-16, 2020

LETTER OF INVITATION **Date:** May 26, 2020

To
Laura Cristina Lima Diniz,
Butantan Institute, Brazil

Re: Letter of Invitation to attend Online event on 3rd Global Congress on Antibiotics, Antimicrobials & Resistance (June 15-16, 2020).

Antibiotics 2020, warmly invites you to attend the **"3rd Global Congress on Antibiotics, Antimicrobials & Resistance"** which will be held from **June 15-16, 2020** via webinar.

We welcome you to join us as a **Speaker** to share your knowledge about **" New insights into antimicrobial peptides isolated from Brazilian natural sources"**. In this regard, on behalf of the Organizing Committee, we are pleased to welcome you to join us at Antibiotics 2020.

The Global Congress on Antibiotics, Antimicrobials & Resistance initiated by editors - *Journal of Infectious Diseases and Medical Microbiology, Research and Reports in Immunology, Journal of Bacteriology and Infectious Diseases* and *Journal of Clinical Research and Pharmacy* will offer you an unforgettable experience in exploring new opportunities, enhance your knowledge, widen your network, stimulate your innovative self and expand your vision.

Further to your registration for the event, Your Speaker slot has been confirmed with us.

For more details about Antibiotics 2020, P.S: https://antibiotics.alliedacademies.com/

We look forward to seeing you via Webcast

Thanking You

Erika Madison

Erika Madison
Conference Director | Antibiotics 2020
114a Bellegrove Road,
Welling, England, DA16 3QR
T: +44 20 3769 1755
E: antibiotics@alliedforums.org

Disclaimer: This invitation is to attend Antibiotics 2020 only

allied academies
25th Anniversary of scientific services

114a Bellegrove Road, Welling, England, DA16 3QR
Toll Free: +44 203 769 1755

Certificate of Recognition

Allied Academies and the Editors of Journal of Infectious Diseases and Medical Microbiology, Journal of Clinical Research and Pharmacy & Clinical Immunology and Infectious Diseases wish to thank

Prof/Dr. Laura Cristina Lima Diniz

Butantan Institute, Brazil

for her phenomenal and worthy oral presentation on

"New insights into antimicrobial peptides isolated from Brazilian natural sources"

at the 3rd Global Congress on Antibiotics, Antimicrobials & Resistance held during June 15-16, 2020 in Webinar

John James Stewart Cadwell
FiberCell Systems Inc., USA

Mohammed Sayed Aly Mohamme
National Research Center
Egypt

Antibiotics 2020 Organizing Committee Members

Farid Menaa
California Innovation corporation
USA

Atef ElGendy
United States Naval Medical Research Unit-3
Egypt

Appendix

Supplementary Material – Chapter 3

Figure S1: Deconvolution of two peptides from the fraction A1 (eluted at 24.8min) corresponding to the fragments 2 -10 and 110-117 of hemoglobin α chain.

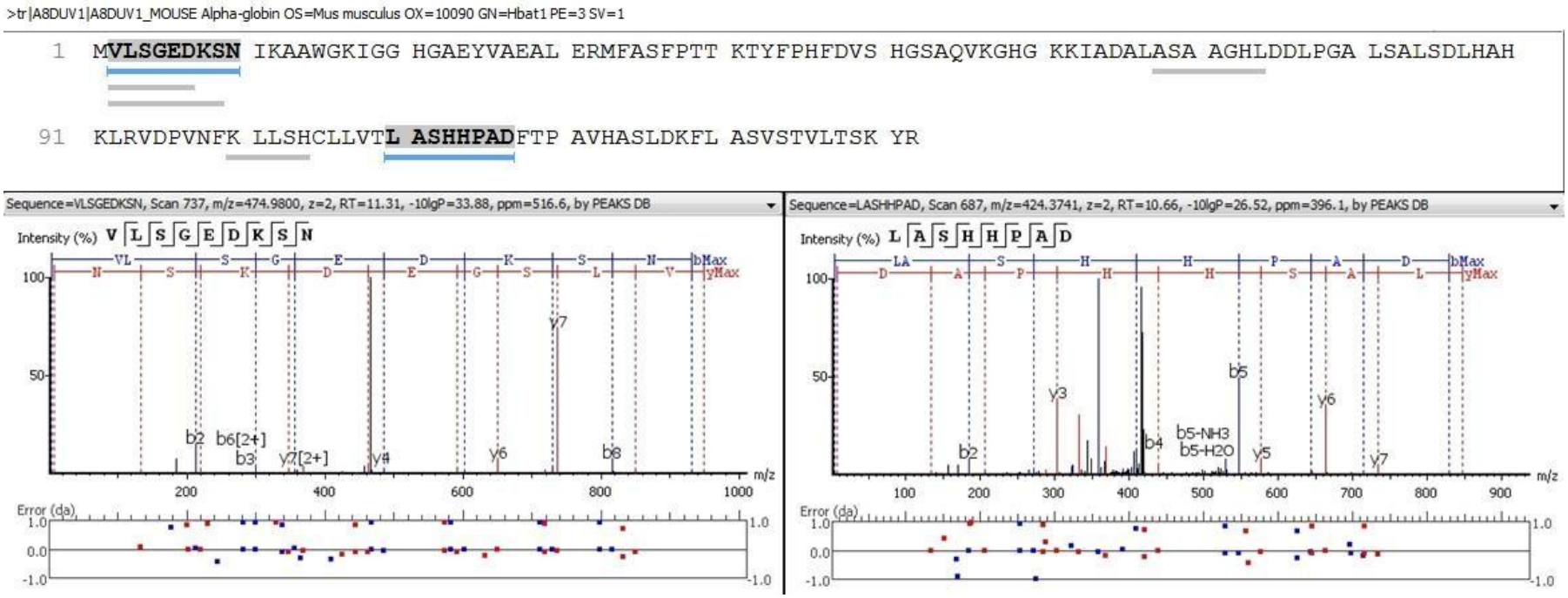

Figure S2: Deconvolution of three peptides from the fraction A2 (eluted at 64.5min) corresponding to the fragments 45-57, 75-95 and 119-145 of hemoglobin α chain.

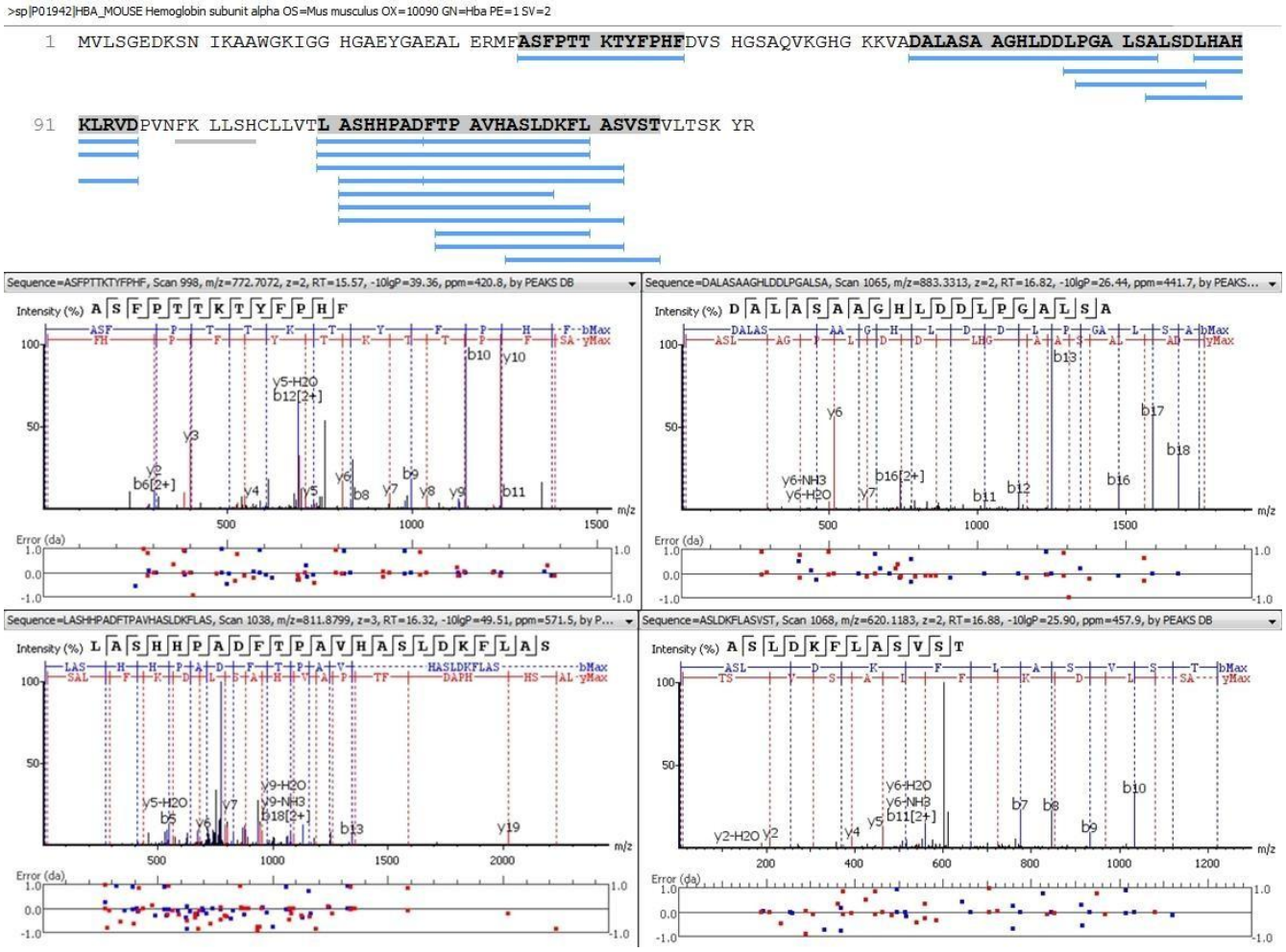

Figure S3: Deconvolution of three peptides from the fraction A3 (eluted at 81.8min) corresponding to the fragments 45-58, 76-104 and 106-147 of hemoglobin α chain

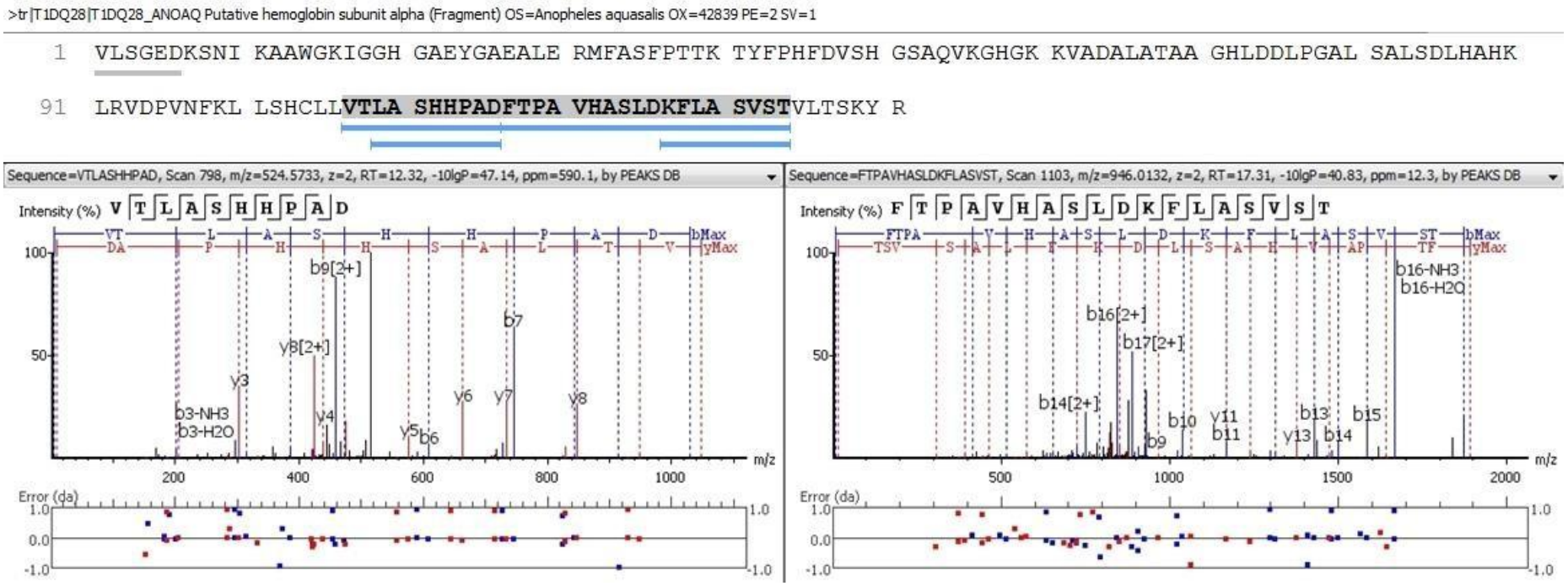

Figure S4: Deconvolution of two peptides from the fraction B1 (eluted at 28.28min) corresponding to the fragments 2-10 and 56-77 of hemoglobin β chain.

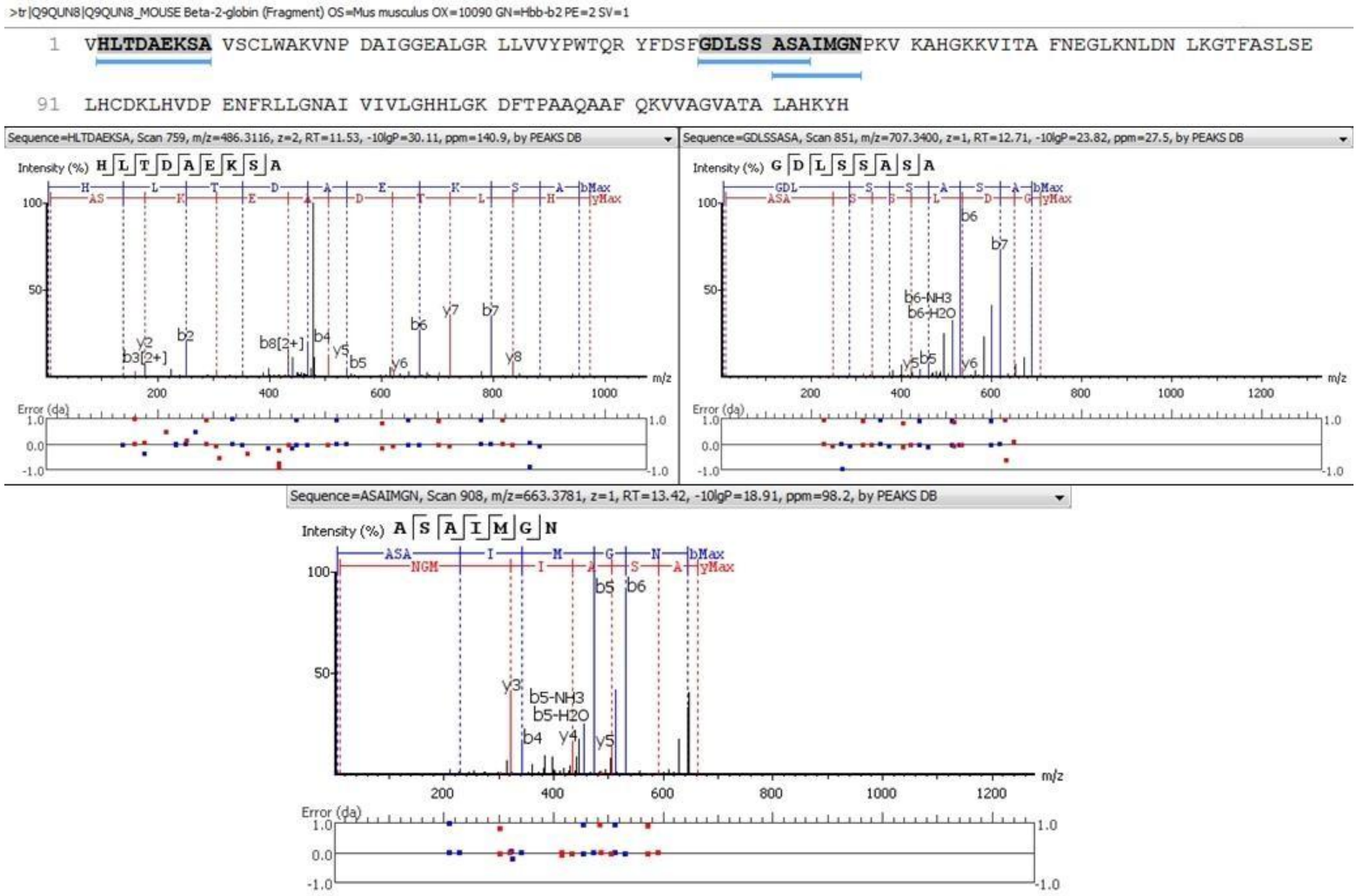

Figure S5: Deconvolution of five peptides from the fraction B2 (eluted at 28.28min) corresponding to the fragments 1-10, 16-27, 49-70, 73-80 and 122-136 of hemoglobin β chain.

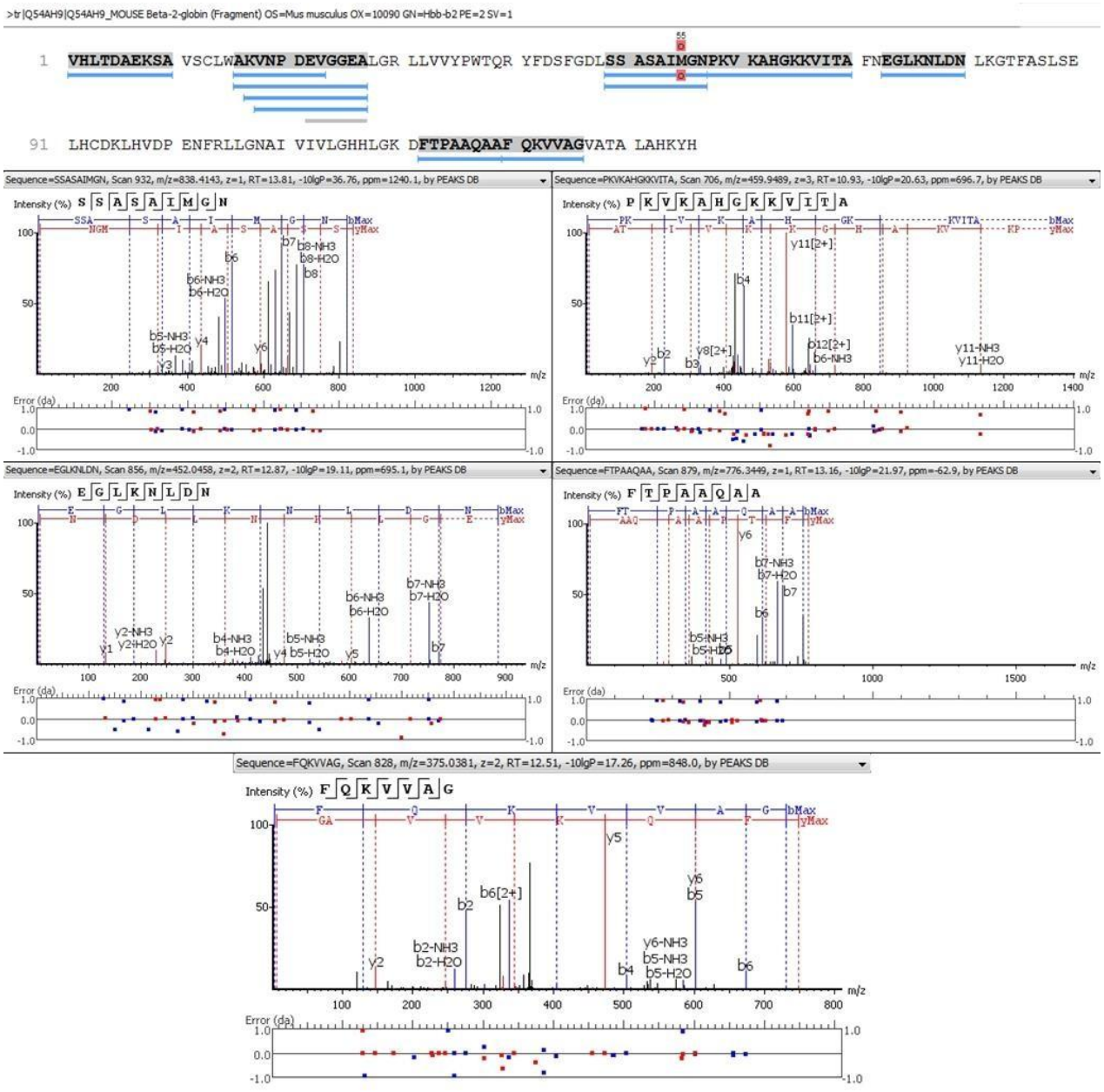

Figure S6: Deconvolution of three peptides from the fraction B3 (eluted at 43min) corresponding to the fragments 1 -12, 58-72 and 112-129 of hemoglobin β chain.

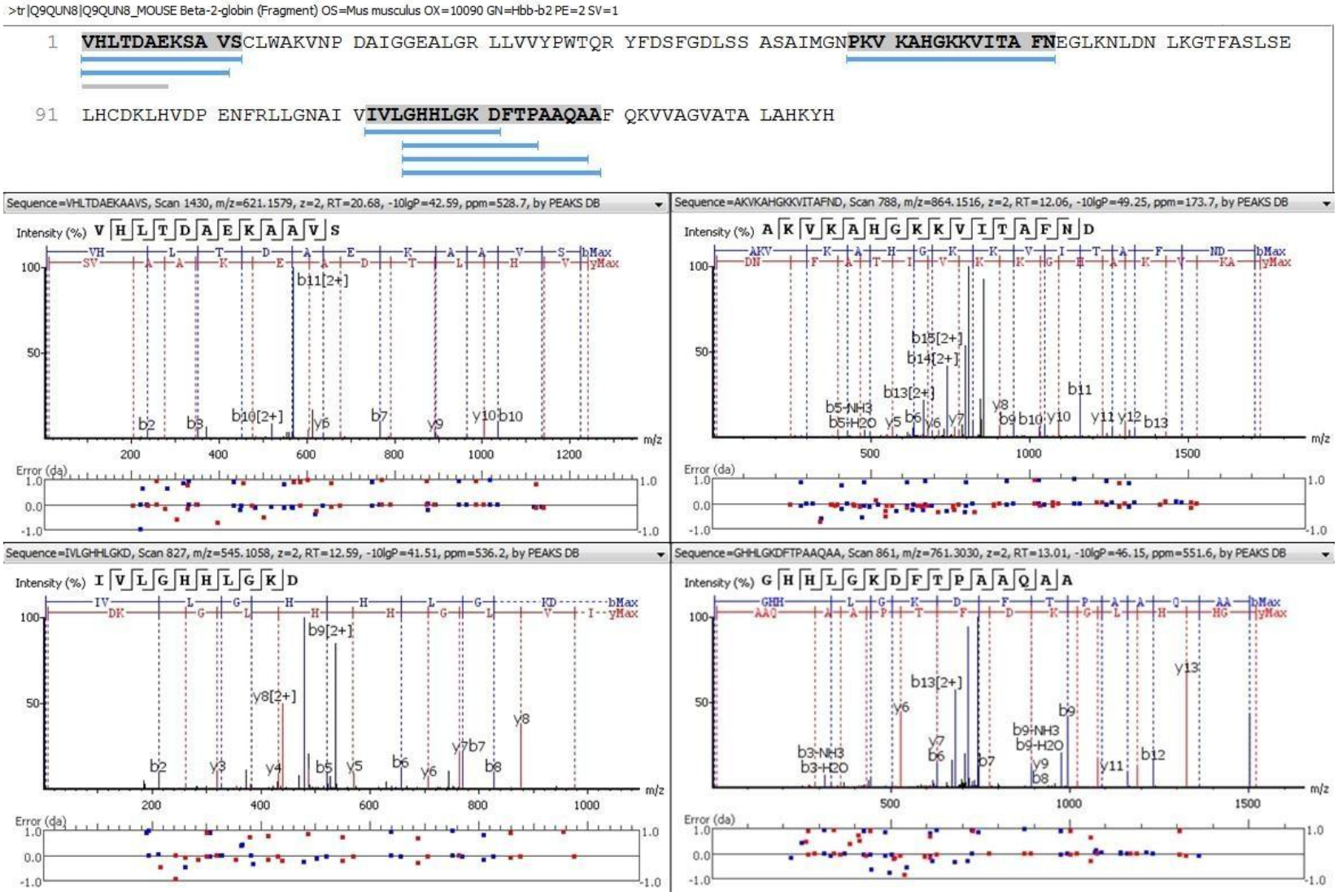

Figure S7: Deconvolution of three peptides from the fraction B4 (eluted at 48.1min) corresponding to the fragments 2-14, 59-88 and 135-147 of hemoglobin β chain.

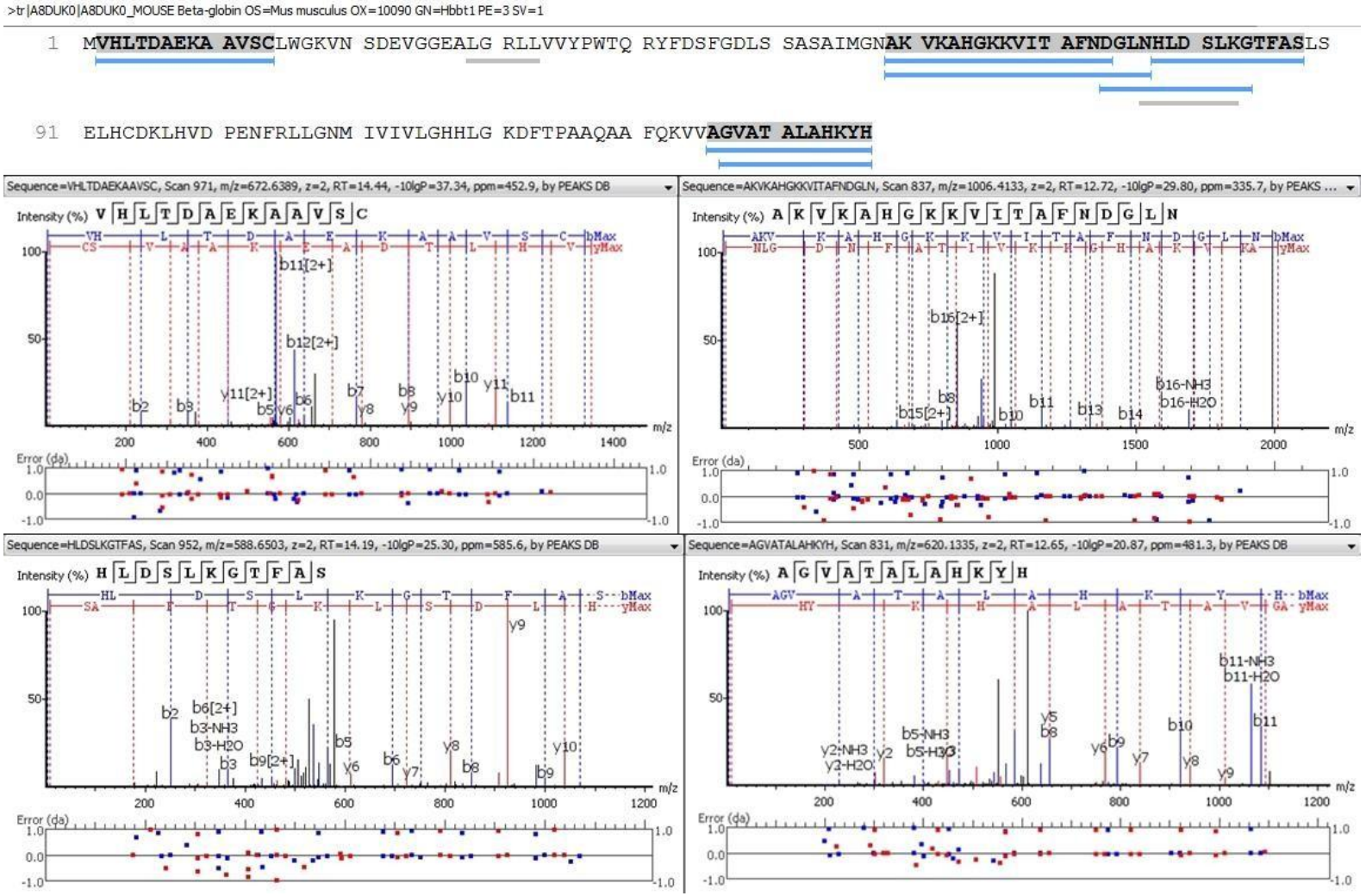

Figure S8: Deconvolution of four peptides from the fraction B5 (eluted at 56.4min) corresponding to the fragments 34-40, 59-71, 75-86 and 90-100 of hemoglobin β chain.

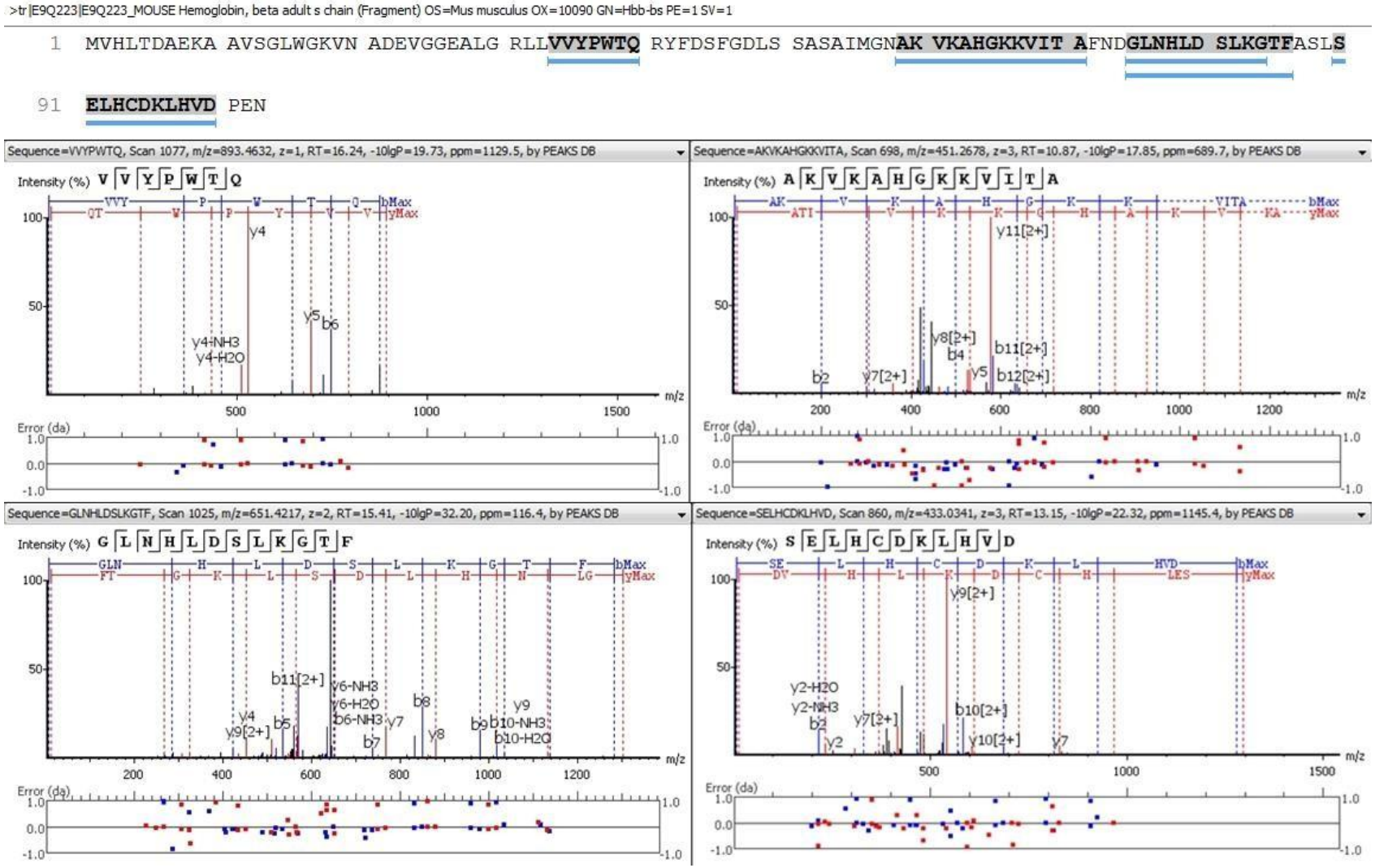

Figure S9: Deconvolution of five peptides from the fraction B6 (eluted at 61.7min) corresponding to the fragments 2-15, 21-33, 90-100, 104-110 and 131-147 of hemoglobin β chain.

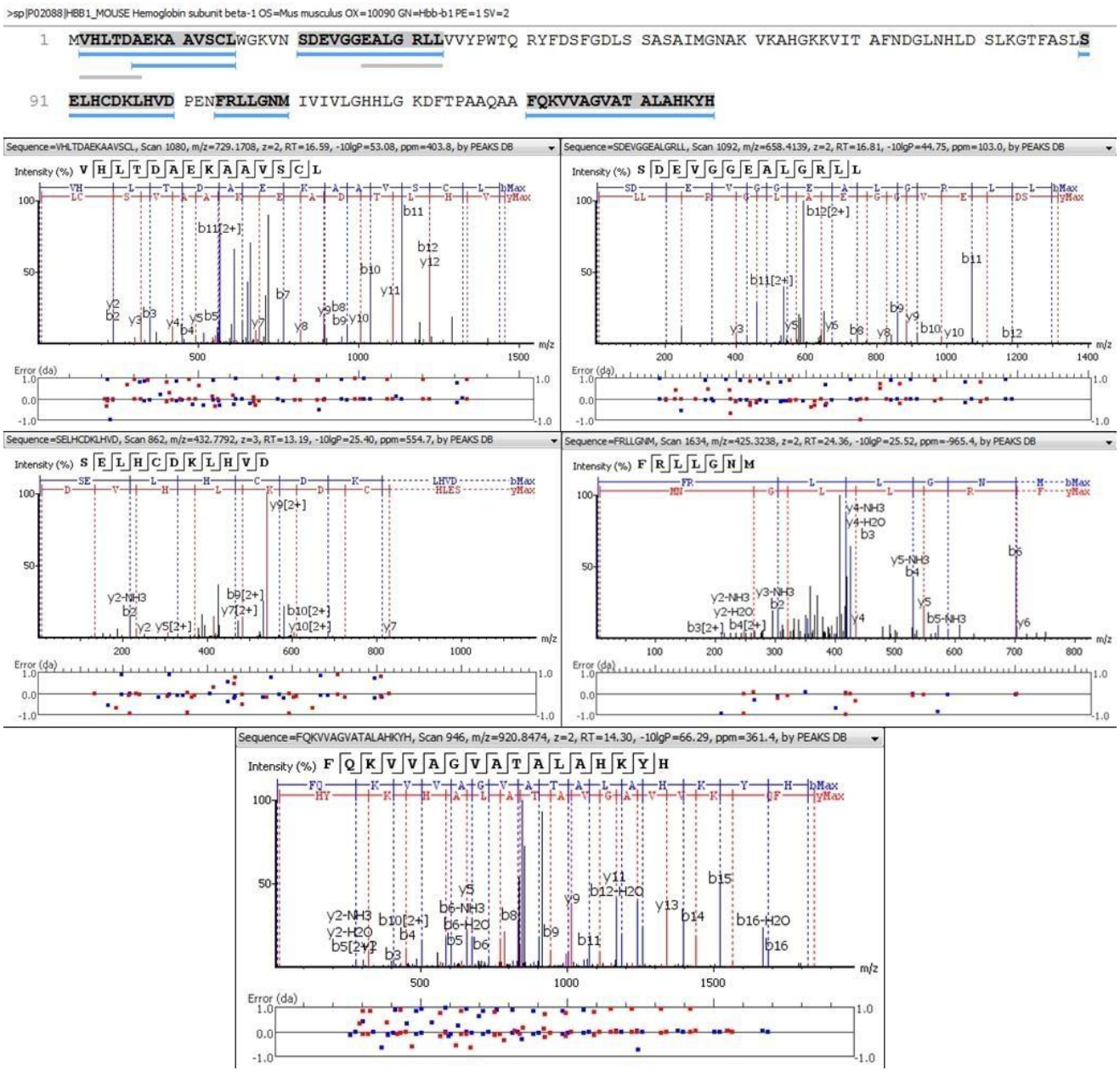

Figure S10: Deconvolution of two peptides from the fraction B2 (eluted at 93.7min) corresponding to the fragments 100-107 and 112-146 of hemoglobin β chain.

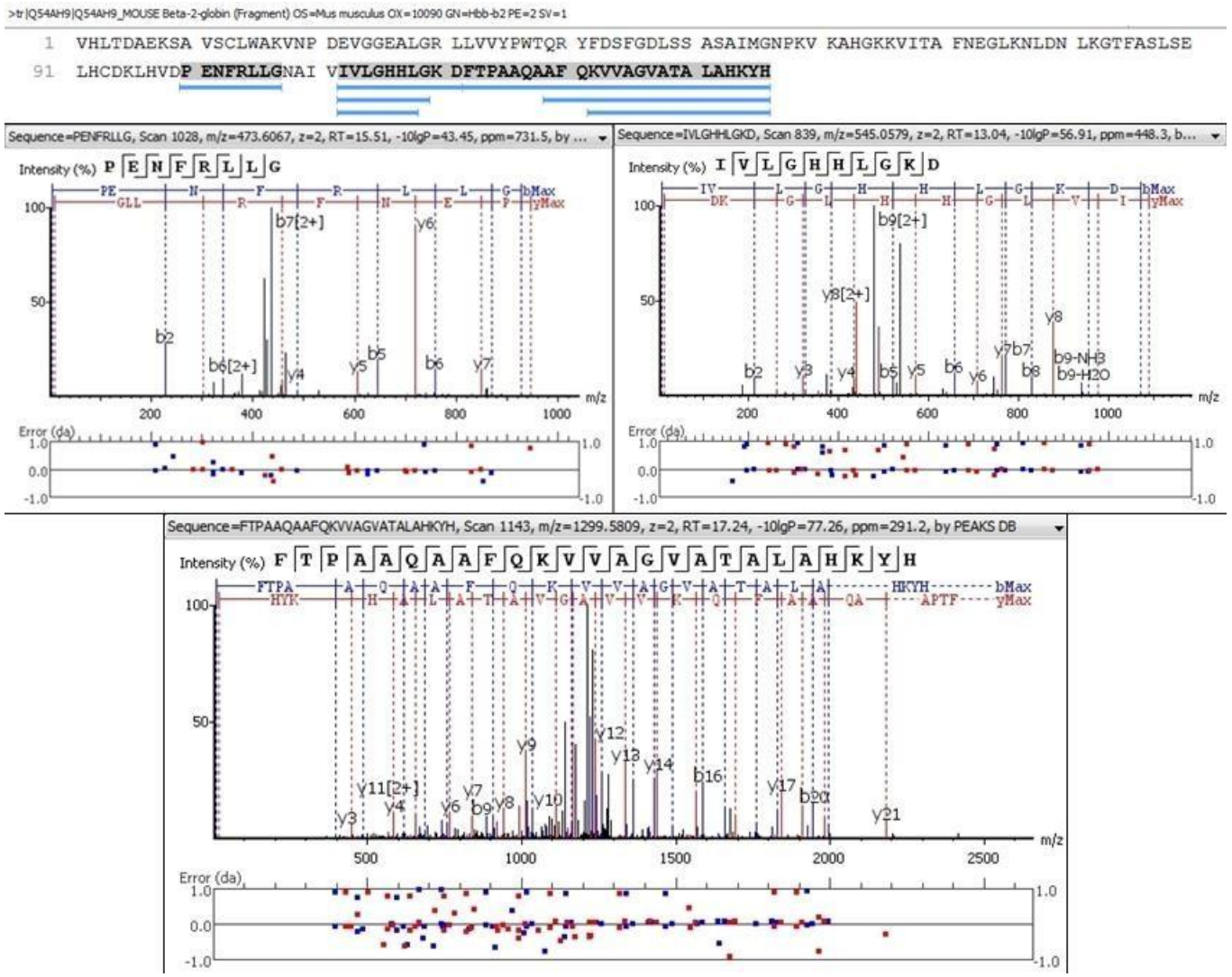

Figure S11: Deconvolution of the main peptide from the fraction A1 (e luted at 24.8min) corresponding to the fragment 2-10 of he moglobin α chain.

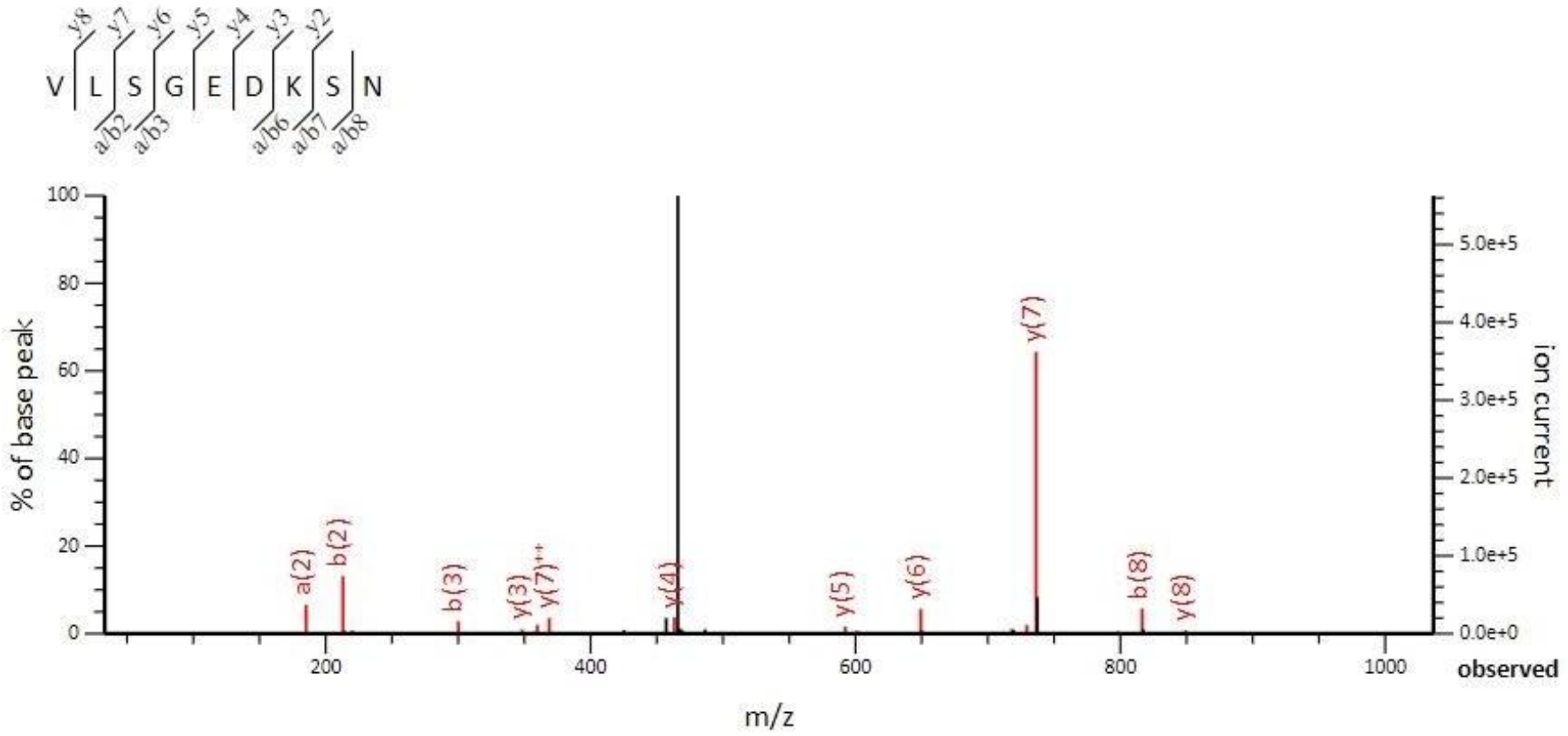

Figure S12: Deconvolution of the main peptide from the fraction A2 (e luted at 64.5 min) corresponding to the fragment 77-95 of he moglobin α chain.

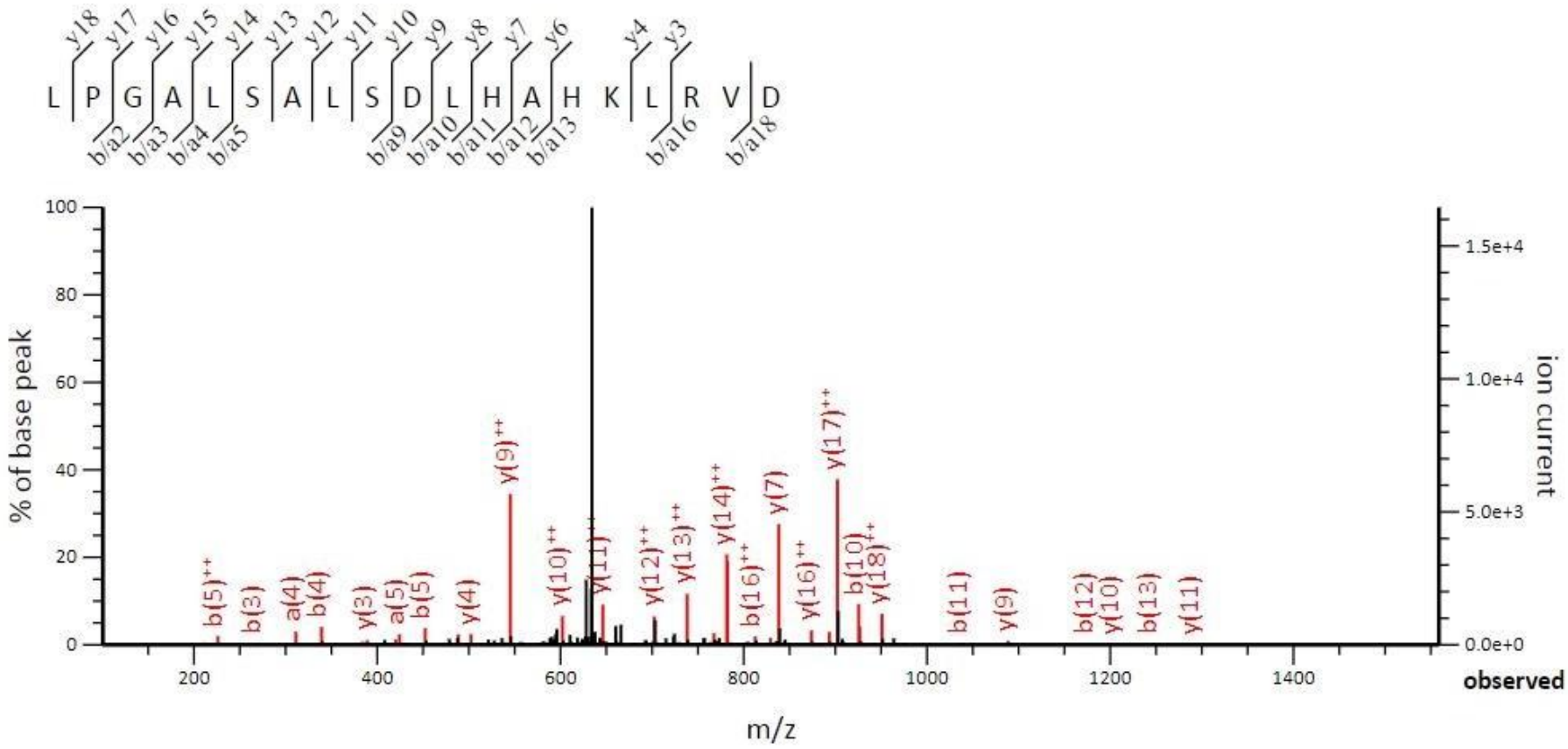

Figure S13: Deconvolution of the main peptide from the fraction A3 (e luted at 81.8 min) corresponding to the fragment 77-95 of he moglobin α chain.

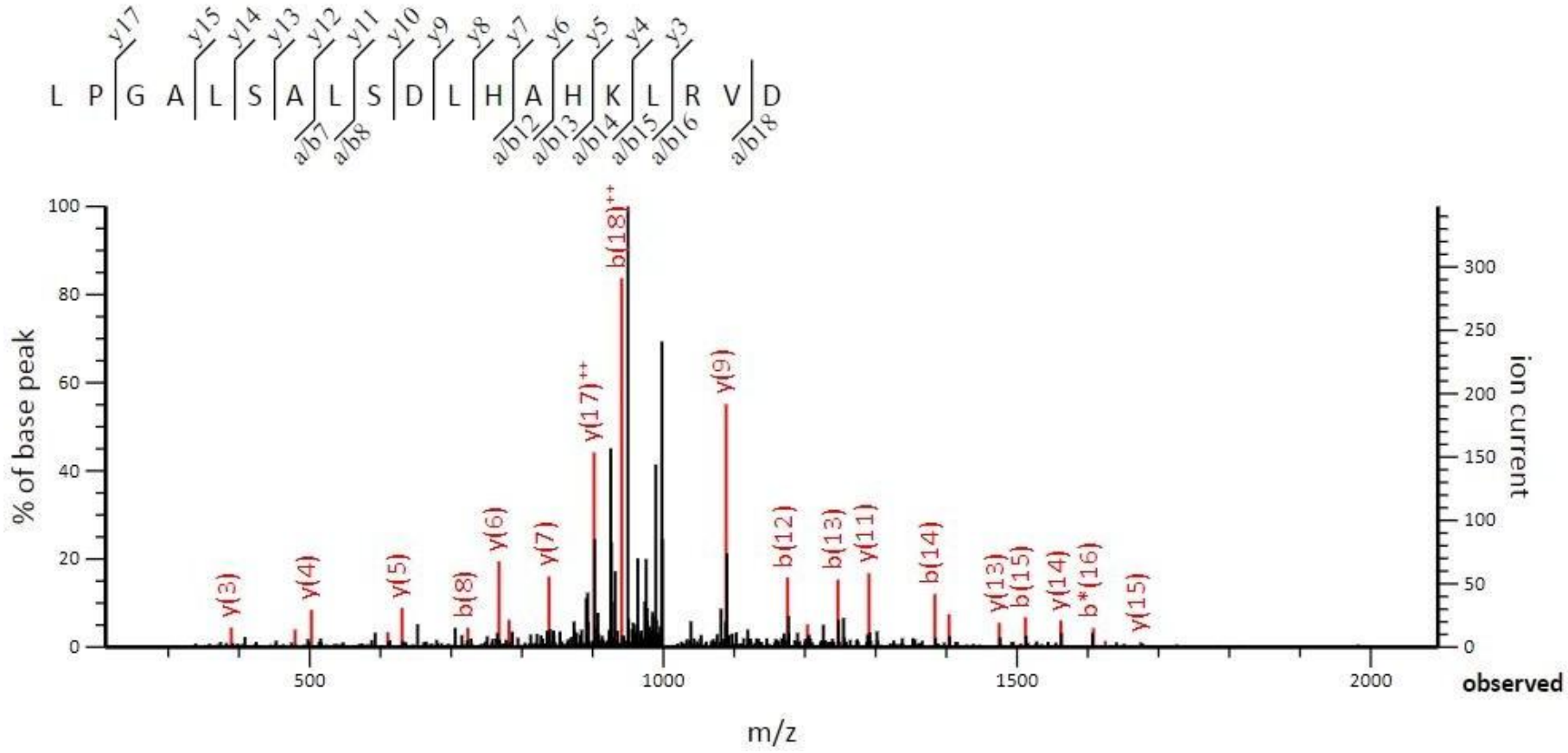

Figure S14: Deconvolution of the main peptide from the fraction B1 (e luted at 28.8 min) corresponding to the fragment 2-10 of he moglobin β2 chain.

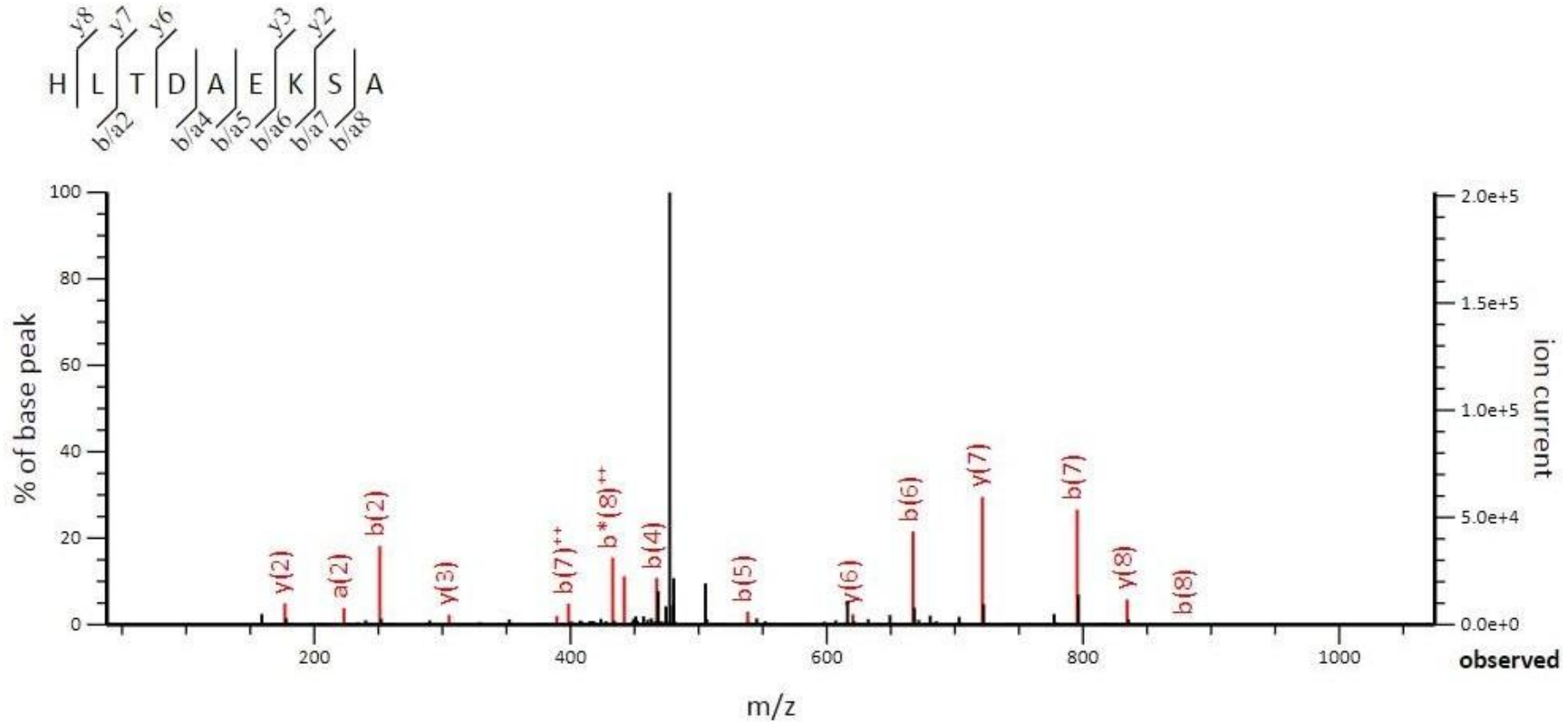

Figure S15: Deconvolution of the main peptide from the fraction B2 (e luted at 35.5 min) corresponding to the fragment 1-10 of he moglobin β2 chain.

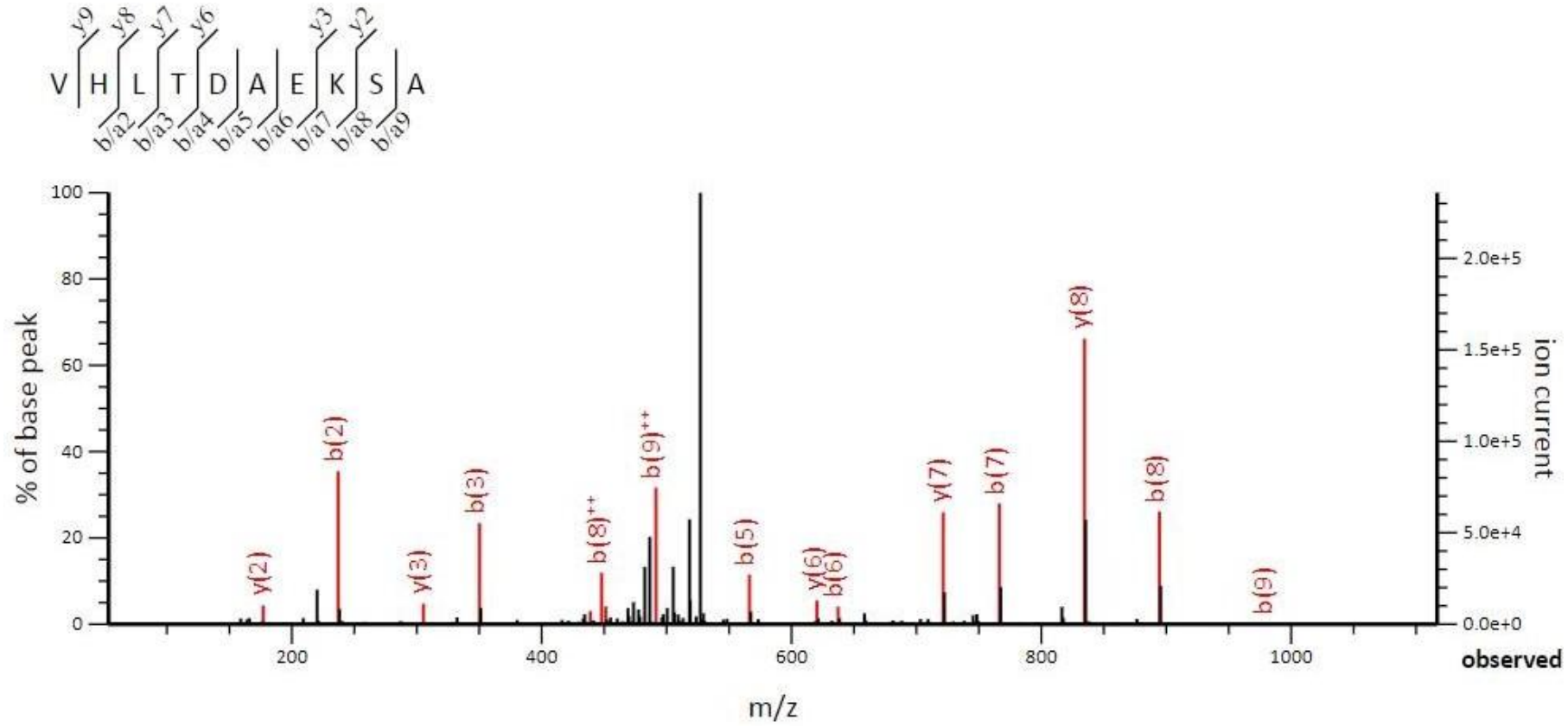

Figure S16: Deconvolution of the main peptide from the fraction B3 (e luted at 43.0 min) corresponding to the fragment 59-74 of he moglobin β1 chain.

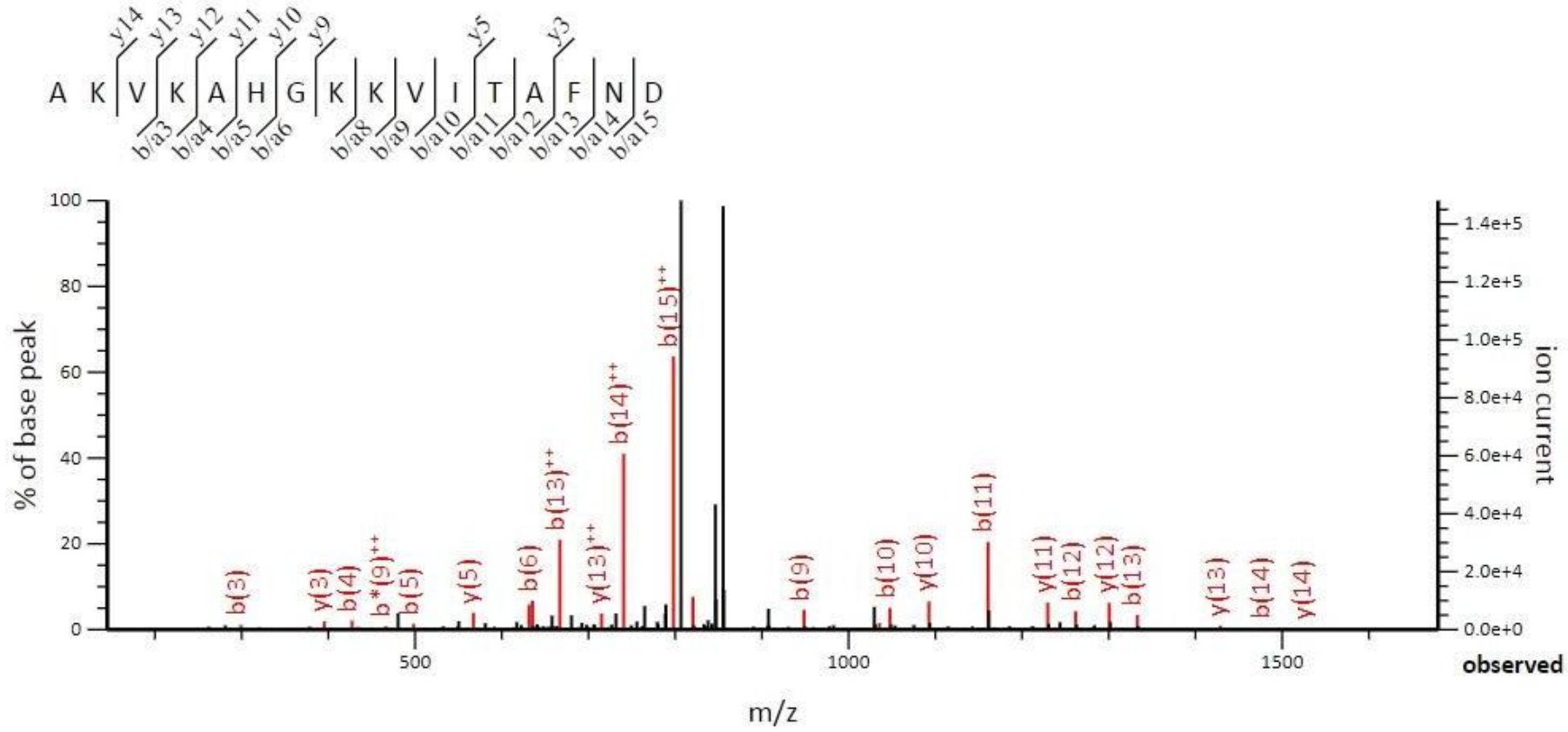

Figure S17: Deconvolution of the main peptide from the fraction B4 (e luted at 48.1 min) corresponding to the fragment 59-77 of he moglobin β1 chain.

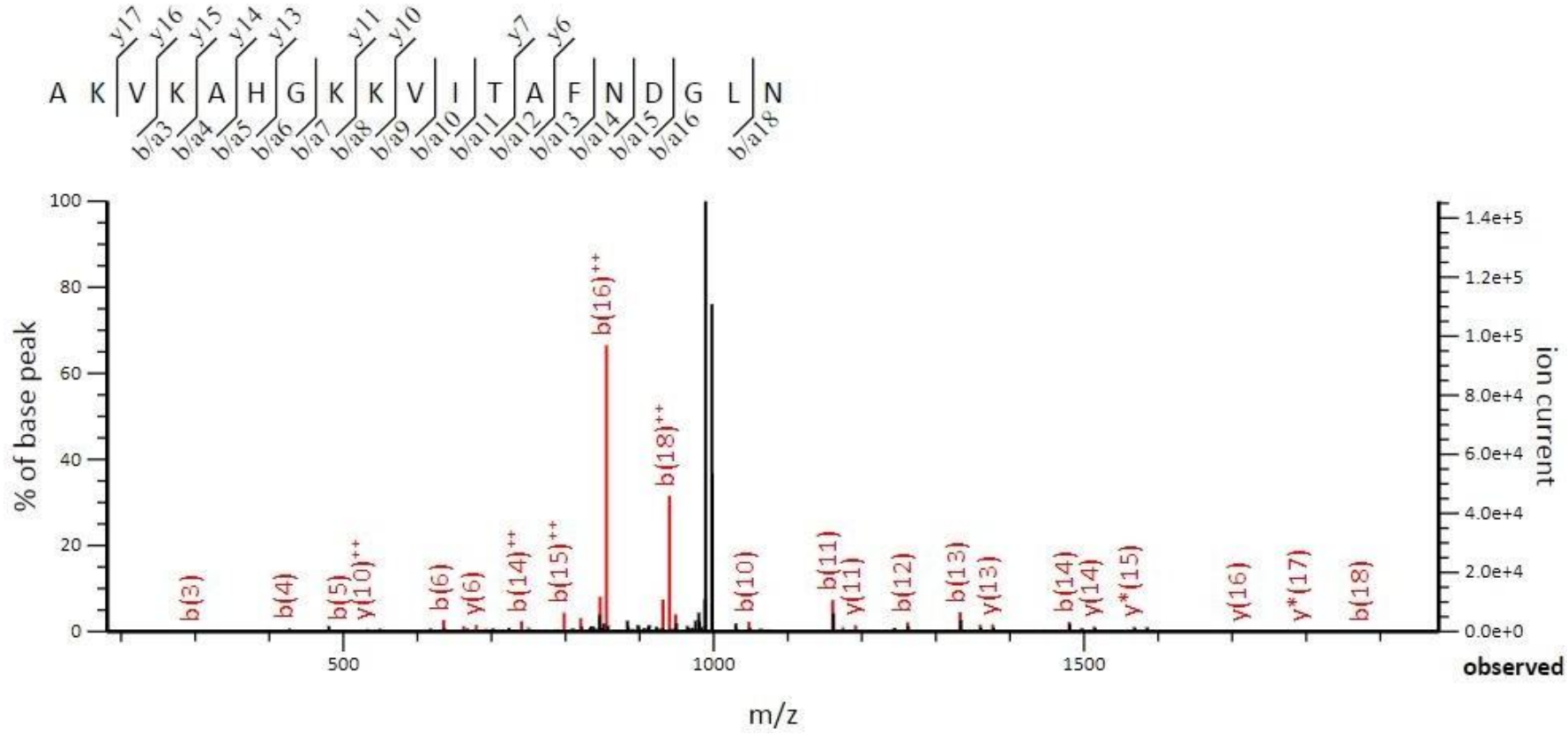

Figure S18: Deconvolution of the main peptide from the fraction B5 (e luted at 56.4 min) corresponding to the fragment 75-84 of he moglobin β1 chain.

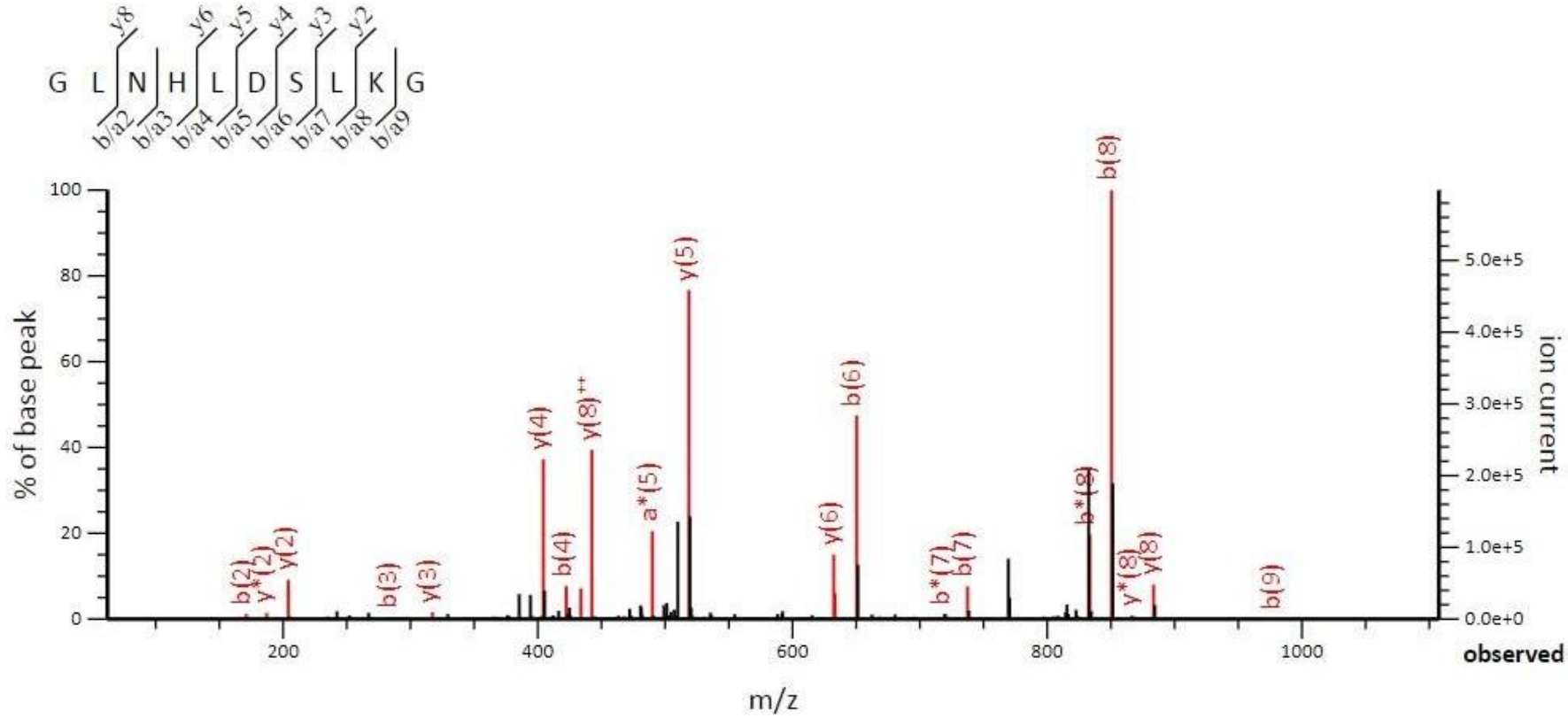

Figure S19: Deconvolution of the main peptide from the fraction B6 (e luted at 61.7 min) corresponding to the fragment 131-147 of he moglobin β1 chain.

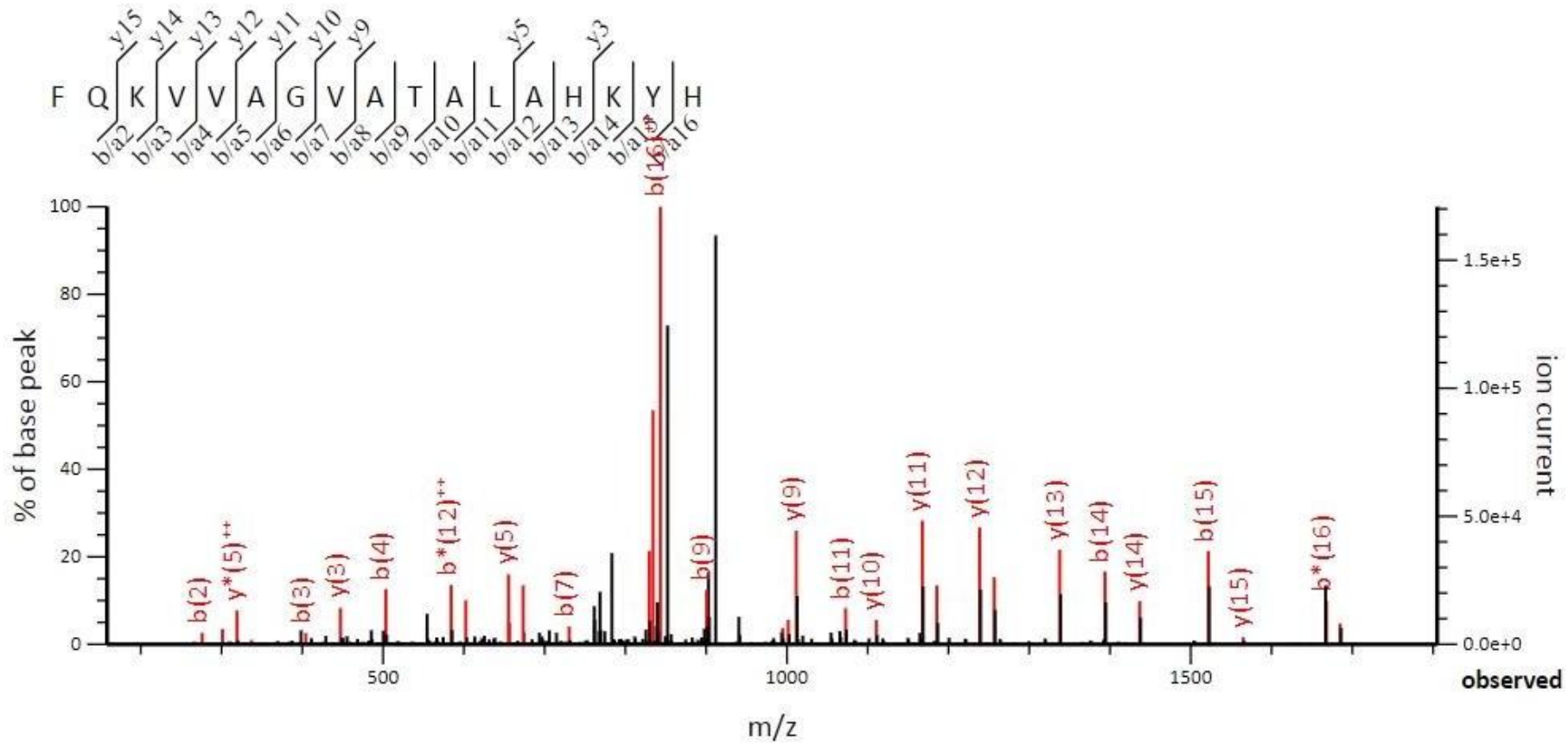

Figure S20: Deconvolution of the main peptide from the fraction B7 (e luted at 93.7 min) corresponding to the fragment 123-147 of he moglobin β2 chain.

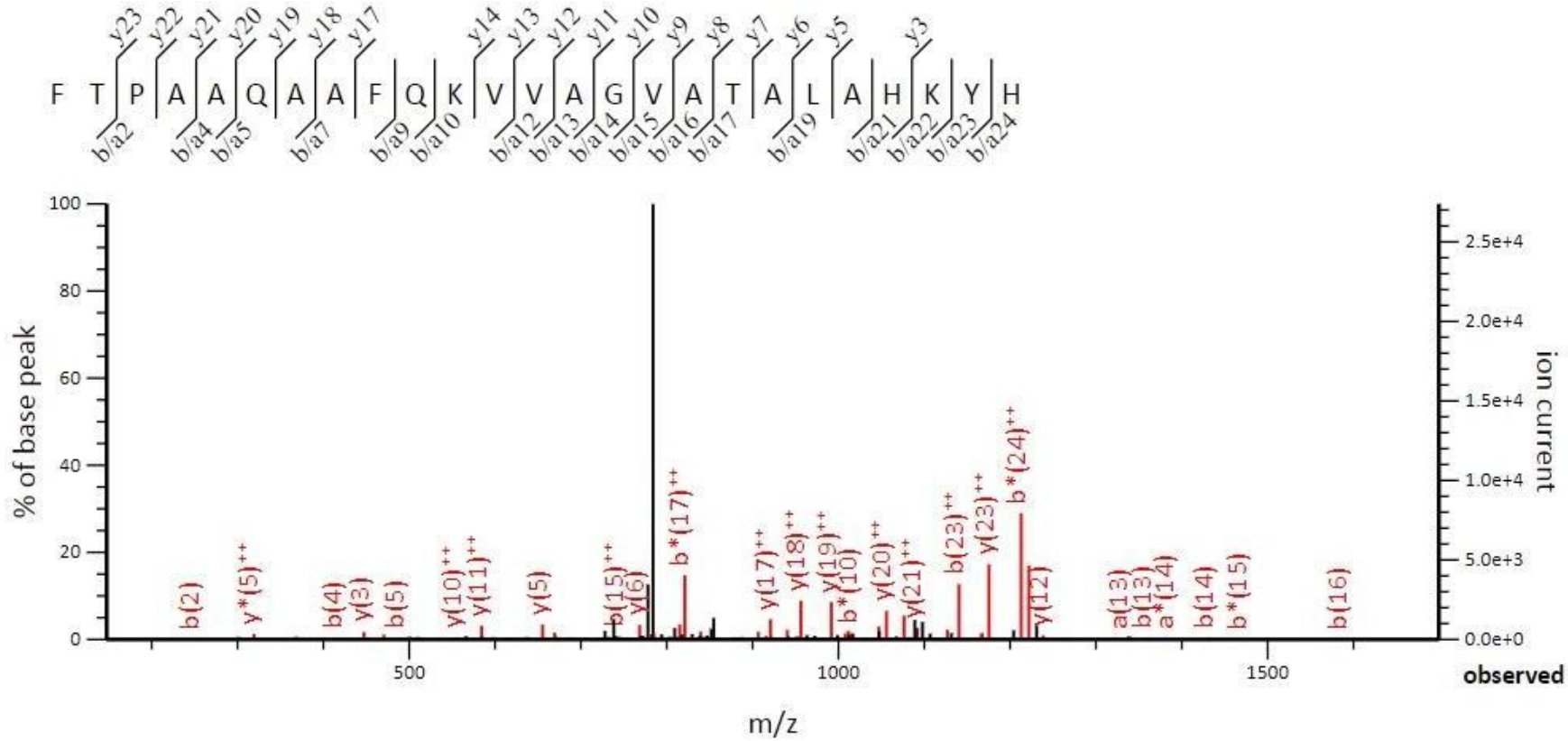

Two Tachykinin-Related Peptides with Antimicrobial Activity Isolated from *Triatoma infestans* Hemolymph

Microbiology Insights
Volume 13: 1–13
© The Author(s) 2020
Article reuse guidelines:
sagepub.com/journals-permissions
DOI: 10.1177/1178636120933635
SAGE

Laura Cristina Lima Diniz[1,2], Flávio Lopes Alves[3], Antonio Miranda[3] and Pedro Ismael da Silva Junior[1,2]

[1]Center of Toxins, Immune-Response and Cell Signaling – CeTICS/CEPID, LAboratory of Applied Toxinology, Butantan Institute, São Paulo, Brazil. [2]Postgraduate Program Interunits in Biotechnology, Department of Biomedical Sciences, USP/IPT/IBU, São Paulo, Brazil. [3]Department of Biophysics, UNIFESP, São Paulo, Brazil.

ABSTRACT: Antimicrobial peptides and proteins (AMPs) are molecules that can interact with microbial cells and lead to membrane disruption or intracellular molecule interactions and death. Several molecules with antimicrobial effects also present other biological activities. One such protein group representing the duplicity of activities is the tachykinin family. Tachykinins (TKs) form a family of neuropeptides in vertebrates with a consensus C-terminal region (F-X-G-Y-R-NH2). Invertebrate TKs and TK-related peptides (TKRPs) are subfamilies found in invertebrates that present high homology with TKs and have similar biological effects. Several of these molecules have already been described but reports of TKRP in Hemiptera species are limited. By analyzing the *Triatoma infestans* hemolymph by reversed-phase high-performance liquid chromatography, biological assays, and mass spectrometry, two antimicrobial molecules were isolated and identified as TKRPs, which we named as TRP1-TINF and TRP2-TINF (tachykinin-related peptides I and II from *T. infestans*). TRP1-TINF is a random secondary structure peptide with 9 amino acid residues. It is susceptible to aminopeptidases degradation and is active mainly against *Micrococcus luteus* (32 μM). TRP2-TINF is a 10-amino acid peptide with a 310 helix secondary structure and is susceptible to carboxypeptidases degradation. It has major antimicrobial activity against both *Pseudomonas aeruginosa* and *Escherichia coli* (45 μM). Neither molecule is toxic to human erythrocytes and both present minor toxicity toward Vero cells at a concentration of 1000 μM. As the first description of TKRPs with antimicrobial activity in *T. infestans*, this work contributes to the wider comprehension of the insects' physiology and describes pharmacological relevant molecules.

KEYWORDS: *Triatoma infestans*, tachykinin-related peptides, antimicrobial peptides, Hemiptera, bioactive molecules

RECEIVED: May 12, 2020. **ACCEPTED:** May 15, 2020.

TYPE: Original Research

FUNDING: The author(s) disclosed receipt of the following financial support for the research, authorship, and/or publication of this article: This work was supported by Fundação de Amparo a Pesquisa do Estado de São Paulo (FAPESP/CeTICS; Grant No. 2013/07467-1) and CNPq Conselho Nacional de Desenvolvimento Cientifico e Tecnologico (Grant Nos 130409/2014-6, 142224/2016-2, and 472744/2012-7).

DECLARATION OF CONFLICTING INTERESTS: The author(s) declared no potential conflicts of interest with respect to the research, authorship, and/or publication of this article.

CORRESPONDING AUTHOR: Pedro Ismael da Silva Junior, Center of Toxins, Immune-Response and Cell Signaling – CeTICS/CEPID, Laboratory of Applied Toxinology, Butantan Institute, 1500 Vital Brazil Avenue, São Paulo, SP 05503-900, Brazil. Email: pisjr@butantan.gov.br

Introduction

Antimicrobial peptides and proteins (AMPs) are cationic and amphipathic molecules that can interact with molecules present on cell membranes and with intracellular pathways in microbes, leading to cell disruption and death.[1]

These bioactive molecules were initially described in insects by Stephens[2] in 1962, followed by Hink and Briggs[3] in 1968, Powning and Davidson[4] in 1973, Boman et al[5] in 1974, and Faye et al[6] in 1975. Subsequent studies led to the characterization of the first 2 antimicrobial molecules in 1981 by Steiner et al.[7] These molecules were isolated from the moth *Hyalophora cecropia*, and thus were entitled cecropins, originating of one of the largest antimicrobial peptide groups. Antimicrobial peptides and proteins show a wide distribution and have been isolated from nearly all living organisms.[8-21]

Beyond their antimicrobial effects, several AMPs have been shown to have other biological activities.[11,22-25] One such protein group that represents the duplicity of activities for the same molecules is the tachykinin family. Tachykinins (TKs) form a family of neuropeptides in vertebrates, represented by compounds such as Neurokinin A,[26] Neurokinin B,[27] hemokinin/endokinin K,[28,29] and substance P (SP), which was the first TK discovered in alcoholic extracts of equine brain[30] and then isolated from the bovine hypothalamus. Its sequence was determined 40 years later.[31]

After the discovery of SP, several other neuropeptides were identified,[32-35] all of which contain a consensus C-terminal region (F-X-G-Y-R-NH_2).[28,36-39] Erspamer,[40] using similar methods as Von Euler and Gaddum,[30] detected a substance in the salivary glands of *Eledone moschata* that was capable of lowering blood pressure, increasing salivation, and stimulating smooth muscle in rabbits and dogs. This substance was named as eledoisin and was the first non-mammalian TK described.[36,37,41,42] Other TKs from frogs and non-mammalian were subsequently described and isolated.[32-34,43,44]

Champagne and Ribeiro[45] identified 2 TKs from the salivary glands of the mosquito *Aedes aegypti*, confirming the presence of peptides related to vertebrate TKs in invertebrates. Following this study, 4 molecules from brain, corpora cardiaca, corpora allata, and subesophageal ganglion extracts of the nervous system of *Locusta migratoria*, named as locust atachykinins, were found to show 30% homology with vertebrate TKs and up to 45% similarity with fish and amphibian TKs.[46-48]

After these discoveries in invertebrates, 2 new molecule subfamilies were established: the invertebrate tachykinins (Inv-TKs) and tachykinin-related peptides (TKRPs). The main

difference between these 2 subfamilies is their C-terminal amino acid composition. Tachykinin-related peptides are clearly related to vertebrate TKs, sharing the same C-terminal region (F-X-G-Y-R-NH_2), whereas Inv-TKs differ in their last 2 residues, containing leucine and methionine (F-X-G-L-M-NH_2). However, they still maintain high homology and exhibit similar biological effects.

Several Inv-TKs and TKRP have been described in species such as *Agrotis ipsilon*,[49] *Apis mellifera*,[50] *Camponotus floridanus*,[51] *Drosophila melanogaster*,[52] *Drosophila pseudoobscura pseudoobscura*,[53] *Leucophaea maderae*,[54] *and Delia radicum*.[55]

Tachykinin-related peptides have been described in other insects in the order Hemiptera, including in *Triatoma infestans*, which was analyzed in the current study. Neupert et al[56] described 6 TKRPs produced by *Nezara viridula, Banasa dimiata, Pyrrhocoris apterus, Oncopeltus fasciatus, Pentatoma rufipes*, and *Euschistus servus*, and Ons et al[57] identified 8 TKRP sequences through neuropeptidome analysis of *Rhodnius prolixus*.

There are no further reports of TKRP in other Hemiptera species. Thus, the aim of this study was to isolate and characterize the first 2 TKRPs in the *T. infestans* hemolymph (Hemiptera: Reduviidae).

Materials and Methods

Microbial strains

The microorganisms *Alcaligenes faecalis* (ATCC 8750), *Aspergillus niger* (bread isolated), *Candida albicans* (IOC 4558), *Candida parapsilosis* (IOC 4564), *Candida tropicalis* (IOC 4560), *Cladosporium sp.* (bread isolated), *Cladosporium herbarum* (ATCC 26362), *Cryptococcus neoformans, Enterobacter cloacae* b-12, *Escherichia coli* (SBS363), *Bacillus megaterium* (ATCC 10778), *Bacillus subtilis* (ATCC 6633), *Micrococcus luteus* (strain A270), *M. luteus* (Nalidixic resistant), *Paecilomyces farinosus* (IBCB-215), *Penicillium expansum* (bread isolated), *Pseudomonas aeruginosa* (ATCC 27853), *Saccharomyces cerevisiae, Serratia marcescens* (ATCC 4112), and *Staphylococcus aureus* (ATCC 29213) were provided by the Special Laboratory of Applied Toxinology from their microorganism library (Butantan Institute, São Paulo, Brazil).

Animals

Both male and female *T. infestans* (Hemipterans: Reduviidae) were provided by the Ecolyzer Group—Entomology Laboratory (São Paulo, Brazil). The insects were maintained under controlled humidity and temperature in the biotherium of the Special Laboratory of Applied Toxinology (Butantan Institute, São Paulo, Brazil) and fed every 2 weeks with human blood (collected from a healthy volunteer donor and stored in citrate buffer [150 mM, pH 7.4]).[58] The study was conducted under exemption from the Institutional Ethics Committee (CEUAIB No. I-1354/15).

Bacteria inoculation and hemolymph collection

Adult *T. infestans* were injured with thin needles soaked in a pool of culture of *Enterobacter cloacae* and *M. luteus* in the logarithmic phase. At 72 hours after induction, hemolymph samples were obtained by excising the metathoracic legs of the insects and pressing gently on the abdomen. Drops were collected with micropipettes and pooled in sterile Eppendorf tubes on ice containing phenylthiourea to avoid activation of the phenol oxidase cascade.[5] The solution was stored at −80°C until use.

Sample fractionation

Intracellular content extraction. To release the intracellular components from the hemolymph, the sample was subjected to acid extraction in the presence of acetic acid (2 M). The supernatant was obtained by centrifugation at 16.000 ×*g* for 30 minutes at 4°C and injected directly into 2 coupled Sep-Pack C18 cartridges (Waters, Milford, MA, USA) equilibrated in 0.1% trifluoroacetic acid (TFA). The sample was eluted with 3 different concentrations of acetonitrile (ACN) in water (5%, 40%, and 80%) and then concentrated in a vacuum centrifuge and reconstituted with ultrapure water.

Reversed-phase high-performance liquid chromatography. Separation steps were performed using high-performance liquid chromatography (HPLC) using a reverse-phase semi-preparative C18 column (Jupiter, 10 × 250 mm; Phenomenex, Torrance, CA, USA) equilibrated in 0.05% TFA. The elution gradient for the fraction eluted with 5% ACN was from 2% solution A (0.05% [v/v] TFA in water) to 20% solution B (0.10% [v/v] TFA in ACN). For the 40% ACN fraction, the elution gradient was 2% to 60% solution B (0.10% [v/v] TFA in ACN). For the 80% ACN fraction, the elution gradient was 20% to 80% solution B (0.10% [v/v] TFA in ACN) in solution A. Each run was performed over 60 minutes at a flow rate of 1.5 mL/min.

Effluent absorbance was monitored at 225 nm, and fractions corresponding to the absorbance peaks were hand-collected, concentrated under vacuum, and reconstituted in ultrapure water.

When necessary, a second chromatography step was performed. The gradient for the second chromatography was determined by evaluation of the molecule's retention time and performed on a VP-ODS analytic C18 column (Shim-pack; Shimadzu, Kyoto, Japan) at a flow rate of 1.0 mL/min for 60 minutes.

Liquid growth inhibition assay

All fractions obtained by HPLC and synthetic peptides were evaluated by antimicrobial screening against the microorganism strains (see section "Microbial Strains")[8,21] using poor

broth nutrient medium (PB: 1.0 g peptone in 100 mL of water containing 86 mM NaCl at pH 7.4; 217 mOsM) and Müller-Hinton medium (peptone 5.0 g/L; casein peptone 17.5 g/L; agar 15.0 g/L; Ca^2+ 20.0-25.0 mg/L; Mg^2+ 10.0-14.5 mg/L; pH 7.4) for bacteria and poor dextrose broth (1/2 PDB: 1.2 g potato dextrose in 100 mL of H_2O at pH 5.0; 79 mOsM) and RPMI 1640 (Roswell Park Memorial Institute medium) medium with MOPS 0.165 mol/L (RPMI without bicarbonate 10.4 g/L; MOPS [3-(*n*-morpholino) propanesulfonic acid] 34.53 g/L; pH 7.0) at half half-strength.[59,60]

Antimicrobial activity was determined in a 5-fold microliter broth dilution assay in 96-well sterile plates at a final volume of 100 µL. The mid-log phase microbial culture was diluted to a final concentration of 1×10^5 colony-forming units per milliliter.[59,61,62]

Lyophilized fractions were dissolved in 500 µL ultrapure water, and 20 µL peptide solution was aliquoted into each well containing 80 µL of the bacterial dilution, giving a final volume of 100 µL. To determine the minimal inhibition concentration, 20 µL peptide stock solution was added to each well of the microtiter plate at a 2-fold serial dilution and added to 80 µL of the bacterial dilution. Sterile water and PB were used as growth controls, and streptomycin was used as a growth inhibitor control.

The microtiter plates were incubated for 18 hours at 30°C, and then growth inhibition was determined by measuring the absorbance at 595 nm.[63,64] To determine the minimal inhibition concentration, the bacterial growth rates were measured after 18 hours of incubation. To determine the minimal bactericidal concentration, the bacterial growth rates were measured at 595 nm after 96 hours.[63,64] All antimicrobial experiments were performed in triplicate.

Mass spectrometry

Active antibacterial fractions were analyzed by liquid chromatography-tandem mass spectrometry on an LTQ-Orbitrap Velos (Thermo Fisher Scientific, Waltham, MA, USA) coupled to an Easy-nLCII liquid nano-chromatography system (Thermo Fisher Scientific). For chromatography, 5 µL of each sample was automatically separated on a C18 pre-column (100 mm I.D. × 50 mm; Jupiter 10 mm; Phenomenex) coupled to a C18 analytical column (75 mm I.D. × 100 mm; ACQUA 5 mm; Phenomenex). The eluate was electro-sprayed at 2 kV and 200°C in positive ion mode. Mass spectra were acquired with a Fourier transform-based mass spectrometer; full scan (MS1) involved using 200-2000 m/z (60 000 resolution at 400 m/z) with a mass scan interval in data-dependent acquisition mode. The 5 most intense ions in each scan were selected for fragmentation by collision-induced dissociation. The minimum threshold for selecting an ion for a fragmentation event (MS2) was set to 5000. The dynamic exclusion time was 15 seconds, repeating at 30-second intervals.

Computational analysis

Mass spectrometry data were analyzed using Mascot Daemon software (version 2.2.2) through database searching using the Swiss-Prot, NCBInr, Hemipteras, and Triatomineos banks for comparison. Homology searching was performed using the PepBank peptide database,[65] Signal Peptide Database,[66] Vector Base,[67] APD3: Antimicrobial Peptide Calculator and Predictor,[68] and BLAST: Basic Local Alignment Search Tool.[69] The results were considered valid only when they were reproducible by different analyses.

Primary structure alignment

Alignment of primary sequences was performed using Clustal W2 version 2 online software[70] with default parameters.

Solid-phase peptide synthesis

Peptides were synthesized using the solid-phase method[71] using methylbenzhydrylamine resin (MBHAR) and employing the *t*-Boc strategy. For synthetic peptide entitled TRP2-TINF, the methionine (second amino acid in the C-terminal region) was changed to norleucine, reducing the molecular weight to 1006 Da. After cleaving the peptides from the resin, the peptides were purified from the lyophilized crude solutions by HPLC on a C18 column. To guarantee high purity and to characterize the peptides, LC-ESI-MS equipment was used.

Synthetic peptide concentration

Peptide concentrations were determined using the Lambert-Beer law using the molar extinction coefficient at 205 nm absorption,[72] obtained using the tool available at http://nickanthis.com/tools/a205.html.

Peptide stability in serum

Aliquots of 20 µL peptide solution (10 mg/mL) were added to 1 mL of 25% non-heat inactivated horse serum (Sigma-Aldrich, St. Louis, MO, USA) in phosphate-buffered saline (PBS) and incubated at 37°C in triplicate for different time intervals (0, 10, 30, 60, and 120 minutes). During incubation, 100 µL of sample was withdrawn incubated with 10 µL of pure TFA at 5°C for 15 minutes. The resulting mixtures were centrifuged at 300 ×*g* for 5 minutes. A volume of 30 µL of the supernatants was injected in an online HPLC coupled to a mass spectrometer (LC-ESI-MS). Peptide consumption was evaluated using a linear gradient of ACN in acidified water from 3% to 57% in 30 minutes at a flow rate of 0.4 mL/min, followed by the measurement of the area decrease of the peak that corresponds to the peptide in the chromatogram.[73]

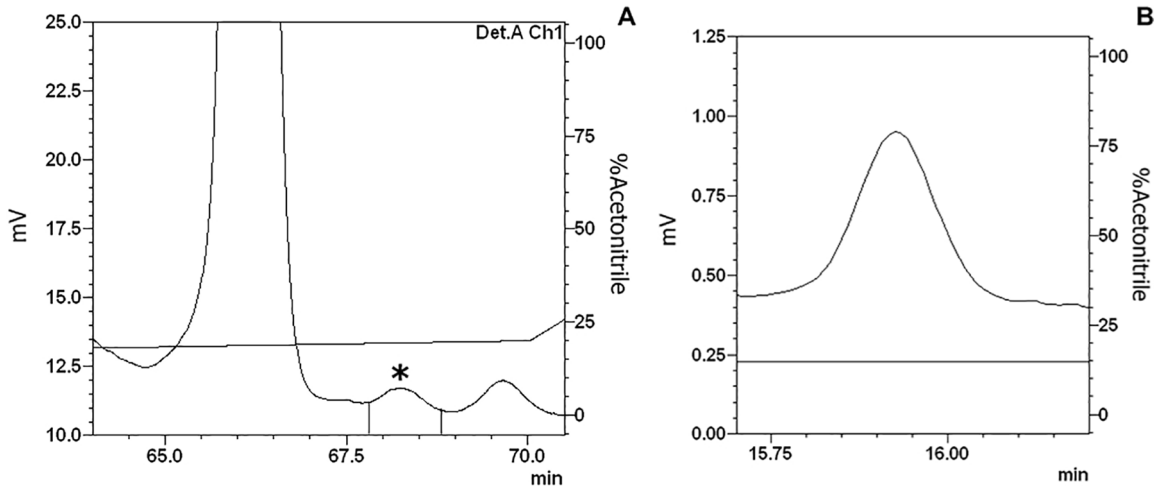

Figure 1. 5% ACN active fraction purification—sample 1: (A) The 5% ACN fraction isolated from *Triatoma infestans* hemolymph was separated by RP-HPLC using a C18 column, eluted over a linear gradient from solution A from 0% to 20% of solution B in 60 minutes. The labeled fraction (*), eluted at 67.3 minutes, exhibited antimicrobial activity and was subjected to a second chromatography step. (B) The second RP-chromatographic step on an analytic VP-ODS C18 column, with an ACN gradient from 13% to 23% solution B in 60 minutes, to guarantee fraction homogeneity.

Circular dichroism

Circular dichroism (CD) measurements were performed on a Jasco J-815 circular dichroism spectropolarimeter (Jasco Corp., Tokyo, Japan). For UV measurements (190-250 nm), CD spectra were recorded after 4 accumulations at 20°C using a 0.5-mm pathlength quartz cell between 250 and 195 nm at 50 nm/min with a bandwidth of 0.5 nm. Both peptides were analyzed in 0%, 10%, 30%, and 50% v/v solutions of 2,2,2 trifluoroethanol in water. Fast Fourier transform was applied to minimize background effects.[74]

Cytotoxic assays

The toxicity of the peptides against Vero cells (African green monkey kidney fibroblasts) was evaluated. Cells were obtained from the American Type Culture Collection (ATCC CCL81; Manassas, VA, USA) and maintained at 37°C in T culture flasks (25 cm^2) containing 5 mL Leibovitz medium (L-15) supplemented with 10% fetal bovine serum, both from Cultilab (Campinas, Brazil) or in a 96-well microplate. Toxicity was determined using the MTT colorimetric assay. Briefly, the cells were seeded into 96-well plates (2×10^5 cells/well) and cultured for 24 hours at 37°C in a humidified atmosphere containing 5% CO_2. Twelve 2-fold serial dilutions of both peptides were performed with L-15 to give solutions with final concentrations ranging from 1.95 to 1000 µM. Varying concentrations were added and allowed to react with the cells for 24 and 48 hours, followed by addition of 20 µL MTT (5 mg/mL in PBS) and incubation for another 4 hours at 37°C. Formazan crystals were dissolved by adding 100 µL dimethyl sulfoxide and incubation at room temperature until all crystals were dissolved. Absorbance at 550 nm was measured using a microplate ELISA reader (1420 Multilabel Counter/Victor3; Perkin Elmer, Waltham, MA, USA). Cell survival was calculated using the following formula: survival (%) = (A550 of peptide-treated cells/A550 of peptide-untreated cells) × 100.[20]

Hemolytic assay

Human erythrocytes from a healthy donor were collected in 0.15 M citrate buffer (pH 7.4) washed 3 times by centrifugation (700 ×*g*, for 10 minutes at 4°C) with 0.15 M PBS containing 137 mM NaCl, 2.7 mM KCI, 10 mM Na_2HPO_4, 1.76 mM KH_2PO_4 (pH 7.4) and resuspended in PBS to a final concentration of 3% (v/v). The peptides (serial 2-fold dilutions in PBS) were added to 80 µL erythrocyte suspension to a final volume of 100 µL and incubated for 1 hour at 37°C. Hemoglobin release was monitored by measuring the supernatant absorbance at 405 nm with a Microplate ELISA Reader (1420 Multilabel Counter/Victor3). The hemolysis percentage was expressed in relation to a 100% lysis control (erythrocytes incubated with 0.1% Triton X-100); PBS was used as a negative control.[12,75,76]

Results and Discussion

Sample fractionation and peptide purification

The hemolymph was processed and separated on a Sep-Pack C18 column using 5%, 40%, and 80% ACN concentrations to elute the main sample into three different fractions (see section "Sample fractionation"). During purification of the 5% ACN sample by RP-HPLC, the fraction eluted at 67.3 minutes (sample 1; Figure 1A) showed antimicrobial against *E. coli*, whereas the fraction eluted at 56.2 minutes during 40% ACN sample purification by RP-HPLC (sample 2; Figure 2A) showed antimicrobial activity against *M. luteus*. Both were completely isolated in the second chromatography step (Figures 1B and 2B).

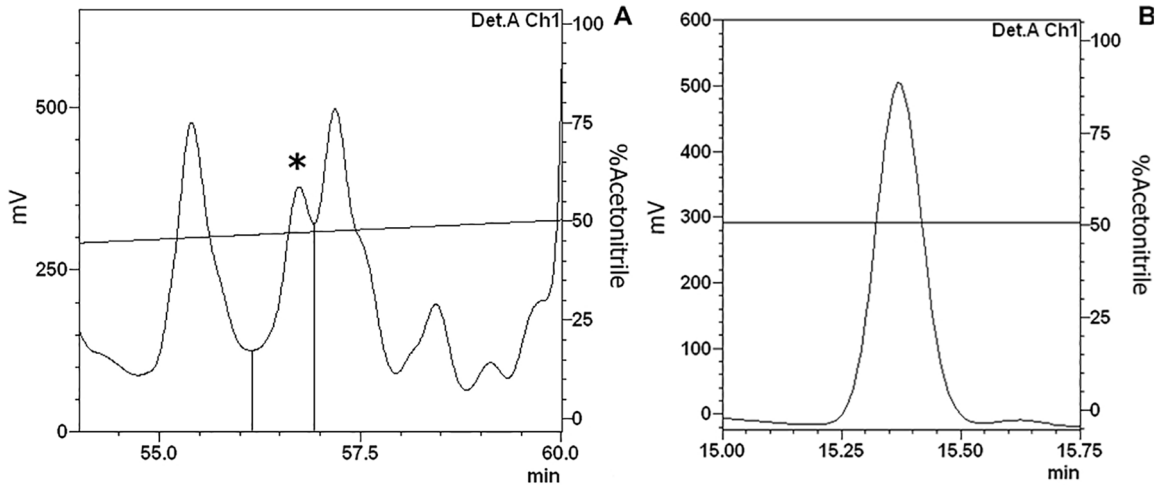

Figure 2. 40% ACN active fraction purification—sample 2: (A) The 40% ACN fraction isolated was separated by RP-HPLC using a C18 column, eluted over a linear gradient from solution A from 2% to 60% of solution B in 60 minutes. The labeled fraction (*), eluted at 56.2 minutes, exhibited antimicrobial activity and was subjected to a second chromatography step. (B) The second RP-chromatographic step on an analytic VP-ODS C18 column with an ACN gradient from 49% to 59% solution B in 60 minutes to guarantee its homogeneity.

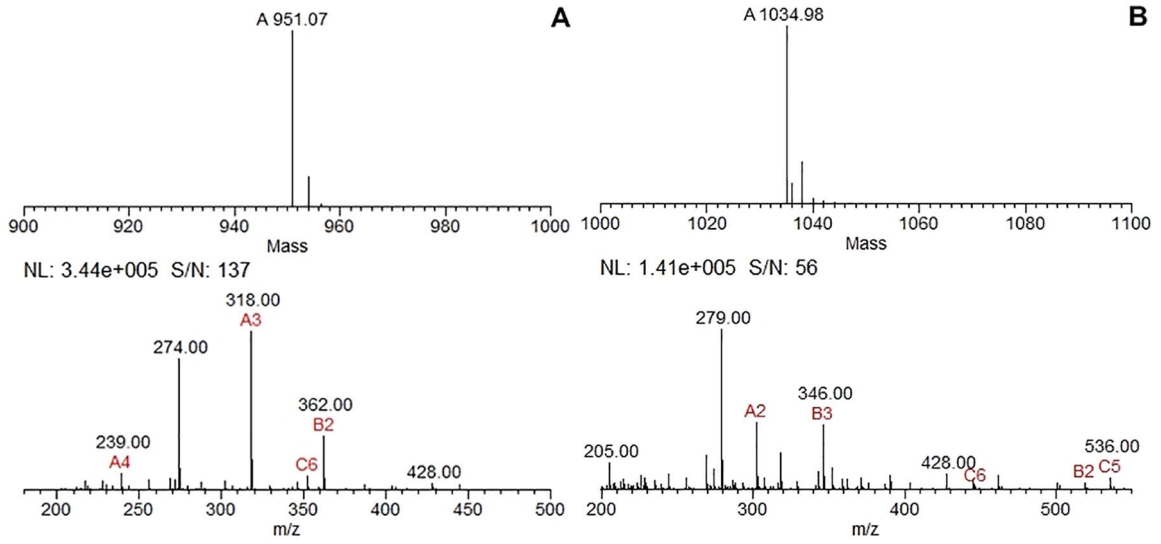

Figure 3. Mass determination using MagTran software: (A) Sample 1 had an approximate mass of 951.07 Da. (B) Sample 2 had an approximate mass of 1034.98 Da.

Peptide identification

After purification, both samples were examined by mass spectrometry and the data were analyzed in MagTran 1.02. We verified that samples 1 and 2 had approximated molecular weights of 951 and 1035 Da, respectively (Figure 3).

To determine the amino acid content and perform protein identification, mass spectrometry data were analyzed with Mascot software with the Fingerprint tool and using the Hemiptera database (118 063 sequences). Both samples showed similarities with tachykinin-related peptides I and II (TRP1 and TRP2), respectively, from different insect species (Figure 4).

According to the official TKRP nomenclature, these peptides were named as TRP1-TINF and TRP2-TINF (tachykinin-related peptides I and II from *T. infestans*). As observed for TRP1-TINF, the first match corresponded to an uncharacterized protein from *Acyrthosiphon pisum*. However, this protein showed an expected threshold P-value $> .05$, and thus this result was discarded. Showing 100% coverage with the corresponding sequences, TRP1-TINF is composed of 9 amino acid residues with the sequence GPSGFLGMR and RP2-TINF is composed of 10 amino acid residues with the sequence APAAGFFGMR.

Tachykinins are proteins that comprise a superfamily initially described by Von Euler and Gaddum[30] and have neurotransmitter/neuromodulator activities as their main physiological functions. A subfamily discovered in insects, named as tachykinin-related peptides (or tachykinin-like peptides), has been widely studied.[36,37] The production of TKRP by species in the order Hemiptera has been described, and all sequences are summarized in Table 1.

Figure 4. Mass spectrometry analysis using MASCOT software: (A) Sample 1 mass spectrometry data compared with a Hemiptera database (118 063 sequences). Sample showed similarity with tachykinin-related peptide I from *Banasa dimiata, Pyrrhocoris apterus, Pentatoma rufipes, Oncopeltus fasciatus, Nezara viridula, Euschistus servus*, and *Acrosternum hilare*. (B) Sample 2 mass spectrometry data compared with a Hemiptera database (118 063 sequences). Sample showed similarity with tachykinin-related peptide II from *B. dimiata, P. rufipes, N. viridula, E. servus*, and *A. hilare*.

Table 1. Relationships with TKRPs from Hemipterans.

SPECIES	PEPTIDE	FAMILY NAME	PEPTIDE SEQUENCE
Acrosternum hilare (*Nezara hilaris*)[a]	Tachykinin-related peptide I	TRP1_ACRHI	GPSGFLGMR
	Tachykinin-related peptide II	TRP2_ACRHI	APAAGFFGMR
	Tachykinin-related peptide III	TRP3_ACRHI	GPSSGFFGMR
	Tachykinin-related peptide IV	TRP4_ACRHI	SPASGFFGMR
	Tachykinin-related peptide V	TRP5_ACRHI	APLMGFQGVR
	Tachykinin-related peptide VI	TRP6_ACRHI	APSMGFMGMR
Banasa dimiata (*Pentatoma dimiata*)[a]	Tachykinin-related peptide I	TRP1_BANDI	GPSGFLGMR
	Tachykinin-related peptide II	TRP2_BANDI	APAAGFFGMR
	Tachykinin-related peptide III	TRP3_BANDI	GPSSGFFGMR
	Tachykinin-related peptide IV	TRP4_BANDI	SPASGFFGMR
	Tachykinin-related peptide V	TRP5_BANDI	APLMGFQGVR
	Tachykinin-related peptide VI	TRP6_BANDI	APSMGFMGMR
Euschistus servus[a]	Tachykinin-related peptide I	TRP1_EUSSE	GPSGFLGMR
	Tachykinin-related peptide II	TRP2_EUSSE	APAAGFFGMR
	Tachykinin-related peptide III	TRP3_EUSSE	GPSSGFFGMR
	Tachykinin-related peptide IV	TRP4_EUSSE	SPASGFFGMR
	Tachykinin-related peptide V	TRP5_EUSSE	APLMGFQGVR
	Tachykinin-related peptide VI	TRP6_EUSSE	APSMGFMGMR

(Continued)

Table 1. (Continued)

SPECIES	PEPTIDE	FAMILY NAME	PEPTIDE SEQUENCE
Nezara viridula (*Cimex viridulus*)[a]	Tachykinin-related peptide I	TRP1_NEZVI	GPSGFLGMR
	Tachykinin-related peptide II	TRP2_NEZVI	APAAGFFGMR
	Tachykinin-related peptide III	TRP3_NEZVI	GPSSGFFGMR
	Tachykinin-related peptide IV	TRP4_NEZVI	SPASGFFGMR
	Tachykinin-related peptide V	TRP5_NEZVI	APSMGFMGMR
	Tachykinin-related peptide VI	TRP6_NEZVI	APLMGFQGVR
Oncopeltus fasciatus[a]	Tachykinin-related peptide I	TRP1_ONCFA	GPSGFLGMR
	Tachykinin-related peptide II	TRP2_ONCFA	APASGFFGMR
	Tachykinin-related peptide III	TRP3_ONCFA	APSSGFFGTR
	Tachykinin-related peptide IV	TRP4_ONCFA	NPASGFFGMR
	Tachykinin-related peptide V	TRP5_ONCFA	APVMGFQGMR
	Tachykinin-related peptide VI	TRP6_ONCFA	APSMGFMGMR
Pentatoma rufipes (*Cimex rufipes*)[a]	Tachykinin-related peptide I	TRP1_PENRU	GPSGFLGMR
	Tachykinin-related peptide II	TRP2_PENRU	APAAGFFGMR
	Tachykinin-related peptide III	TRP3_PENRU	GPSSGFFGMR
	Tachykinin-related peptide IV	TRP4_PENRU	SPASGFFGMR
	Tachykinin-related peptide V	TRP5_PENRU	APLMGFQGVR
	Tachykinin-related peptide VI	TRP6_PENRU	APSMGFMGMR
Pyrrhocoris apterus (*Cimex apterus*)[a]	Tachykinin-related peptide I	TRP1_PYRAP	GPSGFLGMR
	Tachykinin-related peptide II	TRP2_PYRAP	APASGFFGMR
	Tachykinin-related peptide III	TRP3_PYRAP	GPSSGFFGTR
	Tachykinin-related peptide IV	TRP4_PYRAP	TPASGFFGMR
	Tachykinin-related peptide V	TRP5_PYRAP	APSSMGFMGMR
	Tachykinin-related peptide VI	TRP6_PYRAP	APVMGFQGMR
Rhodnius prolixus (Triatomid bug)[b]	Tachykinin-related peptide I	TRP1_RHOPR	SGPGFMGVR
	Tachykinin-related peptide II	TRP2_RHOPR	TSMGFQGVR
	Tachykinin-related peptide III	TRP3_RHOPR	APASGFFGMR
	Tachykinin-related peptide IV	TRP4_RHOPR	TPSDGFMGMR
	Tachykinin-related peptide V	TRP5_RHOPR	APACVGFQGMR
	Tachykinin-related peptide VI	TRP6_RHOPR	GPSSSAFFGMR
	Tachykinin-related peptide VII	TRP7_RHOPR	SPATMGFAGVR
	Tachykinin-related peptide VIII	TRP8_RHOPR	pQERRAMGFVGMR

Relationships of all TKRP sequences described in species in the order Hemiptera.
[a]Neupert et al.[56]
[b]Ons et al.[57]

As *Rhodnius prolixus* is phylogenetically close to *T. infestans*, primary sequence alignment was performed to compare their most similar sequences (Figure 5), which revealed a close resemblance.

Recent studies have shown that a few components of the vertebrate tachykinin family have antimicrobial activity against some bacterial strains such as *S. marcescens* and *P. aeruginosa*.[77-79] Although none of the TKRP sequences mentioned above were

evaluated in antimicrobial assays, urechistachykinin I and urechistachykinin II, which are tachykinin-related neuropeptides isolated from the Echiuroid worm[44] and share the C-terminal region, presented antimicrobial activity against different Gram-positive and Gram-negative bacteria and different fungi.[80]

```
TRP1_RHOPR      -SGPGFMGVR      9
TRP1-TINF       -GPSGFLGMR      9
TRP3_RHOPR      APASGFFGMR      10
TRP2-TINF       APAAGFFGMR      10
                **:*:*
```

Figure 5. Primarily sequence alignment. Tachykinin-related peptides I and II from *Triatoma infestans* (TRP1-TINF and TRP2-TINF) compared with tachykinin-related peptides I and III from *Rhodnius prolixus* (TRP2_RHOPR and TRP3_RHOPR). Amino acid residues highly conserved between the sequences are highlighted in yellow. (*) Position with a single and fully conserved amino acid residue; (:) Position with amino acid residues conserved between groups of strong similar properties; (.) Position with amino acid residues conserved between groups of weakly similar properties.

As a main characteristic of the peptide family, all sequences share the same C-terminal region (F-X-G-Y-R-NH2); thus, it is expected that they have similar biological effects.

Characterization of isolated TKRPs

Bioassays. TRP1-TINF and TRP2-TINF were artificially synthetized. For synthetic TRP2-TINF, the methionine (second amino acid in the C-terminal region) was changed to norleucine, reducing the molecular weight to 1006 Da. For comparison, the synthetic peptides were also tested against *M. luteus* and *E. coli*. Both peptides were active against the two microorganisms, indicating the antimicrobial potential of the synthetic molecules.

The synthetic peptides were tested against a broad range of bacterial, yeast, and fungal species and their antimicrobial activities are reported in Tables 2 and 3. The initial concentration of TRP1-TINF was 128 μM and that of TRP2-TINF was 164 μM.

Both TRP1-TINF and TRP2-TINF could partially or completely inhibit the growth of several bacteria and fungi.

Table 2. Synthetic TRP1-TINF antimicrobial activities against bacterial and fungal strains.

MICROORGANISMS	MIC, μM (MG/ML)			
	MH		PB	
Gram-positive bacteria				
Micrococcus luteus	128 (0.20)		32 (0.05)	
Staphylococcus aureus	NA		NA	
Micrococcus luteus BR2	NA		NA	
Bacillus megaterium	NA		NA	
Bacillus subtilis	NA		NA	
Gram-negative bacteria				
Alcaligenes faecalis	NA		NA	
Enterobacter cloacae	NA		NA	
Serratia marcescens	NA		NA	
Pseudomonas aeruginosa	64 (0.10)		64 (0.10)	
Escherichia coli	NA		100 (0.10)	
MICROORGANISMS	MIC, μM (MG/ML)		MBC, μM (MG/ML)	
	RPMI	PDB	RPMI	PDB
Yeasts				
Candida albicans	NA	NA	NA	NA
Candida parapsilosis	NA	NA	NA	NA
Cryptococcus neoformans	NA	128 (0.20)	NA	128 (0.20)
Saccharomyces cerevisiae	NA	NA	NA	NA
Candida tropicalis	NA	NA	NA	NA

(Continued)

Table 2. (Continued)

MICROORGANISMS	MIC, μM (MG/ML)		MBC, μM (MG/ML)	
	RPMI	PDB	RPMI	PDB
Filamentous fungi				
Cladosporium sp.	NA	NA	NA	NA
Penicillium expansum	128 (0.20)	128 (0.20)	128 (0.20)	128 (0.20)
Aspergillus niger	NA	128 (0.20)	NA	128 (0.20)
Paecilomyces farinosus	NA	NA	NA	NA
Cladosporium herbarum	NA	NA	NA	NA

Abbreviations: MBC, minimal bactericidal concentration values obtained by liquid growth inhibition assay; MH, Müller-Hinton medium; MIC, minimal inhibition concentration; NA, not active at a concentration of 128 μM; PB, poor broth nutrient medium; PDB, potato dextrose broth medium; RPMI, Roswell Park Memorial Institute medium.

Table 3. Synthetic TRP2-TINF antimicrobial activities against bacterial and fungal strains.

MICROORGANISMS	MIC, μM (MG/ML)	
	MH	PB
Gram-positive bacteria		
Micrococcus luteus	NA	164 (0.18)
Staphylococcus aureus	NA	NA
Micrococcus luteus BR2	NA	NA
Bacillus megaterium	NA	NA
Bacillus subtilis	NA	NA
Gram-negative bacteria		
Alcaligenes faecalis	NA	NA
Enterobacter cloacae	NA	NA
Serratia marcescens	NA	NA
Pseudomonas aeruginosa	164 (0.18)	82 (0.09)
Escherichia coli	NA	82 (0.09)

MICROORGANISMS	MIC, μM (MG/ML)		MBC, μM (MG/ML)	
	RPMI	PDB	RPMI	PDB
Yeasts				
Candida albicans	NA	NA	NA	NA
Candida parapsilosis	NA	NA	NA	NA
Cryptococcus neoformans	NA	164 (0.18)	NA	164 (0.18)
Saccharomyces cerevisiae	NA	NA	NA	NA
Candida tropicalis	NA	NA	NA	NA
Filamentous fungi				
Cladosporium sp.	NA	164 (0.18)	NA	164 (0.18)
Penicillium expansum	164 (0.18)	164 (0.18)	164 (0.18)	164 (0.18)
Aspergillus niger	NA	NA	NA	NA
Paecilomyces farinosus	NA	NA	NA	NA
Cladosporium herbarum	NA	NA	NA	NA

Abbreviations: MBC, minimal bactericidal concentration values obtained on the liquid growth inhibition assay; MH, Müller-Hinton medium; MIC, minimal inhibition concentration; NA, not active on a concentration of 164 μM; PB, poor broth nutrient medium; PDB, potato dextrose broth medium; RPMI, Roswell Park Memorial Institute medium.

Neither peptide showed specific activities, although both could disrupt bacterial cells at a lower concentration than that required for disrupting fungi cells. For instance, TRP1-TINF was active against Gram-positive and Gram-negative bacteria (*M. luteus* with 32 μM and *P. aeruginosa* with 64 μM), and TRP2-TINF has predilection toward Gram-negative bacteria, presenting activity with lower concentrations toward *P. aeruginosa* and *E. coli*.

Hemolysis percentages of 0.9% and 0.6% were observed when red blood cells were incubated with 300 μM of TRP1-TINF and 360 μM of TRP2-TINF, respectively. Thus, the peptides showed no significant hemolytic activity ($P < .05$).

In contrast, when incubated Vero cells with the highest tested concentration of both peptides (1000 μM), cell viability was approximately 84% and 90% after exposure to TRP1-TINF and TRP2-TINF, respectively (Figure 6). The selectivity index was not calculated, as no median lethal dose values were found at the maximum evaluated concentrations.

To investigate the physicochemical dynamics of the peptides, we performed tridimensional structure analysis and degradation analysis in plasma assays. In CD analysis, the structural conformation of asymmetric molecules was obtained from the patterns of absorption and refraction of the absorbance of right- and left-handed circularly polarized light[81,82] as a hygroscopic liquid was added to the original solution.

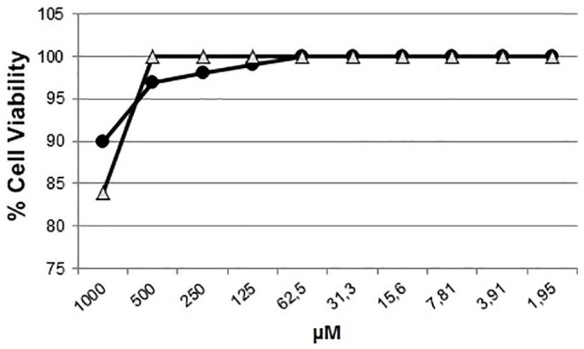

Figure 6. TRP1-TINF and TRP2-TINF toxicity assays. Cytotoxicity of TRP1-TINF (Δ) and TRP2-TINF (•) over Vero cells in a 2-fold series dilution at a maximum concentration of 1000 μM.

As shown on the CD spectra, TRP1-TINF (Figure 7A) tended to assume a random coil conformation, whereas TRP2-TINF (Figure 7B) tended to assume a Poly (Pro) II (PPII) or helix-3_1 conformation.

TRP1-TINF showed a random secondary structure because of 2 main factors. It is formed of less than 10 amino acid residues and nearly half of these residues have small and neutral side chains (3 glycine residues and 2 proline residues), lowering the possibility of forming a stable secondary structure.

Stable PPII structures presents turns of approximately 120° (3 amino acid residues per turn) and contain 10 atoms in each turn with a hydrogen bridge/bond.[83,84] As TRP2-TINF has a PPII conformation and is composed of 10 amino acid residues, it represents a structure with 3 turns.

Tachykinin-related peptides are present in different insect tissues because of hemolymph circulation,[41] thus it is crucial to determine their degradation rate in the plasma to develop improve the understanding of the peptide bioavailability. The percentages of available peptides in the plasma after different incubation times are shown in Figure 8.

Within 15 minutes, the percentage of TRP1-TINF decreased to 69% peptide remaining; this process occurs gradually, with only 16% of the whole peptides remaining in solution at 120 minutes.

TRP2-TINF was more susceptible to degradation. In 15 minutes, the peptide concentration decreased to 34% and in 30 minutes decreased to 14%. By 60 minutes, 2.3% of the peptide remained, and no peptide was detected at 120 minutes. The molecular weight of each peptide and the degradation curves were analyzed by mass spectrometry to determine the amino acid loss (Table 4).

By observing the amino acid loss at each time point, it is possible to determine if the sequence was degraded by aminopeptidases, carboxypeptidases, or endopeptidases. After

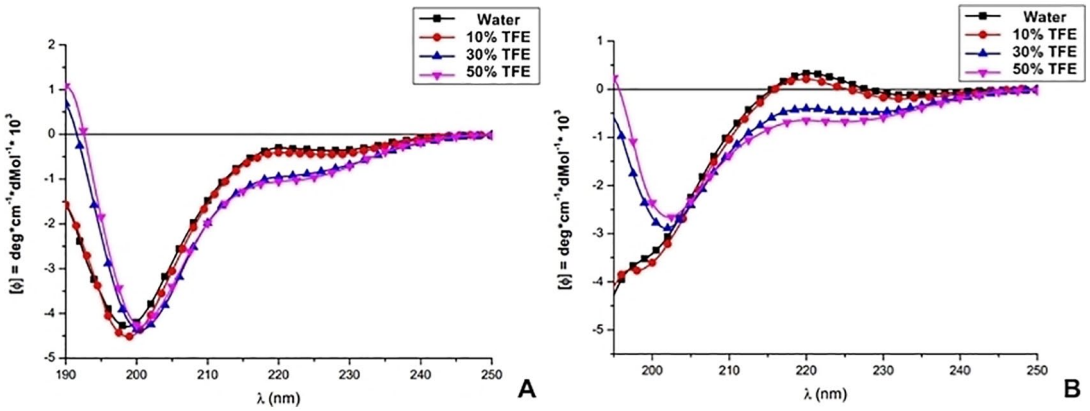

Figure 7. TRP1-TINF and TRP2-TINF CD spectra: (A) Diffraction pattern of polarized light of TRP1-TINF, corresponding to a random structure. (B) Diffraction pattern of polarized light of TRP2-TINF, corresponding to a PPII structure.

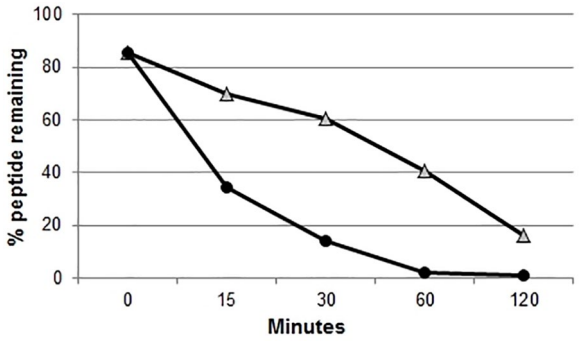

Figure 8. Degradation of TRP1-TINF and TRP2-TINF in the plasma. Percentage of whole peptides per incubation time (0-120 minutes). TRP1-TINF is represented by Δ and 16% of the peptides were not degraded after 120 minutes. TRP2-TINF is represented by (•) and was entirely degraded after 120 minutes.

Table 4. Amino acid loss by degradation in plasma.

TIME (MINUTES)	MOLECULAR WEIGHT (DA)	AMINO ACID RELEASED
TRP1-TINF (GPSGFLGNR – 903 Da)		
0	903	No degradation
15	749, 846	-G, -PG
30	604, 661, 749, 846	-G, -PG, -SPG, -GSPG
60	604, 661, 749, 846	-G, -PG, -SPG, -GSPG
120	457, 604, 661, 749, 846	-G, -PG, -SPG, GPSG-, -GSPG
TRP2-TINF (APAAGFFGNR – 1006 Da)		
0	1006	No degradation
15	736, 850	-R, -NR
30	681, 736, 850	-R, -NR, -GNR
60	681, 736, 850	-R, -NR, -GNR
120	681, 736, 850	-R, -NR, -GNR

The molecular weight determined by mass spectrometry analyses during incubation indicates which amino acid was released. Amino acid residues list: G, glycine; P, proline; S, serine; F, phenylalanine; L, leucine; N, norleucine; R, arginine; A, alanine.

15 minutes of incubation, 3 molecular weights were detected, and 903, 846, and 749 Da were also registered. These molecular weights correspond to the entire sequence and loss of G and G-P, respectively. Additional amino acid losses continually occurred until 120 minutes. At the last time point, 5 molecular weights corresponding to the full sequence without G (846 Da), G-P (749 Da), G-P-S (661 Da), G-P-S-G (604 Da), and G-P-S-G-F (457 Da) were observed. These losses indicate the susceptibility of the peptides to degradation by aminopeptidase enzymes.[85]

The degradation profile of TRP2-TINF is compatible with degradation by a carboxypeptidase. Within 15 minutes, fragments with molecular weights of 850 and 736 Da were detected, corresponding to the entire sequence without R and RN. In agreement with this, at 30, 60, and 120 minutes RNG loss was observed (681 Da). This degradation is indicative of carboxypeptidase activity.[86]

Conclusions

These results increase the understanding of triatomines physiology and represent a pharmacological relevant study object, providing the first description of TKRP molecules produced by *T. infestans* and demonstrating the antimicrobial potency and physicochemical features of the isolated molecules.

Acknowledgements

The authors are thankful to the referees for critical review of the manuscript, and to colleagues of the laboratory who helped during the procedures, mainly to Dr Ronaldo Zucatelli Mendonça and Juliana Cuoco Badari for their help with the cell culture experiments and Ivan Ferreira for helping with English editing.

Author Contributions

LCLD was responsible for the development of all experiments and writing the manuscript; PIdS Jr participated during the purification experiments, mainly HPLC, and all of the mass spectrometry analysis; AdM participated during peptide synthesis, in plasma degradation, circular dichroism, and mass spectrometry analysis; and FLA participated during circular dichroism experiments. All the authors approve the entire manuscript content and ensure the accuracy and integrity of any part of the work.

ORCID iDs

Laura Cristina Lima Diniz https://orcid.org/0000-0002-4985-8329

Pedro Ismael da Silva Junior https://orcid.org/0000-0001-6619-6489

REFERENCES

1. Li Y, Xiang Q, Zhang Q, Huang Y, Su Z. Overview on the recent study of antimicrobial peptides: origins, functions, relative mechanisms and application. *Peptides*. 2012;37:207-215. doi:10.1016/j.peptides.2012.07.001.
2. Stephens JM. Bactericidal activity of the blood of actively immunized wax moth larvae. *Can J Microbiol*. 1962;8:491-499. doi:10.1139/m62-064.
3. Hink WF, Briggs JD. Bactericidal factors in hemolymph from normal and immune wax moth larvae, Galleria mellonella. *J Insect Physiol*. 1968;14:10.
4. Powning RF, Davidson WJ. Studies on insect bacteriolytic enzymes. I. Lysozyme in haemolymph of Galleria mellonella and Bombyx mori. *Comp Biochem Physiol B*. 1973;45:669-686.
5. Boman HG, Nilsson-Faye I, Paul K, Rasmuson T Jr. Insect immunity. I. Characteristics of an inducible cell-free antibacterial reaction in hemolymph of Samia cynthia pupae. *Infect Immun*. 1974;10:136-145.
6. Faye I, Pye A, Rasmuson T, Boman HG, Boman IA. Insect immunity. 11. Simultaneous induction of antibacterial activity and selection synthesis of some hemolymph proteins in diapausing pupae of Hyalophora cecropia and Samia cynthia. *Infect Immun*. 1975;12:1426-1438.
7. Steiner H, Hultmark D, Engström A, Bennich H, Boman HG. Sequence and specificity of two antibacterial proteins involved in insect immunity. *Nature*. 1981;292:246-248. doi:10.1038/292246a0.
8. Silva PI Jr, Daffre S, Bulet P. Isolation and characterization of gomesin, an 18-residue cysteine-rich defense peptide from the spider Acanthoscurria gomesiana

hemocytes with sequence similarities to horseshoe crab antimicrobial peptides of the tachyplesin family. *J Biol Chem*. 2000;275:33464-33470. doi: 10.1074/jbc.M001491200.
9. Ayroza G, Ferreira ILC, Sayegh RSR, Tashima AK, da Silva PI Jr. Juruin: an antifungal peptide from the venom of the Amazonian Pink Toe spider, Avicularia juruensis, which contains the inhibitory cystine knot motif. *Front Microbiol*. 2012;3:324-324. doi:10.3389/fmicb.2012.00324.
10. Abreu TF, Sumitomo BN, Nishiyama MY Jr, et al. Peptidomics of Acanthoscurria gomesiana spider venom reveals new toxins with potential antimicrobial activity. *J Proteomics*. 2017;151:232-242. doi:10.1016/j.jprot.2016.07.012.
11. Candido-Ferreira IL, Kronenberger T, Sayegh RSR, Batista IdFC, da Silva PI Jr. Evidence of an antimicrobial peptide signature encrypted in HECT E3 uubiquitin ligases. *Front Immunol*. 2017;7:664. doi:10.3389/fimmu.2016.00664.
12. Chaparro E, da Silva PI Jr. Lacrain: the first antimicrobial peptide from the body extract of the Brazilian centipede Scolopendra viridicornis. *Int J Antimicrob Agents*. 2016;48:277-285. doi:10.1016/j.ijantimicag.2016.05.015.
13. Chaparro-Aguirre E, Segura-Ramírez PJ, Alves FL, Riske KA, Miranda A, Silva Júnior PI. Antimicrobial activity and mechanism of action of a novel peptide present in the ecdysis process of centipede Scolopendra subspinipes subspinipes. *Scientific Reports*. 2019;9:13631. doi:10.1038/s41598-019-50061-y.
14. Díaz-Roa A, Espinoza-Culupú A, Torres-García O, et al. Sarconesin II, a new antimicrobial peptide isolated from sarconesiopsis magellanica excretions and secretions. *Molecules*. 2019;24:2077. doi:10.3390/molecules24112077.
15. Díaz-Roa A, Patarroyo MA, Bello FJ, Da Silva PI. Sarconesin: sarconesiopsis magellanica blowfly larval excretions and secretions with antibacterial properties. *Front Microbiol*. 2018;9:2249. doi:10.3389/fmicb.2018.02249.
16. Diniz LCL, Miranda A, da Silva PI Jr. Human antimicrobial peptide isolated from triatoma infestans haemolymph, trypanosoma cruzi-transmitting vector. *Front Cell Infect Microbiol*. 2018;8:354. doi:10.3389/fcimb.2018.00354.
17. Nascimento S, Martins L, Oliveira U, Moraes R, Mendonça R, da Silva Junior P. A new lysozyme found in the haemolymph from pupae of Lonomia obliqua (Lepidoptera: Saturniidae). *Trends Entomol*. 2016;12:13-23.
18. Segura-Ramírez PJ, Silva Júnior PI. Loxosceles gaucho spider venom: an untapped source of antimicrobial agents. *Toxins (Basel)*. 2018;10:522. doi:10 .3390/toxins10120522.
19. Pushpanathan M, Gunasekaran P, Rajendhran J. Antimicrobial peptides: versatile biological properties. *Int J Pept*. 2013;2013:675391-675391. doi:10.1155 /2013/675391.
20. Sayegh RS, Batista IF, Melo RL, et al. Longipin: an amyloid antimicrobial peptide from the harvestman acutisoma longipes (arachnida: opiliones) with preferential affinity for anionic vesicles. *PLoS ONE*. 2016;11:e0167953. doi:10.1371/ journal.pone.0167953.
21. Riciluca KC, Sayegh RS, Melo RL, Silva PI Jr. Rondonin an antifungal peptide from spider (Acanthoscurria rondoniae) haemolymph. *Results Immunol*. 2012;2:66-71. doi:10.1016/j.rinim.2012.03.001
22. Pasupuleti M, Schmidtchen A, Malmsten M. Antimicrobial peptides: key components of the innate immune system. *Crit Rev Biotechnol*. 2012;32:143-171. doi :10.3109/07388551.2011.594423.
23. Sutti R, Rosa BB, Wunderlich B, da Silva Junior PI, Rocha EST. Antimicrobial activity of the toxin VdTX-I from the spider Vitalius dubius (Araneae, Theraphosidae). *Biochem Biophys Rep*. 2015;4:324-328. doi:10.1016/j.bbrep.2015.09.018.
24. Diniz LCL, da Silva Junior PI. Hemoglobin reassembly of antimicrobial fragments from the midgut of triatoma infestans. *Biomolecules*. 2020;10:261. doi:10 .3390/biom10020261.
25. Lei J, Sun L, Huang S, et al. The antimicrobial peptides and their potential clinical applications. *Am J Transl Res*. 2019;11:3919-3931.
26. Kangawa K, Minamino N, Fukuda A, Matsuo H. Neuromedin K: a novel mammalian tachykinin identified in porcine spinal cord. *Biochem Biophys Res Commun*. 1983;114:533-540. doi:10.1016/0006-291x(83)90813-6.
27. Kimura S, Okada M, Sugita Y, Kanazawa I, Munekata E. Novel neuropeptides, neurokinin alpha and beta isolated from porcine spinal cord. *Proc Japan Acad, Ser B*. 1983;59:101-104. doi:10.2183/pjab.59.101.
28. Steinhoff MS, von Mentzer B, Geppetti P, Pothoulakis C, Bunnett NW. Tachykinins and their receptors: contributions to physiological control and the mechanisms of disease. *Physiol Rev*. 2014;94:265-301. doi:10.1152/physrev.00031.2013.
29. Satake H. Chapter 9 – Tachykinin family. In: Takei Y, Ando H, Tsutsui K, eds. *Handbook of Hormones*. 1st ed. Academic Press, Oxford, London, UK. 2016;72-73.
30. Von Euler US, Gaddum JH. An unidentified depressor substance in certain tissue extracts. *J Physiol*. 1931;72:74-87. doi:10.1113/jphysiol.1931.sp002763.
31. Chang MM, Leeman SE, Niall HD. Amino-acid sequence of substance P. *Nature New Biology*. 1971;232:86-87. doi:10.1038/newbio232086a0.
32. Erspamer V. The tachykinin peptide family. *Trends Neurosci*. 1981;4:267-269. doi:10.1016/0166-2236(81)90084-9.
33. Maggio JE. Tachykinins. *Ann Rev Neurosci*. 1988;11:13-28. doi:10.1146/annurev. ne.11.030188.000305.
34. Helke CJ, Krause JE, Mantyh PW, Couture R, Bannon MJ. Diversity in mammalian tachykinin peptidergic neurons: multiple peptides, receptors, and regulatory mechanisms. *FASEB J*. 1990;4:1606-1615.
35. Mussap CJ, Geraghty DP, Burcher E. Tachykinin receptors: a radioligand binding perspective. *J Neurochem*. 1993;60:1987-2009. doi:10.1111/j.1471-4159.1993. tb03484.x.
36. Vanden Broeck J, Torfs H, Poels J, et al. Tachykinin-like peptides and their receptors. *Ann N Y Acad Sci*. 1999;897:374-387. doi:10.1111/j.1749-6632.1999. tb07907.x.
37. Severini C, Improta G, Falconieri-Erspamer G, Salvadori S, Erspamer V. The tachykinin peptide family. *Pharmacol Rev*. 2002;54:285-322. doi:10.1124/ pr.54.2.285.
38. Satake H, Kawada T. Overview of the primary structure, tissue-distribution, and functions of tachykinins and their receptors. *Curr Drug Targets*. 2006;7:963-974. doi:10.2174/138945006778019273.
39. Satake H, Aoyama M, Sekiguchi T, Kawada T. Insight into molecular and functional diversity of tachykinins and their receptors. *Protein Pept Lett*. 2013;20: 615-627. doi:10.2174/0929866511320060002.
40. Erspamer V. Ricerche preliminari sulla moschatina. *Experientia*. 1949;5:79-81. doi:10.1007/BF02153737.
41. Satake H, Kawada T, Nomoto K, Minakata H. Insight into tachykinin-related peptides, their receptors, and invertebrate tachykinins: a review. *Zoolog Sci*. 2003;20:533-549. doi:10.2108/zsj.20.533.
42. Van Loy T, Vandersmissen HP, Poels J, Van Hiel MB, Verlinden H, Vanden Broeck J. Tachykinin-related peptides and their receptors in invertebrates: a current view. *Peptides*. 2010;31:520-524. doi:10.1016/j.peptides.2009.09.023.
43. Anastasi A, Erspamer V, Cei JM. Isolation and amino acid sequence of physalaemin, the main active polypeptide of the skin of physalaemus fuscumaculatus. *Arch Biochem Biophys*. 1964;108:341-348. doi:10.1016/0003-9861(64)90395-9.
44. Ikeda T, Minakata H, Nomoto K, Kubota I, Muneoka Y. Two novel tachykinin-related neuropeptides in the echiuroid worm, Urechis unicinctus. *Biochem Biophys Res Commun*. 1993;192:1-6. doi:10.1006/bbrc.1993.1373.
45. Champagne DE, Ribeiro JM. Sialokinin I and II: vasodilatory tachykinins from the yellow fever mosquito Aedes aegypti. *Proc Natl Acad Sci U S A*. 1994;91: 138-142. doi:10.1073/pnas.91.1.138.
46. Schoofs L, Holman GM, Hayes TK, Kochansky JP, Nachman RJ, De Loof A. Locustatachykinin III and IV: two additional insect neuropeptides with homology to peptides of the vertebrate tachykinin family. *Regul Pept*. 1990;31:199-212. doi:10.1016/0167-0115(90)90006-i.
47. Schoofs L, Holman GM, Hayes TK, Nachman RJ, De Loof A. Locustatachykinin I and II, two novel insect neuropeptides with homology to peptides of the vertebrate tachykinin family. *FEBS Lett*. 1990;261:397-401. doi:10.1016/0014 -5793(90)80601-e.
48. Schoofs L, Veelaert D, Vanden Broeck J, De Loof A. Peptides in the Locusts, Locusta migratoria and Schistocerca gregaria11Taken in part from a paper presented at a satellite symposium on Insect Neuropeptides during the Seventh Annual Neuropeptide Conference, February 1–6, 1996, Breckenridge, CO. *Peptides*. 1997;18:145-156. doi:10.1016/S0196-9781(96)00236-7.
49. Diesner M, Gallot A, Binz H, et al. Mating-induced differential peptidomics of neuropeptides and protein hormones in agrotis ipsilon moths. *J Proteome Res*. 2018;17:1397-1414. doi:10.1021/acs.jproteome.7b00779.
50. Takeuchi H, Yasuda A, Yasuda-Kamatani Y, Kubo T, Nakajima T. Identification of a tachykinin-related neuropeptide from the honeybee brain using direct MALDI-TOF MS and its gene expression in worker, queen and drone heads. *Insect Mol Biol*. 2003;12:291-298. doi:10.1046/j.1365-2583.2003.00414.x.
51. Bonasio R, Zhang G, Ye C, et al. Genomic comparison of the ants Camponotus floridanus and Harpegnathos saltator. *Science*. 2010;329:1068-1071. doi:10.1126/ science.1192428.
52. Siviter R, Winther Nachman ÅR, et al. Expression and functional characterization of a Drosophila neuropeptide precursor with homology to mammalian preprotachykinin A. *J Biol Chem*. 2000;275:23273-23280.
53. Richards S, Liu Y, Bettencourt BR, et al. Comparative genome sequencing of Drosophila pseudoobscura: chromosomal, gene, and cis-element evolution. *Genome Res*. 2005;15:1-18. doi:10.1101/gr.3059305.
54. Muren JE, Nässel DR. Seven tachykinin-related peptides isolated from the brain of the madeira cockroach: evidence for tissue-specific expression of isoforms11taken in part from a paper presented at a satellite symposium on insect neuropeptides during the seventh annual neuropeptide conference, February 1–6, 1996, Breckenridge, CO. *Peptides*. 1997;18:7-15. doi:10.1016/S0196-9781(96)00236-7.
55. Zoephel J, Reiher W, Rexer KH, Kahnt J, Wegener C. Peptidomics of the agriculturally damaging larval stage of the cabbage root fly Delia radicum (Diptera: Anthomyiidae). *PLoS ONE*. 2012;7:e41543. doi:10.1371/journal.pone.0041543.
56. Neupert S, Russell WK, Russell DH, López JD Jr, Predel R, Nachman RJ. Neuropeptides in Heteroptera: identification of allatotropin-related peptide and tachykinin-related peptides using MALDI-TOF mass spectrometry. *Peptides*. 2009;30:483-488. doi:10.1016/j.peptides.2008.11.009.

57. Ons S, Richter F, Urlaub H, Pomar RR. The neuropeptidome of Rhodnius prolixus brain. *Proteomics*. 2009;9:788-792. doi:10.1002/pmic.200800499.
58. Martins LPA, Castanho REP, Da Rosa JA, Tokumo MO, De Godoy CAP, Rosa RM. Estudo comparativo entre duas técnicas de xenodiagnóstico artificial aplicado empacientes chagásicos cronicos. *Revista de Patologia Tropical*. 2001;30:8. doi:10.5216/rpt.v30i1.15813.
59. Bulet P. Strategies for the discovery, isolation, and characterization of natural bioactive peptides from the immune system of invertebrates. *Methods Mol Biol*. 2008;494:9-29. doi:10.1007/978-1-59745-419-3_2.
60. Wiegand I, Hilpert K, Hancock RE. Agar and broth dilution methods to determine the minimal inhibitory concentration (MIC) of antimicrobial substances. *Nat Protoc*. 2008;3:163-175. doi:10.1038/nprot.2007.521.
61. Hetru C, Bulet P. Strategies for the isolation and characterization of antimicrobial peptides of invertebrates. *Methods Mol Biol*. 1997;78:35-49. doi:10.1385/0-89603-408-9:35.
62. Pöppel AK, Vogel H, Wiesner J, Vilcinskas A. Antimicrobial peptides expressed in medicinal maggots of the blow fly Lucilia sericata show combinatorial activity against bacteria. *Antimicrob Agents Chemother*. 2015;59:2508-2514. doi:10.1128/AAC.05180-14.
63. Hancock RE. *Modifies MIC Method for Cationic Antimicrobial Peptides*. University of British Columbia. http://cmdr.ubc.ca/bobh/method/modified-mic-method-for-cationic-antimicrobial-peptides/. Accessed November 27, 2017.
64. Yamamoto LG. Chapter 4. Inhibitory and bactericidal principles (MIC & MBC). In: *Case Based Pediatrics for Medical Students and Residents*. 2003. https://www.hawaii.edu/medicine/pediatrics/pedtext/s06c04.html
65. Shtatland T, Guettler D, Kossodo M, Pivovarov M, Weissleder R. PepBank – a database of peptides based on sequence text mining and public peptide data sources. *BMC Bioinformatics*. 2007;8:280. doi:10.1186/1471-2105-8-280.
66. Choo KH, Tan TW, Ranganathan S. SPdb – a signal peptide database. *BMC Bioinformatics*. 2005;6:249. doi:10.1186/1471-2105-6-249.
67. Giraldo-Calderon GI, Emrich SJ, MacCallum RM, et al. VectorBase: an updated bioinformatics resource for invertebrate vectors and other organisms related with human diseases. *Nucleic Acids Res*. 2015;43:D707-D713. doi:10.1093/nar/gku1117.
68. Wang G, Li X, Wang Z. APD3: the antimicrobial peptide database as a tool for research and education. *Nucleic Acids Res*. 2016;44:D1087-D1093. doi:10.1093/nar/gkv1278.
69. Altschul SF, Gish W, Miller W, Myers EW, Lipman DJ. Basic local alignment search tool. *J Mol Biol*. 1990;215:403-410. doi:10.1016/S0022-2836(05)80360-2.
70. Larkin MA, Blackshields G, Brown NP, et al. Clustal W and Clustal X version 2.0. *Bioinformatics*. 2007;23:2947-2948. doi:10.1093/bioinformatics/btm404.
71. Miranda A, Koerber SC, Gulyas J, et al. Conformationally restricted competitive antagonists of human/rat corticotropin-releasing factor. *J Med Chem*. 1994;37:1450-1459. doi:10.1021/jm00036a010.
72. Anthis NJ, Clore GM. Sequence-specific determination of protein and peptide concentrations by absorbance at 205 nm. *Protein Sci*. 2013;22:851-858. doi:10.1002/pro.2253.
73. Fazio MA, Jouvensal L, Vovelle F, et al. Biological and structural characterization of new linear gomesin analogues with improved therapeutic indices. *Biopolymers*. 2007;88:386-400. doi:10.1002/bip.20660.
74. Alves FL, Oliveira VX Jr, Miranda A. Angiotensin II analogues with N-terminal lactam bridge cyclization: an overview on AT1 receptor activation and tachyphylaxis. *Chem Biol Drug Des*. 2016;88:677-682. doi:10.1111/cbdd.12795.
75. Hao G, Shi YH, Tang YL, Le GW. The membrane action mechanism of analogs of the antimicrobial peptide Buforin 2. *Peptides*. 2009;30:1421-1427. doi:10.1016/j.peptides.2009.05.016.
76. Nan YH, Bang JK, Jacob B, Park IS, Shin SY. Prokaryotic selectivity and LPS-neutralizing activity of short antimicrobial peptides designed from the human antimicrobial peptide LL-37. *Peptides*. 2012;35:239-247. doi:10.1016/j.peptides.2012.04.004.
77. Hansen CJ, Burnell KK, Brogden KA. Antimicrobial activity of Substance P and Neuropeptide Y against laboratory strains of bacteria and oral microorganisms. *J Neuroimmunol*. 2006;177:215-218. doi:10.1016/j.jneuroim.2006.05.011.
78. El Karim IA, Linden GJ, Orr DF, Lundy FT. Antimicrobial activity of neuropeptides against a range of micro-organisms from skin, oral, respiratory and gastrointestinal tract sites. *J Neuroimmunol*. 2008;200:11-16. doi:10.1016/j.jneuroim.2008.05.014.
79. Berger A, Tran AH, Dedier H, Gardam MA, Paige CJ. Antimicrobial properties of hemokinin-1 against strains of Pseudomonas aeruginosa. *Life Sci*. 2009;85:700-703. doi:10.1016/j.lfs.2009.09.011.
80. Sung WS, Park SH, Lee DG. Antimicrobial effect and membrane-active mechanism of Urechistachykinins, neuropeptides derived from Urechis unicinctus. *FEBS Lett*. 2008;582:2463-2466. doi:10.1016/j.febslet.2008.06.015.
81. Kelly SM, Jess TJ, Price NC. How to study proteins by circular dichroism. *Biochim Biophys Acta*. 2005;1751:119-139. doi:10.1016/j.bbapap.2005.06.005.
82. Greenfield NJ. Using circular dichroism spectra to estimate protein secondary structure. *Nat Protoc*. 2006;1:2876-2890. doi:10.1038/nprot.2006.202.
83. Cooley RB, Arp DJ, Karplus PA. Evolutionary origin of a secondary structure: pi-helices as cryptic but widespread insertional variations of alpha-helices that enhance protein functionality. *J Mol Biol*. 2010;404:232-246. doi:10.1016/j.jmb.2010.09.034.
84. Weaver TM. The pi-helix translates structure into function. *Protein Sci*. 2000;9:201-206. doi:10.1110/ps.9.1.201.
85. Taylor A. Aminopeptidases: structure and function. *FASEB J*. 1993;7:290-298. doi:10.1096/fasebj.7.2.8440407.
86. Barber AK, Fisher JR. A mechanism of action for carboxypeptidase A. *Proc Natl Acad Sci U S A*. 1972;69:2970-2974. doi:10.1073/pnas.69.10.2970.